

AD-A094 628

CALIFORNIA UNIV LOS ANGELES SCHOOL OF ENGINEERING A--ETC F/8 20/9
CHAOTIC SOLUTIONS OF NONLINEAR WAVE-WAVE INTERACTING SYSTEMS IN--ETC(U)
JUN 80 K MASUI AFOSR-79-0050

UNCLASSIFIED

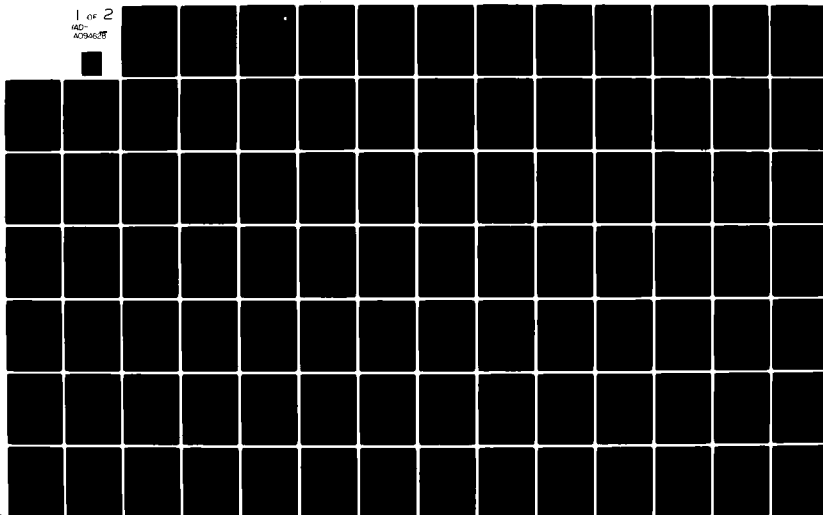
UCLA-ENG-8026

AFOSR-TR-81-0074

NL

1 of 2

AD-
ADONIS



UNCLASSIFIED

SECURITY CLASSIFICATION OF THIS PAGE (When Data Entered)

REPORT DOCUMENTATION PAGE		READ INSTRUCTIONS BEFORE COMPLETING FORM
1. REPORT NUMBER AFOSR/IR-81-0074	2. GOVT ACCESSION NO. D-1094628	3. RECIPIENT'S CATALOG NUMBER
4. TITLE (and Subtitle) Chaotic Solutions of Nonlinear Wave-Wave Interacting Systems in Plasmas	5. TYPE OF REPORT & PERIOD COVERED INTERIM	
7. AUTHOR(s) Koshiro/Masui	6. PERFORMING ORG. REPORT NUMBER UCLA-ENG-8026	8. CONTRACT OR GRANT NUMBER(s) AFOSR-79-0050
9. PERFORMING ORGANIZATION NAME AND ADDRESS School of Engineering and Applied Science University of California, Los Angeles, CA 90024	10. PROGRAM ELEMENT, PROJECT, TASK AREA & WORK UNIT NUMBERS 61102F, 2301/A7	
11. CONTROLLING OFFICE NAME AND ADDRESS AFOSR Bolling AFB, DC 20332	12. REPORT DATE June 1980	13. NUMBER OF PAGES 136
14. MONITORING AGENCY NAME & ADDRESS LEVEL	15. SECURITY CLASS. (of this report) UNCLASSIFIED	
15a. DECLASSIFICATION/DOWNGRADING SCHEDULE		
16. DISTRIBUTION STATEMENT (of this Report) Approved for Public Release; Distribution Unlimited.		
17. DISTRIBUTION STATEMENT (of the abstract entered in Block 20, if different from Report) DTIC ELECTED FEB 5 1981		
18. SUPPLEMENTARY NOTES		
19. KEY WORDS (Continue on reverse side if necessary and identify by block number) Chaotic oscillations, plasma turbulence, nonlinear phenomena, wave-wave interactions		
20. ABSTRACT (Continue on reverse side if necessary and identify by block number) We study the chaotic behavior and phase locking in wave-wave interacting systems with linear damping or growth terms. For a two or three-wave interaction, the system equations are reducible to a real three-dimensional equation on a certain set Σ in the state space. For a three-wave interaction, the phases of the waves are locked on Σ . We consider only systems of positive-energy waves whose reduced equations may have chaotic behavior for almost all initial conditions. Hence, we discard those systems which have the following properties: The corresponding reduced equation has only one equilibrium point, or there is an open set R_0 in		

DD FORM 1473

EDITION OF 1 NOV 65 IS OBSOLETE

UNCLASSIFIED

SECURITY CLASSIFICATION OF THIS PAGE (When Data Entered)

DDC FILE COPY

UNCLASSIFIED

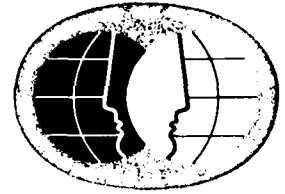
SECURITY CLASSIFICATION OF THIS PAGE(When Data Entered)

Accession For	
DTIC GCMR	<input checked="" type="checkbox"/>
DTIC TAB	<input type="checkbox"/>
Unannounced	<input type="checkbox"/>
Justification	
Evaluation	
Distribution/	
Availability Codes	
Dist	
A	

the state space such that if the initial point is in R_0 , the whole trajectory is in R_0 and converges to an equilibrium point or diverges to infinity as $t \rightarrow \infty$. We obtain sufficient conditions for asymptotic phase locking as $t \rightarrow \infty$ in three-wave interacting systems, which depend on the sizes of the attractors for the trajectories. Under the foregoing selection rule, only two of the remained cases have no growth terms and have parametric instability. Numerical experiments show that in one of the two systems, the phases of the waves are locked asymptotically as $t \rightarrow \infty$ for a wide range of parameter values (i.e., the damping coefficients and the external wave amplitude). In the other system, the phases are nearly locked most of the time for certain values of the parameters, but not asymptotically locked as $t \rightarrow \infty$. The trajectory behavior of the reduced equations is studied numerically in detail. For certain values of the parameters, the first return mappings of the trajectories have properties which are similar to those of one-dimensional mappings having parabolic graphs. Simple models are introduced to explain schematically the transition of attractors for the trajectories. Finally, we consider certain statistical properties of the first return mappings in the light of the known theorems for one-dimensional mappings. Numerical results suggest that the systems with parametric instability are in a turbulent state for certain values of the parameters.

UNCLASSIFIED

SECURITY CLASSIFICATION OF THIS PAGE(When Data Entered)



This work was supported by the
U.S. Air Force Office of Scientific Research
under Grant No. AFOSR-79-0050

UCLA-ENG-8026
JUNE 1980

CHAOTIC SOLUTIONS OF NONLINEAR WAVE-WAVE
INTERACTING SYSTEMS IN PLASMAS

K. MASUI

Approved for public release;
distribution unlimited.

UCLA 81 2 2 071
SCHOOL OF ENGINEERING AND APPLIED SCIENCE

Chaotic Solutions of Nonlinear Wave-Wave

Interacting Systems in Plasmas

by

Koshiro Masui

School of Engineering and Applied Science

University of California

Los Angeles, California 90024

This work was supported by the
U.S. Air Force Office of Scientific Research
Under Grant No. AFOSR-79-0050

AIR FORCE OFFICE OF SCIENTIFIC RESEARCH (AFSC)
NOTICE OF WORKING COPY TO 1000
This document is a working copy and has been reviewed and is
approved for release under FAR AIR 190-12 (7b).
Distribution is unlimited.
A. D. Masui
Information Officer

TABLE OF CONTENTS

	Page
List of Tables.....	vi
List of Figures.....	vii
ACKNOWLEDGMENTS.....	viii
VITA.....	ix
ABSTRACT.....	x
CHAPTER 1 INTRODUCTION.....	1
1.1 Turbulence in Plasmas.....	3
1.2 Outline of Dissertation.....	6
CHAPTER 2 WAVE-WAVE INTERACTIONS.....	8
2.1 Wave-Wave Interacting Systems $\dot{Y} = \hat{F}(Y)$	8
2.2 Reduced Systems $\dot{X} = F(X)$	15
2.3 Phase Locking.....	24
2.3.1 Differential Equations of Phase Differences $\dot{\xi} = \Phi \xi$	27
2.3.2 Sufficient Conditions for Convergence of $\xi(t)$ to θ_{ξ}	28
2.3.3 Sufficient Conditions for Convergence of $Y(t)$ to Σ	31
CHAPTER 3 REDUCED EQUATIONS.....	39
3.1 Analysis of Reduced Equations.....	41
3.1.1 System (3).....	41
3.1.2 System (4).....	45
3.1.3 System (5).....	51
3.1.4 System (7).....	53
3.1.5 System (2) and (6).....	55
3.2 Physical Interpretation for Reduced Systems.....	60

	Page
3.2.1 System (2).....	60
3.2.2 System (3).....	63
3.2.3 System (4).....	64
3.2.4 System (5).....	65
3.2.5 System (6).....	66
3.2.6 System (7).....	66
3.3 Systems with Parametric Instability.....	67
3.3.1 Sufficient Conditions for Convergence of $\xi(t)$ to θ_ξ	69
3.3.2 Attractor in X-space.....	70
3.3.3 Phase Locking and Chaotic Solutions.....	72
3.3.4 Local Properties of Original Systems.....	75
3.3.5 Energy of Original Systems.....	79
CHAPTER 4 NUMERICAL EXPERIMENTS.....	82
4.1 Behavior of Original Systems (3') and (6').....	82
4.2 Behavior of Reduced Systems (3) and (6)..	89
4.2.1 System (3).....	90
4.2.2 System (6).....	92
4.2.3 Sizes of Attractors.....	98
4.2.4 Periodic Solutions and Bifurcations.....	99
4.3 Simple Models Describing Attractors.....	100
CHAPTER 5 FIRST RETURN MAPPINGS AND STATISTICAL PROPERTIES.....	109
5.1 First Return Mappings of (3) and (6).....	109
5.2 One-Dimensional Mappings.....	115
5.2.1 Period Three Implies Chaos.....	115
5.2.2 Statistical Properties of $\{G^n(p)\}$	118

	Page
5.3 Statistical Properties of (3) and (6)....	120
5.3.1 Mixing Property.....	120
5.3.2 Unbounded Solutions of System (6)..	121
CHAPTER 6 CONCLUSIONS.....	126
6.1 Summary of Results.....	126
6.2 Remarks on Further Research.....	127
REFERENCES.....	130
APPENDIX.....	134

Accession For	
FILE NO.	
DATE	
BY	
REMARKS	
A	

LIST OF TABLES

Table		Page
2.1	Frequency Matching.....	10
2.2	Wave-Wave Interacting Systems $\dot{Y} = \hat{F}(Y)$	14
2.3	Parameter for Chaotic Solutions.....	16
2.4	Reduced Systems $\dot{X} = F(X)$	22
2.5	Parameters for Chaotic Solutions of Systems (3) and (4).....	25
2.6	Differential Equations of Phase Differences $\dot{\xi} = \Phi \xi$	29
2.7	Sufficient Conditions for Convergence of $\xi(t)$ to θ_{ξ}	32
3.1	Frequency Matching and Decay Diagrams.....	61
3.2	Systems for Chaotic Solutions.....	68

LIST OF FIGURES

Figure		Page
2.1	Phase-Locked Trajectory.....	19
2.2	Diverging Trajectory of (3).....	24
2.3	Sketches of Sets in (S.2.3).....	37
3.1	Sketches of Root Locus of (3).....	44
3.2	Sketches of Root Locus of (4).....	49
3.3	Sketches of S and W_{\pm} in (6).....	57
3.4	Dynamics of Energy of (2).....	62
3.5	Attractors $\hat{\Delta}$ and $\tilde{\Delta}$ of (3).....	72
3.6	Necessary Conditions for $\hat{\Delta} \subset \hat{\Gamma}$	73
3.7	Dynamics of Energy of (3').....	80
4.1	Time Variations of Phase Difference of (3')..	84
4.2	Plots of Wave Amplitude of (3').....	86
4.3	Projections of Trajectories of (3).....	91
4.4	First Return Mapping.....	92
4.5	Projections of Trajectories of (6).....	93
4.6	Schematic Diagram of Bifurcation of (6).....	100
4.7	Simple Models for (3).....	102
4.8	Simple Models for (6).....	103
4.9	Multi-Loop Attractors.....	107
5.1	First Return Mappings of x_1	110
5.2	Autocovariance $R(\tau)$ of x_1	122
5.3	Density $P_T(\chi)$ of Distribution of x_1	125

ACKNOWLEDGMENT

I would like to acknowledge the guidance provided by Professor Paul K. C. Wang during the research of this dissertation. Without his advice and encouragement, this work would have never been completed. Sincere thanks are also extended to Professors Earl A. Coddington, Nhan N. Levan, George J. Morales and Richard E. Mortensen for serving on the dissertation committee.

Appreciation is expressed for the support provided by the Office of Scientific Research of the U. S. Air Force under Grant AFOSR 79-0050.

Special appreciation is made to Faith Flagg for her help for finishing this manuscript.

CHAPTER 1

INTRODUCTION

The nonlinear interaction of waves in plasma has been studied extensively [1-9]. Recently, it has been shown that certain nonlinear wave-wave interacting systems with a small number of degrees of freedom exhibit chaotic behaviors [10-15]. Studies of this phenomenon may lead to new theories for turbulence in fluids and plasmas.

In the classical Landau-Lifshitz theory of turbulence [16], the physical variables describing a turbulent motion are quasi-periodic functions of time:

$$x(t) = f(\omega_1 t, \omega_2 t, \dots, \omega_N t), \quad (1.1)$$

where f is composed of periodic motions with frequencies $\omega_1, \dots, \omega_N$ which are irrationally related. As the number N of modes becomes large, $x(t)$ generally exhibits a very complicated behavior. The motion described by (1.1) can be produced by a sequence of successive bifurcations of periodic motions. As certain parameters vary, a stable equilibrium point becomes unstable and a stable periodic orbit appears. Then, the periodic orbit becomes unstable and a stable periodic orbit with two frequencies appears. This bifurcation process continues on.

It is known that a quasi-periodic function of time does not have the mixing property (i.e., the autocovariance

$R(t)$ of x does not decay to zero as $t \rightarrow \infty$). This implies intuitively that the temporal variation of x is not sensitive to initial conditions, thus contradicting an important physical feature of turbulent states. Furthermore, a quasi-periodic function is unstable in the sense that a small perturbation of the parameter could lead to a periodic motion [17]. Hence, the quasi-periodic motion does not provide a satisfactory description of the turbulent states. It is also known that some physical systems exhibit abrupt transition from a nonturbulent state into a turbulent state without the appearance of periodic motions. Such phenomenon cannot be explained by the above mentioned mechanism.

Recently, Ruelle and Takens [18] proposed the following definition for a turbulent state: In this state, the trajectories of the system model are attracted to a nonempty set called the "strange attractor" which is a positive limit set of trajectories consisting of neither periodic orbits nor equilibrium point. On this attractor, the system trajectories behave in a chaotic manner resembling a turbulent state.

According to the above notion of a turbulent state, it is possible that simple models described by finite dimensional systems of ordinary differential equations could have chaotic behavior. A well known example is the Lorenz model [19] describing the convection in a fluid layer forced by a linear temperature gradient:

$$\left. \begin{aligned} \dot{x}_1 &= -\sigma x_1 + \sigma x_2, \\ \dot{x}_2 &= rx_1 - x_2 - x_1 x_3, \\ \dot{x}_3 &= -bx_3 + x_1 x_2, \end{aligned} \right\} \quad (1.2)$$

where σ , r and b are constant real parameters. The Lorenz system exhibits abrupt transition into a very complicated behavior when the parameters pass through certain threshold values. Many numerical experiments have been performed on this system and their results suggest the existence of strange attractors and the mixing property, but they have not been verified mathematically. In this work, the term "chaotic solutions" refers to those solutions which lie on a strange attractor. If a solution exhibits complicated behavior but without a mathematical proof as being a "chaotic solution", it will be referred to as a "pseudo-chaotic solution". Hence, "pseudo-chaotic solutions" may be periodic solutions with long periods, or may correspond to trajectories converging to a stable closed orbit or an equilibrium point in a complicated manner. Many simple mathematical models having chaotic or pseudo-chaotic solutions have been found in such areas as geophysics [20], biology [21,22], chemistry [23] and laser physics [24].

1.1 Turbulence in Plasmas

In the conventional theory of turbulence in plasmas, turbulence is described as the state in which a large number

of collective degrees of freedom are strongly excited [25]. This means that the energy of the collective modes is much larger than the thermal fluctuation level, and that the number of modes is so large that the plasma has a complicated behavior. The energy of the unstable modes is distributed to other modes by nonlinear processes and then dissipated through some form of damping mechanisms. When the energy transfer between the modes is balanced, a stationary broad spectrum corresponding to stationary turbulence appears. When the energy of each mode is small and the nonlinear coupling between various modes is weak, and when the linear growth and damping terms can be neglected, the random-phase approximation can be used to obtain the turbulent state. In this approximation, it is assumed that the phase of each mode varies randomly. On the other hand, if the linear growth or damping terms are not negligible, the phase of each mode is no longer independent even when the nonlinear coupling of modes is weak. In spite of this limitation, the random-phase approximation is often used for expedience.

As mentioned earlier, the existence of a large number of modes does not necessarily mean that the system is in a turbulent state. Furthermore, the assumption of independent phases between the modes is usually made without justification. At the initial stage of turbulent states, it is reasonable to assume independent phases since the randomness of thermal fluctuation at the initial time is retained. On

the other hand, once the energy of turbulence is far from the equilibrium, there must be some mechanisms which maintain the random phases. Flynn and Manheimer [10] showed that even when the modes have no linear growth or damping over an interval of wave numbers, the phases are completely coupled when the linearly growing and damping modes are introduced outside the interval. This means that the random-phase approximation is not suitable even in the interval over which both the linear growth and damping are negligible.

At present, there are a few known models in plasma physics having a small number of modes which exhibit chaotic behaviors [11-15]. Flynn and Manheimer's model [10] consisting of ten modes, two of which are linearly growing and damped, has chaotic behavior. Rabinovich and his coworkers introduced following two simple models of wave-wave interaction having chaotic motions [11-13].

$$\left. \begin{aligned} \dot{A}_1 - \gamma_1 A_1 &= -i\{A_2^2 + A_1(v_1|A_1|^2 + w_1|A_2|^2)\}, \\ \dot{A}_2 + \gamma_2 A_2 &= -i\{A_1 A_2^* + A_2(v_2|A_1|^2 + w_2|A_2|^2)\}, \end{aligned} \right\} \quad (1.3)$$

and

$$\left. \begin{aligned} \dot{A}_1 + \gamma_1 A_1 &= -i(A_2 A_3 + v A_0 A_2^*), \\ \dot{A}_2 + \gamma_2 A_2 &= -i(A_1 A_3^* + v A_0 A_1^*), \\ \dot{A}_3 + \gamma_3 A_3 &= -i A_1 A_2^*, \end{aligned} \right\} \quad (1.4)$$

where A_i is a normalized complex wave amplitude; all

parameters are real numbers and $\gamma_i > 0$. System (1.3) describes the interaction of two plasma waves belonging to different branches. Chaotic motion appears only when a small frequency mismatching is introduced. System (1.4) describes a three-wave interaction such that an external wave with a constant amplitude decays into two waves which have another resonant wave. Numerical experiments for these systems suggest that they have strange attractors and mixing properties. Hence, they could represent turbulent states. We should note that in these systems, the linear instability may lead directly to a turbulent state, and that the chaotic behavior is intrinsic to the equations and no additional assumption of randomness is necessary.

1.2 Outline of Dissertation

In this dissertation, three-wave interacting systems having chaotic behaviors are studied in detail. Asymptotic phase locking of the waves as $t \rightarrow \infty$ are also studied, which is a special property of wave-wave interaction with linear damping terms. Once the phase are locked, the system reduces to a three-dimensional one.

In Chapter 2, the systems to be studied in this work are presented. All these systems are obtained from the equations for a set of interacting oscillators. The reduced three-dimensional equation is obtained for each system. We also give sufficient conditions for the reduced equations to

describe the asymptotic behavior of the original system.

In Chapter 3, the reduced equations are studied mainly by a root locus analysis of the characteristic equations of the linearized vector field at the equilibrium points. From the results, we choose those systems whose reduced equations may have periodic or pseudo-chaotic solutions for almost all initial conditions. Based on physical considerations, two systems are selected for detailed study.

In Chapter 4, the results of numerical experiments for two chosen systems are presented. The transition between periodic and pseudo-chaotic motions are shown in detail. Simple two-dimensional models are introduced which are used to explain the transition of behaviors.

In Chapter 5, we obtain the first return mappings of the trajectories for the chosen systems, some of which resemble one-dimensional mappings. We discuss certain statistical properties of general one-dimensional mappings and the first return mappings of our systems.

CHAPTER 2

WAVE-WAVE INTERACTIONS

In this chapter, we introduce the systems of wave-wave interactions to be studied in subsequent chapters. All these systems are derived from the equations describing a set of nonlinearly interacting oscillators. A wave-wave interaction which does not belong to this framework is not considered here.

2.1 Wave-Wave Interacting Systems $\dot{Y} = \hat{F}(Y)$

We begin with the equations for a set of nonlinearly interacting oscillators described by

$$\begin{aligned} \ddot{x}_i + 2\gamma_i \dot{x}_i + \omega_i^2 x_i = & \sum_{j,k \in Z_N} v_{jk} x_j x_k \\ & + \sum_{j,k,l \in Z_N} v_{jkl} x_j x_k x_l, \quad i \in Z_N \triangleq \{1, \dots, N\}, \end{aligned} \quad (2.1)$$

where x_i is the displacement, ω_i is the natural frequency, and γ_i is the growth or damping coefficient for the i -th oscillator; v_{jk} and v_{jkl} are the nonlinear coupling coefficients of the oscillators. All the variables and parameters are real numbers. We assume that the linear damping and growth rates are small (i.e., $\gamma_i \ll \omega_i$) and the nonlinear terms are also small (i.e., $|v_{jk} x_j|, |v_{jkl} x_j x_k| \ll \omega_i^2$). Then, we can express $x_i(t)$ in the form:

$$x_i(t) = a_i(t)\exp(i\omega_i t) + a_i^*(t)\exp(-i\omega_i t),$$

$$i \in Z_N, \quad (2.2)$$

where a_i is a slowly time-varying component. We also assume frequency matching:

$$\omega_i = \sum_{j \in Z_N} \mu_j \omega_j, \quad \mu_j \in \{-1, 1\}, \quad i \in Z_N, \quad (2.3)$$

where $\omega_i > 0$ and $\omega_i \neq \omega_j$ if $i \neq j$. Then, the frequency matching conditions for $N = 2, 3, 4$ are shown in Table 2.1, where it is assumed that the v_{ijk} 's in (2.1) are zero for $N = 3, 4$. For $N = 3$, the first frequency matching condition has two degrees of freedom and the remaining ones have only one degree of freedom. For $N = 4$, we assume that one of the waves is an external wave with fixed amplitude. Then, there is one degree of freedom in the first three cases and none in the rest. The energy of the waves is obtained by an integration over the frequency domains. Here, for $N = 3$, the energy contribution of the last two cases is negligible as compared to that of the first case. In what follows, we consider only the first case. Similarly, for $N = 4$, only the first three cases will be studied.

For $N = 2$, substituting (2.2) into (2.1) and normalizing the variables, we have

$$\left. \begin{aligned} \dot{A}_i + \gamma_i A_i &= -i\{v A_j^2 + A_i(v_{iii}|A_i|^2 + v_{ijj}|A_j|^2)\}, \\ \dot{A}_j + \gamma_j A_j &= -i\{A_i A_j^* + A_j(v_{jii}|A_i|^2 + v_{jjj}|A_j|^2)\}, \end{aligned} \right\} \quad (2.4)$$

Table 2.1 Frequency Matching

N = 2	$(\omega_i, \omega_j) = (2\omega_j, \omega_j)$
N = 3	$(\omega_i, \omega_j, \omega_k)$
	$(\omega_j + \omega_k, \omega_j, \omega_k), (2\omega_j, \omega_j, 3\omega_j), (4\omega_k, 2\omega_k, \omega_k)$
N = 4	$(\omega_i, \omega_j, \omega_k, \omega_l)$
	$(\sigma\omega_k + v\omega_l, \omega_i/2, \omega_k, \omega_l),$ $(2\omega_j, \sigma\omega_k + v\omega_l, \omega_k, \omega_l), (\sigma, v) \in \{(1,1), (1,-1), (-1,1)\},$ $(\omega_j + \omega_k, \omega_k + \sigma\omega_l, \omega_k, \omega_l), \sigma \in \{-1, 1\},$ $(8\omega_l, 4\omega_l, 2\omega_l, \omega_l), (4\omega_k, 2\omega_k, \omega_k, 3\omega_k),$ $(4\omega_k, 2\omega_k, \omega_k, 6\omega_k), (4\omega_k, 2\omega_k, \omega_k, 5\omega_k),$ $(2\omega_j, \omega_j, 3\omega_j, (3/2)\omega_j), (2\omega_j, \omega_j, 6\omega_j, 3\omega_j)$

where

$$\begin{aligned} A_i &= (v_{ij}/2\omega_i) a_i, \quad A_j = v(|v_{jj}v_{ij}|/2\omega_i\omega_j)^{\frac{1}{2}} a_j, \quad v = \text{sgn}(v_{jj}v_{ij}), \\ V_{iii} &= \{(2\omega_j/v_{jj})^2/2\omega_i\} v_{iii}, \quad V_{ijj} = \{(4\omega_i\omega_j/|v_{ij}v_{jj}|)/2\omega_i\} v_{ijj}, \\ V_{jii} &= \{(2\omega_j/v_{ij})^2/2\omega_j\} v_{jii}, \quad V_{jjj} = \{(4\omega_i\omega_j/|v_{ij}v_{jj}|)/2\omega_j\} v_{jjj}. \end{aligned}$$

For $N = 3$, we have

$$\left. \begin{aligned} \dot{A}_i + \gamma_i A_i &= -i v_i A_j A_k, \\ \dot{A}_j + \gamma_j A_j &= -i v_j A_k^* A_i, \\ \dot{A}_k + \gamma_k A_k &= -i v_k A_i A_j^*, \end{aligned} \right\} \quad (2.5)$$

where

$$\begin{aligned} A_i &= (|v_{ij}v_{ki}|/4\omega_j\omega_k)^{\frac{1}{2}} a_i, \quad A_j = (|v_{ij}v_{jk}|/4\omega_i\omega_k)^{\frac{1}{2}} a_j, \\ A_k &= (|v_{ki}v_{jk}|/4\omega_i\omega_j)^{\frac{1}{2}} a_k, \quad v_j = \text{sgn}(v_{ij}v_{ki}). \end{aligned}$$

For $N = 4$, we have three cases as follows:

Case (i):

$$\left. \begin{aligned} \dot{A}_i + \gamma_i A_i &= -i(v_i' v A_j A_k), \\ \dot{A}_j + \gamma_j A_j &= -i(v_j' v A_i A_k^* + v_j A_k A_1), \\ \dot{A}_k + \gamma_k A_k &= -i(v_k' v A_i A_j^* + v_k A_j A_1^*), \\ \dot{A}_1 + \gamma_1 A_1 &= -i(v_1 A_j A_k^*), \end{aligned} \right\} \quad (2.6)$$

where

$$\begin{aligned}
A_i &= (|v_{ij}v_{ik}|/4\omega_j\omega_k)^{\frac{1}{2}}a_i/v, \quad A_j = (|v_{jk}v_{jl}|/4\omega_k\omega_l)^{\frac{1}{2}}a_j, \\
A_k &= (|v_{kl}v_{jk}|/4\omega_j\omega_l)^{\frac{1}{2}}a_k, \quad A_l = (|v_{jk}v_{jl}|/4\omega_j\omega_k)^{\frac{1}{2}}a_l, \\
v &= (|v_{jl}/v_{ij}|\omega_l/\omega_i)^{\frac{1}{2}}, \quad v_i' = \text{sgn}(v_{ij}v_{ik}), \quad v_j' = \text{sgn}(v_{ij}v_{jk}), \\
v_k' &= \text{sgn}(v_{ik}v_{jk}), \quad v_j = \text{sgn}(v_{jk}v_{jl}), \quad v_k = \text{sgn}(v_{kl}v_{jk}), \\
v_l &= \text{sgn}(v_{jl}v_{kl}).
\end{aligned}$$

Here, without loss of generality, we set $\omega_i = \omega_j + \omega_k$, $\omega_j = \omega_k + \omega_l$, since if $\sigma = -1$, the substitutions $A_i \rightarrow -A_i$, $A_j \rightarrow -A_j$, $A_l \rightarrow -A_l^*$ and $v_k \rightarrow -v_k$ lead to the same equation as (2.6).
Case (ii):

$$\left. \begin{aligned}
\dot{A}_i + \gamma_i A_i &= -i(v_i' v A_j^2 + v_i A_k A_l), \\
\dot{A}_j + \gamma_j A_j &= -i(v A_i A_j^*), \\
\dot{A}_k + \gamma_k A_k &= -i(v_k A_i A_l^*), \\
\dot{A}_l + \gamma_l A_l &= -i(v_l A_i A_k^*),
\end{aligned} \right\} \quad (2.7)$$

where

$$\begin{aligned}
A_i &= (|v_{il}v_{ik}|/4\omega_k\omega_l)^{\frac{1}{2}}a_i, \quad A_j = (|v_{ij}v_{jj}|/4\omega_i\omega_j)^{\frac{1}{2}}a_j/v, \\
A_k &= (|v_{ik}v_{kl}|/4\omega_i\omega_l)^{\frac{1}{2}}a_k, \quad A_l = (|v_{il}v_{kl}|/4\omega_i\omega_l)^{\frac{1}{2}}a_l, \\
v &= (v_{ij}/2\omega_j)(4\omega_k\omega_l/|v_{il}v_{ik}|)^{\frac{1}{2}}, \quad v_i = \text{sgn}(v_{ik}v_{il}), \\
v_i' &= \text{sgn}(v_{ij}v_{jj}), \quad v_k = \text{sgn}(v_{ik}v_{kl}), \quad v_l = \text{sgn}(v_{il}v_{kl}),
\end{aligned}$$

and $\omega_i = 2\omega_j = \omega_k + \omega_l$.

Case (iii):

$$\left. \begin{aligned} \dot{A}_i + \gamma_i A_i &= -i(v_i v A_j^2), \\ \dot{A}_j + \gamma_j A_j &= -i(v A_i A_j^* + v_j A_k A_l), \\ \dot{A}_k + \gamma_k A_k &= -i(v_k A_j A_l^*), \\ \dot{A}_l + \gamma_l A_l &= -i(v_l A_j A_k^*), \end{aligned} \right\} \quad (2.8)$$

where

$$\begin{aligned} A_i &= (v_{ij}/2\omega_j) a_j / v, \quad A_j = (|v_{jk} v_{jl}|/4\omega_k \omega_l)^{1/2} a_j, \\ A_k &= (|v_{jk} v_{kl}|/4\omega_j \omega_l)^{1/2} a_k, \quad A_l = (|v_{jl} v_{kl}|/4\omega_j \omega_k)^{1/2} a_l, \\ v &= (|v_{ij} v_{jj}|/4\omega_i \omega_j)^{1/2} (4\omega_k \omega_l / |v_{jk} v_{jl}|)^{1/2}, \quad v_i = \text{sgn}(v_{ij} v_{jj}), \\ v_j &= \text{sgn}(v_{jk} v_{jl}), \quad v_k = \text{sgn}(v_{jk} v_{kl}), \quad v_l = \text{sgn}(v_{jl} v_{kl}), \end{aligned}$$

and $\omega_i = 2\omega_j$, $\omega_j = \omega_k + \omega_l$.

As mentioned earlier, we fix the amplitude of one of the waves as an external wave for $N = 4$. We choose the external wave so that the equation is nonlinear, since linear equations do not have chaotic solutions. Then, from (2.6), (2.7) and (2.8), we obtain five distinct three-wave interacting systems. Thus, we have seven systems which may have chaotic solutions and they are listed in Table 2.2. Here, without loss of generality, A_0 is taken to be real. Also, the substitutions $A_0 \rightarrow A_0/v$, $A_m \rightarrow A_m/v$, $m = i, j, l$ and $v \rightarrow 1/v$ have been used to derive (5') and (7').

In Table 2.2, some systems with certain values of

Table 2.2 Wave-wave Interacting Systems $\dot{Y} = \hat{F}(Y)$

N=2	(ω_i, ω_j) $= (2\omega_j, \omega_j)$	$\begin{aligned}\dot{A}_i + \gamma_i A_i &= -i\{v A_j^2 + A_i(v_{iii} A_i ^2 + v_{ijj} A_j ^2)\}, \\ \dot{A}_j + \gamma_j A_j &= -i\{A_i A_j^* + A_j(v_{jii} A_i ^2 + v_{jjj} A_j ^2)\}, \\ v &\in \{-1, 1\}\end{aligned}\quad (1')$
N=3	$(\omega_i, \omega_j, \omega_k)$ $= (\omega_j + \omega_k, \omega_j, \omega_k)$	$\begin{aligned}\dot{A}_i + \gamma_i A_i &= -i v_i A_j A_k, \quad v_m \in \{-1, 1\} \\ \dot{A}_j + \gamma_j A_j &= -i v_j A_i A_k^*, \\ \dot{A}_k + \gamma_k A_k &= -i v_k A_i A_j^*\end{aligned}\quad (2')$
N=4	$(\omega_i, \omega_j, \omega_k, \omega_l) = (\omega_j + \omega_k, \omega_k + \omega_l, \omega_k, \omega_l)$	$\begin{aligned}\dot{A}_j + \gamma_j A_j &= -i(v_j A_k A_l + v_j' v A_0 A_k^*), \quad A_0 = A_i, \\ \dot{A}_k + \gamma_k A_k &= -i(v_k A_j A_l^* + v_k' v A_0 A_j^*), \quad v_m \in \{-1, 1\}, \\ \dot{A}_l + \gamma_l A_l &= -i(v_l A_j A_k^*)\end{aligned}\quad (3')$
	$(\omega_i, \omega_j, \omega_k, \omega_l) = (\omega_k + \omega_l, \omega_i/2, \omega_k, \omega_l)$	$\begin{aligned}\dot{A}_i + \gamma_i A_i &= -i(v_i A_k A_l + v_i' v A_0^2), \quad A_0 = A_j, \\ \dot{A}_k + \gamma_k A_k &= -i(v_k A_i A_l^*), \quad v_m \in \{-1, 1\}, \\ \dot{A}_l + \gamma_l A_l &= -i(v_l A_i A_k^*)\end{aligned}\quad (4')$
		$\begin{aligned}\dot{A}_i + \gamma_i A_i &= -i(v_i' A_j^2 + v_i v A_0 A_l), \quad A_0 = A_k, \\ \dot{A}_j + \gamma_j A_j &= -i(A_i A_j^*), \quad v_m \in \{-1, 1\}, \\ \dot{A}_l + \gamma_l A_l &= -i(v_l v A_0 A_i)\end{aligned}\quad (5')$
	$(\omega_i, \omega_j, \omega_k, \omega_l) = (2\omega_j, \omega_k + \omega_l, \omega_k, \omega_l)$	$\begin{aligned}\dot{A}_j + \gamma_j A_j &= -i(v_j A_k A_l + v A_0 A_j^*), \quad A_0 = A_i, \\ \dot{A}_k + \gamma_k A_k &= -i(v_k A_j A_l^*), \quad v_m \in \{-1, 1\}, \\ \dot{A}_l + \gamma_l A_l &= -i(v_l A_j A_k^*)\end{aligned}\quad (6')$
		$\begin{aligned}\dot{A}_i + \gamma_i A_i &= -i(v_i' A_j^2), \quad A_0 = A_k, \\ \dot{A}_j + \gamma_j A_j &= -i(A_i A_j^* + v_j v A_0 A_l), \quad v_m \in \{-1, 1\}, \\ \dot{A}_l + \gamma_l A_l &= -i(v_l v A_0 A_j)\end{aligned}\quad (7')$

parameters obviously have no chaotic solutions. For example, consider system (3') with $\gamma_j, \gamma_l > 0$, $\gamma_k < 0$, $v_m = 1$, $m = j, k, l$ and $v'_m = 1$, $m = j, k$. By direct computation, we have

$$\begin{aligned} & (d/dt)(|A_j|^2 - |A_k|^2 + 2|A_l|^2)/2 \\ & = -\gamma_j |A_j|^2 - \gamma_k |A_k|^2 - 2\gamma_l |A_l|^2. \end{aligned} \quad (2.9)$$

Hence, the quantity $|A_j(t)|^2 - |A_k(t)|^2 + 2|A_l(t)|^2$ decreases as t increases and therefore, the trajectory of (3') diverges to infinity as $t \rightarrow \infty$ for almost all initial conditions. In a similar manner, we can discard certain systems in Table 2.2, and only those cases in Table 2.3 may possess chaotic solutions.

In what follows, we use subscript 1,2,3,... in place of i,j,k,\dots . For example, subscripts j,k and l of (3') are replaced by 1,2 and 3, respectively. Moreover, we denote systems (2') - (7') by

$$\dot{Y} = \hat{F}(Y), \quad (2.10)$$

where $Y \triangleq (y_1, z_1, y_2, z_2, y_3, z_3)^T$, and $y_j = \text{Re}(A_j)$ and $z_j = \text{Im}(A_j)$, $j = 1, 2, 3$. We also denote the solution of (2.10) at time t corresponding to initial condition Y_0 at $t = 0$ by $Y(t, Y_0)$, and the positive semi-orbit by $Y^+(Y_0) \triangleq \{Y : Y = Y(t, Y_0), t \geq 0\}$.

2.2 Reduced Systems $\dot{X} = F(X)$

System (1') in Table 2.3 is identical to (1.3). That is, model (1.3) [11] is the only two-wave interacting system

Table 2.3 Parameters for Chaotic Solutions

(1')	$v = 1$	$(\text{sgn}(\gamma_i), \text{sgn}(\gamma_j)) = (-1, 1)$
(2')	(v_i, v_j, v_k)	$(\text{sgn}(\gamma_i), \text{sgn}(\gamma_j), \text{sgn}(\gamma_k))$
	$(1, 1, 1)$	$(-1, 1, 1)$
(3')	$(v_j', v_k'), (v_j, v_k, v_l)$	$(\text{sgn}(\gamma_j), \text{sgn}(\gamma_k), \text{sgn}(\gamma_l))$
	$(1, 1), (1, 1, 1)$	$(\pm 1, \pm 1, \pm 1), (1, \pm 1, -1), (-1, \pm 1, 1)$
	$(1, -1, -1)$	$(1, 1, \pm 1)$
	$(-1, 1, -1)$	$(1, 1, \pm 1)$
	$(-1, -1, 1)$	$(\pm 1, \pm 1, \pm 1), (\pm 1, 1, -1), (\pm 1, -1, 1)$
	$(1, -1), (1, 1, 1)$	$(1, -1, \pm 1), (-1, 1, \pm 1)$
	$(1, -1, -1)$	$(\pm 1, \pm 1, \pm 1), (1, -1, \pm 1), (-1, 1, \pm 1)$
	$(-1, 1, -1)$	$(1, \pm 1, -1), (-1, 1, \pm 1), (\pm 1, -1, 1)$
	$(-1, -1, 1)$	$(1, -1, \pm 1), (-1, 1, \pm 1)$
(5')	(v_i', v_i, v_l)	$(\text{sgn}(\gamma_i), \text{sgn}(\gamma_j), \text{sgn}(\gamma_l))$
	$(1, 1, 1)$	$(1, \pm 1, -1), (-1, 1, \pm 1), (\pm 1, -1, 1)$
	$(1, 1, -1)$	$(\pm 1, \pm 1, \pm 1), (1, -1, \pm 1), (-1, 1, \pm 1)$
	$(-1, 1, 1)$	$(-1, -1, -1), (1, \pm 1, -1), (-1, \pm 1, 1)$
	$(-1, 1, -1)$	$(\pm 1, \pm 1, \pm 1), (\pm 1, 1, -1), (\pm 1, -1, 1)$
(7')	(v_i', v_i, v_l)	$(\text{sgn}(\gamma_i), \text{sgn}(\gamma_j), \text{sgn}(\gamma_l))$
	$(1, 1, 1)$	$(1, -1, \pm 1), (\pm 1, 1, -1), (-1, \pm 1, 1)$
	$(1, 1, -1)$	$(\pm 1, \pm 1, \pm 1), (1, -1, \pm 1), (-1, 1, \pm 1)$
	$(-1, 1, 1)$	$(-1, -1, -1), (1, \pm 1, -1), (-1, \pm 1, 1)$
	$(-1, 1, -1)$	$(\pm 1, \pm 1, \pm 1), (\pm 1, 1, -1), (\pm 1, -1, 1)$

which may have chaotic solutions. Equation (1') is rewritten as a three-dimensional equation:

$$\left. \begin{aligned} \dot{x}_1 &= -\gamma_1 x_1 - \delta \omega x_2 + 2x_1 x_2 - x_2 \{ (V_{111} - 2V_{211})(x_1^2 + x_2^2) \\ &\quad + (V_{122} - 2V_{222})x_3 \}, \\ \dot{x}_2 &= -\gamma_1 x_2 + \delta \omega x_1 + x_3 - 2x_1^2 + x_1 \{ (V_{111} - 2V_{211})(x_1^2 + x_2^2) \\ &\quad + (V_{122} - 2V_{222})x_3 \}, \\ \dot{x}_3 &= -2\gamma_2 x_3 - 2x_2 x_3, \quad x_3 \geq 0, \end{aligned} \right\} \quad (2.11)$$

where $x_1 = r_1 \cos \phi$, $x_2 = r_1 \sin \phi$, $x_3 = r_2^2$, $r_1 = |A_1|$, $r_2 = |A_2|$, $\phi = 2\text{Arg}(A_2) - \text{Arg}(A_1)$ and $\delta \omega$ is a frequency mismatching $\omega_1 - 2\omega_2$. Equation (2.11) has pseudo-chaotic solutions with or without the third order terms, and its behavior has been studied [11,13,14].

Now, we shall show that systems (2')-(7') also reduce to three-dimensional equations on certain subsets of the original six-dimensional space. We choose equation (3') as an example. Let $A_j = r_j \exp(i\theta_j)$, $r_j \geq 0$, $j = 1, 2, 3$. Then, equation (3') can be written as

$$\left. \begin{aligned} \dot{r}_1 + ir_1 \dot{\theta}_1 + \gamma_1 r_1 &= -i[v_1 r_2 r_3 \exp\{-i(\theta_1 - \theta_2 - \theta_3) \\ &\quad + v_1' v A_0 r_2 \exp\{-i(\theta_1 + \theta_2)\}\}], \\ \dot{r}_2 + ir_2 \dot{\theta}_2 + \gamma_2 r_2 &= -i[v_2 r_1 r_3 \exp\{i(\theta_1 - \theta_2 - \theta_3) \\ &\quad + v_2' v A_0 r_1 \exp\{-i(\theta_1 + \theta_2)\}\}], \end{aligned} \right\} \quad (2.12)$$

$$\dot{r}_3 + ir_3 \dot{\theta}_3 + \gamma_3 r_3 = -iv_3 r_1 r_2 \exp\{i(\theta_1 - \theta_2 - \theta_3)\}.)$$

Let us define the sets:

$$\Sigma_\theta = \{Y : \cos(\theta_1 - \theta_2 - \theta_3) = \cos(\theta_1 + \theta_2) = 0, \theta_3 = \theta,$$

$$r_j \neq 0, j = 1, 2, 3\},$$

$$\Sigma_r = \bigcup_{\theta} \Sigma_\theta$$

$$\Sigma_n = \{Y : r_i = 0, i = 1, 2 \text{ and/or } 3\},$$

$$\Sigma_0 = \{Y : r_1 = r_2 = 0\},$$

$$\hat{\Sigma}_0 = \{Y : r_i = \dot{r}_i = 0, i = 1, 2 \text{ or } 3\} - \Sigma_0,$$

$$\tilde{\Sigma}_0 = \Sigma_n - \{\Sigma_0 \cup \hat{\Sigma}_0\}.$$

Obviously, Σ_θ is not closed, and Σ_n and $\Sigma_n \cup \Sigma_\theta$ are closed. Furthermore, $\Sigma_n \cap \Sigma_\theta = \emptyset$. Hence, $\bar{\Sigma}_\theta - \Sigma_\theta$ is nonempty and $\bar{\Sigma}_\theta - \Sigma_\theta \subset \Sigma_n$. An example of $\bar{\Sigma}_\theta$ is shown in Figure 2.1. The set Σ_n is located at the origins.

We assume that $V(0, Y_0) = Y_0 \in \Sigma_{\theta_0}$. From (2.12), $\theta_j(t) = 0, j = 1, 2, 3$, if $V(t, Y_0) \in \Sigma_{\theta_0}$. Hence, $V^+(t_0) \in \Sigma_{\theta_0}$ or there exists a $t_1 > 0$ such that $V(t, Y_0) \in \Sigma_{\theta_0}$ for $t \in [0, t_1)$ and $V(t_1, Y_0) \in \bar{\Sigma}_{\theta_0} - \Sigma_{\theta_0} \subset \Sigma_n$. Since $\Sigma_n = \Sigma_0 \cup \hat{\Sigma}_0 \cup \tilde{\Sigma}_0$ and Σ_0 is an invariant set (i.e., if $Y_0 \in \Sigma_0, V(t, Y_0) \in \Sigma_0$ for $t \geq 0$), $V(t_1, Y_0) \in \hat{\Sigma}_0 \cup \tilde{\Sigma}_0$. Suppose that $V(t_1, Y_0) \in \tilde{\Sigma}_0$. Then, $V(t_1, Y)$ is located at one of the three origins in Figure 2.1. Since $\hat{F}(Y)$ is transverse to $\tilde{\Sigma}_0$ at $Y = V(t_1, Y_0)$ and $\hat{F}(Y)$ of (3') is differentiable, $V(t_1 + \epsilon, Y_0) \in \Sigma_{\theta_0}$ for arbitrarily small $\epsilon > 0$.

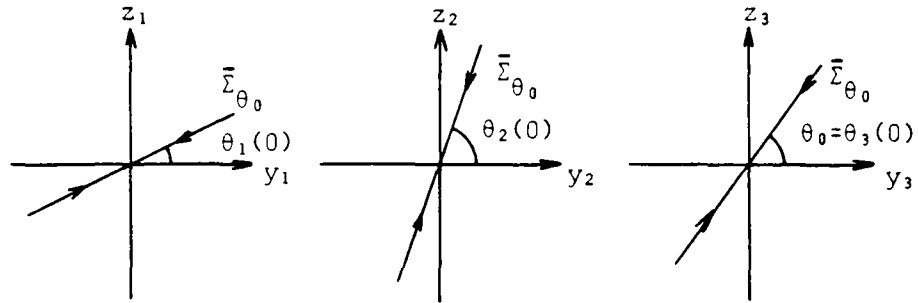


Figure 2.1 Phase-Locked Trajectory

Suppose that $V(t_1, Y_0) \in \hat{\Sigma}_0$. Then, $V(t_1, Y_0)$ is located at two of the three origins in Figure 2.1. For $\hat{F}(Y)$ of (3'), there is no $\tau > 0$ such that $V(t, Y_0) \in \hat{\Sigma}_0$ for $t \in [t_1, t_1 + \tau)$. Moreover, $\hat{F}(Y)$ of (3') is continuously differentiable. Hence, $V(t_1 + \epsilon, Y_0) \in \Sigma_{\theta_0}$ for arbitrary small $\epsilon > 0$. Thus, the set $\bar{\Sigma}_{\theta_0}$ is an invariant set, and the set Σ_{θ_0} is invariant in the sense that if $Y_0 \in \Sigma_{\theta_0}$, $V(t, Y_0) \in \Sigma_{\theta_0}$ for almost all t except when $r_i(t) = 0$, $i = 1, 2$ and/or 3 . Thus, $V^+(Y_0)$, $Y_0 \in \Sigma_{\theta_0}$, is contained in $\bar{\Sigma}_{\theta_0}$.

If $V(0, Y_0) \in (\tilde{\Sigma}_0 \cup \hat{\Sigma}_0) \cap \bar{\Sigma}_r$, by the above used arguments, $V(\epsilon, Y_0) \in \Sigma_{\theta_0}$ for arbitrarily small $\epsilon > 0$. Here,

$$\theta_0 = \lim_{t \rightarrow 0} \theta_3(t).$$

Such a limit θ_0 exists, since $\hat{F}(Y)$ of (3') is continuous.

Hence, $V^+(Y_0) \in \bar{\Sigma}_{\theta_0}$ if $Y_0 \in (\tilde{\Sigma}_0 \cup \hat{\Sigma}_0) \cap \bar{\Sigma}_r$. Thus, if we define a set Σ_{r0} :

$$\Sigma_{r0} = \Sigma_r \cup \{(\hat{\Sigma}_0 \cup \tilde{\Sigma}_0) \cap \bar{\Sigma}_r\},$$

$V^+(Y_0) \in \bar{\Sigma}_{\theta_0}$ for all $Y_0 \in \Sigma_{r0}$, where if $Y_0 \in \Sigma_r$, $\theta_0 = \theta_1(0)$ and if $Y_0 \in (\hat{\Sigma}_0 \cup \tilde{\Sigma}_0) \cap \bar{\Sigma}_r$, $\theta_0 = \lim_{t \rightarrow 0} \theta_3(t)$.

Now, we introduce a reduced equation of (3'). If $V(0, Y_0) \in \Sigma_{\theta_0}$,

$$\theta_i(t) = \theta_i(0) + \pi n_i(t), \quad i = 1, 2, 3, \quad (2.13)$$

where $\theta_3(0) = \theta_0$ and n_i is an integer-valued step function having discontinuities only when $r_i(t) = 0$. Let us define a vector $X \triangleq (x_1, x_2, x_3)^T$:

$$\left. \begin{aligned} x_1(t) &= v\sigma r_1(t) \exp\{in_1(t)\}, \\ x_2(t) &= vr_2(t) \exp\{in_2(t)\}, \\ x_3(t) &= v\sigma r_3(t) \exp\{in_3(t)\}, \end{aligned} \right\} \quad (2.14)$$

where $v = \sin(\theta_1(0) - \theta_2(0) - \theta_3(0))$ and $\sigma = \sin(\theta_1(0) + \theta_2(0))$. Then, x_i is real, and at the time t when $V(t, Y_0) \in \Sigma_{\theta_0}$, equation (2.12) reduces to

$$\left. \begin{aligned} \dot{x}_1 &= -\gamma_1 x_1 - v_1 x_2 x_3 - v_1' v A_0 x_2, \\ \dot{x}_2 &= -\gamma_2 x_2 + v_2 x_1 x_3 - v_2' v A_0 x_1, \\ \dot{x}_3 &= -\gamma_3 x_3 + v_3 x_1 x_2. \end{aligned} \right\} \quad (2.15)$$

This equation actually holds at the time t when $V(t, Y_0) \in \bar{\Sigma}_{\theta_0} - \Sigma_{\theta_0}$, since its trajectory stays in $\bar{\Sigma}_{\theta_0} - \Sigma_{\theta_0}$ momentarily.

If $Y_0 \in \bar{\Sigma}_r \cap (\hat{\Sigma}_0 \cup \tilde{\Sigma}_0)$, the solution of (2.15) is identical to that of (2.12). For, the trajectory of (2.15)

momentarily stays in the set in the X-space corresponding to $\bar{\Sigma}_r \cap (\hat{\Sigma}_0 \cup \tilde{\Sigma}_0)$. Furthermore, equation (2.15) has a solution $X(t) \equiv \theta_X$, the zero-vector in the X-space, or $X(t) = (0, 0, x_3(0)\exp(-\gamma_3 t))^T$ on the set in the X-space corresponding to Σ_0 , and they are identical to those of (2.12) on Σ_0 . Thus, equation (2.12) reduces to (2.15) for all $Y_0 \in \bar{\Sigma}_{r0} \cup \Sigma_0$. If $Y_0 \in \bar{\Sigma}_{r0} - \Sigma_0$, $\gamma^+(Y_0) \subset \bar{\Sigma}_{r0} - \Sigma_0$ and if $Y_0 \in \Sigma_0$, $\gamma^+(Y_0) \subset \Sigma_0$.

Similarly, each of the remaining systems in Table 2.2 reduces to a three-dimensional equation on a certain invariant set. These equations are given in Table 2.4 along with the definitions of variables and Σ_r . Systems (2)-(7) and their solution will be denoted by

$$\dot{X} = F(X), \quad (2.16)$$

and $X(t, X_0)$, respectively, where X_0 is an initial value. Moreover, we denote the positive semi-orbit by $X^+(X_0) \triangleq \{X : X = X(t, X_0), t \geq 0\}$.

For some reduced equations, $\|X(t)\| \rightarrow \infty$ or 0 as $t \rightarrow \infty$ for initial points in certain open subsets of the X-space. Let us consider (3) with $(v_1^1, v_2) = (1, 1)$, $(v_1, v_2, v_3) = (1, 1, 1)$ and $(\text{sgn}(\gamma_1), \text{sgn}(\gamma_2), \text{sgn}(\gamma_3)) = (1, 1, -1)$ as an example (see Table 2.3). It is not determined whether the original system (3') with such parameters has a diverging trajectory. On the other hand, from (3),

$$(d/dt)\{(x_3 - (3/2)vA_0)^2 - x_1^2 - 2x_2^2\}$$

Table 2.4 Reduced Systems $\dot{X} = F(X)$

	Variables	Σ_r	Reduced Equation
(2)	$x_j(t) = v r_j(t) \exp(in_j(t)\pi),$ $j = 1, 2, 3,$ $v = \sin(\theta_1(0) - \theta_2(0) - \theta_3(0))$	$\cos(\theta_1 - \theta_2 - \theta_3) = 0$	$\dot{x}_1 = -\gamma_1 x_1 - v_1 x_2 x_3,$ $\dot{x}_2 = -\gamma_2 x_2 + v_2 x_1 x_3,$ $\dot{x}_3 = -\gamma_3 x_3 + v_3 x_1 x_2$
(3)	$x_1(t) = v \sigma r_1(t) \exp(in_1(t)\pi),$ $x_2(t) = v r_2(t) \exp(in_2(t)\pi),$ $x_3(t) = v \sigma r_3(t) \exp(in_3(t)\pi),$ $v = \sin(\theta_1(0) - \theta_2(0) - \theta_3(0)),$ $\sigma = \sin(\theta_1(0) + \theta_2(0))$	$\cos(\theta_1 - \theta_2 - \theta_3) = 0,$ $\cos(\theta_1 + \theta_2) = 0$	$\dot{x}_1 = -\gamma_1 x_1 - v_1 x_2 x_3 - v_1' v A_0 x_2,$ $\dot{x}_2 = -\gamma_2 x_2 + v_2 x_1 x_3 - v_2' v A_0 x_1,$ $\dot{x}_3 = -\gamma_3 x_3 + v_3 x_1 x_2$
(4)	$x_1(t) = v \sigma r_1(t) \exp(in_1(t)\pi)$ $+ (v_1' / \gamma_1) v A_0^2,$ $x_2(t) = v \sigma r_2(t) \exp(in_2(t)\pi),$ $x_3(t) = v r_3(t) \exp(in_3(t)\pi),$ $v = \sin(\theta_1(0) - \theta_2(0) - \theta_3(0)),$ $\sigma = \sin \theta_1(0)$	$\cos(\theta_1 - \theta_2 - \theta_3) = 0,$ $\cos \theta_1 = 0$	$\dot{x}_1 = -\gamma_1 x_1 + v_1 x_2 x_3,$ $\dot{x}_2 = -\gamma_2 x_2 - v_2 x_1 x_3 + (v_1' v_2 / \gamma_1) v A_0^2 x_3,$ $\dot{x}_3 = -\gamma_3 x_3 - v_3 x_1 x_2 + (v_1' v_3 / \gamma_1) v A_0^2 x_2$

	Variables	Σ_r	Reduced Equation
(5)	$x_1(t) = vr_1(t)\exp(in_1(t)\pi),$ $x_2(t) = vr_2(t)\exp(in_2(t)\pi),$ $x_3(t) = vor_3(t)\exp(in_3(t)\pi),$ $v = \sin(\theta_1(0) - 2\theta_2(0)),$ $\sigma = \sin(\theta_1(0) - \theta_3(0))$	$\cos(\theta_1 - 2\theta_2) = 0,$ $\cos(\theta_1 - \theta_3) = 0$	$\dot{x}_1 = -\gamma_1 x_1 - v_1' x_2^2 - v_1 v A_0 x_3,$ $\dot{x}_2 = -\gamma_2 x_2 + x_1 x_2,$ $\dot{x}_3 = -\gamma_3 x_3 + v_3 v A_0 x_1$
(6)	$x_j(t) = vr_j(t)\exp(in_j(t)\pi),$ $j = 1, 2, 3,$ $v = \sin(\theta_1(0) - \theta_2(0) - \theta_3(0)),$ $\sigma = \sin(2\theta_1(0))$	$\cos(\theta_1 - \theta_2 - \theta_3) = 0,$ $\cos(2\theta_1) = 0$	$\dot{x}_1 = -(\gamma_1 + \sigma v A_0) x_1 - v_1 x_2 x_3,$ $\dot{x}_2 = -\gamma_2 x_2 + x_1 x_3,$ $\dot{x}_3 = -\gamma_3 x_3 + x_1 x_2$
(7)	$x_1(t) = vr_1(t)\exp(in_1(t)\pi),$ $x_2(t) = vr_2(t)\exp(in_2(t)\pi),$ $x_3(t) = vor_3(t)\exp(in_3(t)\pi),$ $v = \sin(\theta_1(0) - 2\theta_2(0)),$ $\sigma = \sin(\theta_1(0) - \theta_3(0))$	$\cos(\theta_1 - 2\theta_2) = 0,$ $\cos(\theta_1 - \theta_3) = 0$	$\dot{x}_1 = -\gamma_1 x_1 - v_1' x_2^2,$ $\dot{x}_2 = -\gamma_2 x_2 + x_1 x_2 + v_2 v A_0 x_3,$ $\dot{x}_3 = -\gamma_3 x_3 - v_3 v A_0 x_2$

$$= \gamma_1 x_1^2 + 2\gamma_2 x_2^2 + \gamma_3 (x_3 - (3/2)vA_0)^2 - (9/4)\gamma_3 |vA_0|^2.$$

Hence, if $(0, X_0)$ is inside the elliptic cone $C: x_1^2 + 2x_2^2 = (x_3 - (3/2)vA_0)^2$ and outside the ellipsoid $E: \gamma_1 x_1^2 + 2\gamma_2 x_2^2 + \gamma_3 (x_3 - (3/2)vA_0)^2 = (9/4)\gamma_3 |vA_0|^2$, $\|X(t)\| \rightarrow \infty$ as $t \rightarrow \infty$ where $X(t) = (t, X_0)$ (Fig. 2.2). Similarly, for some cases of (3) and (4) in Table 2.3, there exist open sets R_0 such that if $X_0 \in R_0$, $\|X(t)\| \rightarrow \infty$ as $t \rightarrow \infty$ where $X(t) = X(t, X_0)$. These systems will be discarded in Chapter 3, since they do not have periodic or chaotic solutions for almost all initial conditions. The remaining cases are shown in Table 2.5.

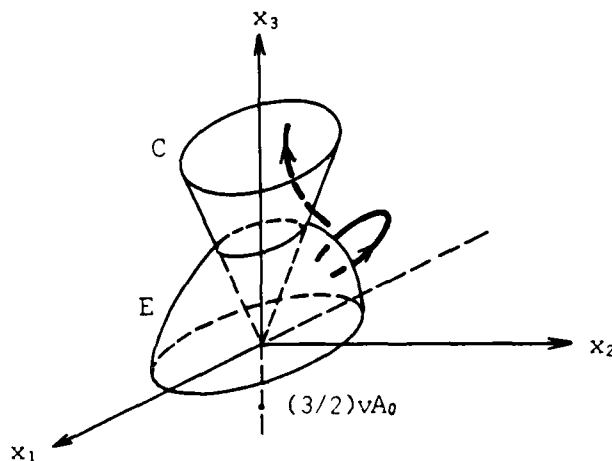


Figure 2.2 Diverging Trajectory of (3)

2.3 Phase Locking

In the previous section, we have shown that if the phases are locked at the initial time (i.e., $\psi(0, Y_0) \in \Sigma_{r_0}$),

Table 2.5 Parameters for Chaotic Solutions
of Systems (3) and (4)

(3)	(v_1', v_2')	(v_1, v_2, v_3)	$(\text{sgn}(\gamma_1), \text{sgn}(\gamma_2), \text{sgn}(\gamma_3))$
	(1,1)	(1,1,1)	(1,1,1), (-1,1,1)
		(1,-1,-1)	(1,1,1)
		(-1,1,-1)	(1,1,1), (1,1,-1)
		(-1,-1,1)	(1,-1,1)
	(1,-1)	(1,1,1)	(-1,1,1)
		(-1,1,-1)	(1,1,-1)
		(-1,-1,1)	(1,-1,1)
(4)	(v_1, v_2, v_3)		$(\text{sgn}(\gamma_1), \text{sgn}(\gamma_2), \text{sgn}(\gamma_3))$
	(1,1,1)		(1,1,1), (1,1,-1)
	(-1,-1,1)		(1,-1,1)
	(-1,1,-1)		(1,1,-1)
	(1,-1,-1)		(1,1,1)

they remain locked for almost all t (i.e., $Y(t, Y_0) \in \Sigma_{r0}$ for almost all $t \geq 0$ except when $Y(t, Y_0) \in \bar{\Sigma}_{r0} - \Sigma_{r0}$). Furthermore, on $\bar{\Sigma}_{r0} \cup \Sigma_0$, the original equation reduces to a three-dimensional one. It is meaningful to study the reduced equation, if it describes the asymptotic behavior of the original equation in the limit $t \rightarrow \infty$. Otherwise, the solutions of the reduced equation may not resemble those of the original one. In order to find whether the reduced equation represents the original one in the above sense, we shall obtain sufficient conditions for a subset Δ of $\bar{\Sigma}_{r0} \cup \Sigma_0$ to be an attractor in the Y -space. Here, we call Δ an attractor in the Y -space, if there is a neighborhood O of Δ in the Y -space such that if $Y_0 \in O$, then $Y^+(Y_0) \subset O$ and $Y(t) = Y(t, Y_0)$ converges to Δ as $t \rightarrow \infty$, that is,

$$\liminf_{t \rightarrow \infty} \|Y(t) - Y\| = 0. \quad (2.17)$$

If O is the whole Y -space, the phases become locked asymptotically as $t \rightarrow \infty$ for any initial conditions. Even when O is a small subset of the Y -space, it is theoretically easy to choose the initial conditions for phase locking, since the volume of O is nonzero. Hence, if a neighborhood O exists, it is meaningful to study the behavior of the reduced equation.

We again choose system (3') as an example. According to Pikovskii et al. [12], the set $\bar{\Sigma}_r$ is always an attractor if all of the γ_i 's, ν_i 's and ν_i' 's are positive. It can be

readily shown that their analysis is inaccurate (see Appendix). Here, we shall give a more detailed analysis for the general cases of (3'). Similar arguments hold for other systems also.

2.3.1 Differential Equations of Phase Differences $\dot{\underline{\xi}} = \Phi \underline{\xi}$

Equation (2.12) suggests studying the time variation of the quantities $A_1 A_2^* A_3^*$ and $A_1 A_2$, since they include the phase differences $\theta_1 - \theta_2 - \theta_3$ and $\theta_1 + \theta_2$ which are of important here. Taking the time derivative of $A_1 A_2^* A_3^*$, $A_1 A_2$, $A_2^2 A_3$ and $A_1^2 A_3^*$, we have

$$\begin{bmatrix} \dot{\xi}_1 \\ \dot{\xi}_2 \\ \dot{\xi}_3 \\ \dot{\xi}_4 \end{bmatrix} = \begin{bmatrix} -(\gamma_1 + \gamma_2 + \gamma_3) & 0 & -v_1' v A_0 & -v_2' v A_0 \\ 0 & -(\gamma_1 + \gamma_2) & v_1 & v_2 \\ -2v_2' v A_0 & -(2v_2 |A_3|^2 + v_3 |A_2|^2) & -(2\gamma_2 + \gamma_3) & 0 \\ -2v_1' v A_0 & -(2v_1 |A_3|^2 - v_3 |A_1|^2) & 0 & -(2\gamma_1 + \gamma_3) \end{bmatrix} \begin{bmatrix} \xi_1 \\ \xi_2 \\ \xi_3 \\ \xi_4 \end{bmatrix} \quad (2.18)$$

or

$$\dot{\underline{\xi}}(t) = \Phi(|A_2(t)|^2, |A_3(t)|^2) \underline{\xi}(t), \quad (2.19)$$

where $\xi_1 = \text{Re}(A_1 A_2^* A_3^*)$, $\xi_2 = \text{Re}(A_1 A_2)$, $\xi_3 = \text{Im}(A_2^2 A_3)$ and $\xi_4 = \text{Im}(A_1^2 A_3^*)$. The system of equations (2.18) is not closed, but it can be regarded as a closed time-varying linear differential equation:

$$\dot{\underline{\xi}}(t) = \hat{\Phi}(t) \underline{\xi}(t). \quad (2.20)$$

Let us consider the set

$$\Sigma \triangleq \{Y : \underline{\xi} = \theta_{\xi}\}. \quad (2.21)$$

where θ_{ξ} is the zero vector in the $\underline{\xi}$ -space. From (2.18), Σ is an invariant set. As shown later, if $\underline{\xi}(t) \rightarrow \theta_{\xi}$ as $t \rightarrow \infty$, the corresponding $Y(t)$ converges to Σ as $t \rightarrow \infty$. Since $\Sigma - (\bar{\Sigma}_r \cup \Sigma_0)$ is not an invariant set, $Y(t)$ does not converge to $\Sigma - (\bar{\Sigma}_r \cup \Sigma_0)$ as $t \rightarrow \infty$. Hence, $Y(t)$ converges to $\bar{\Sigma}_r$ and/or to Σ_0 as $t \rightarrow \infty$. As mentioned in Section 2.2, system (3') reduces to (3) on $\bar{\Sigma}_{r0} \cup \Sigma_0$ and therefore, on $\bar{\Sigma}_r \cup \Sigma_0$. Hence, if $\underline{\xi}(t) \rightarrow \theta_{\xi}$ as $t \rightarrow \infty$, then system (3) describes the asymptotic behavior of (3').

Similarly, an equation in the form (2.19) is obtained for each system of (2'), (4') - (7'). Moreover, if $\underline{\xi}(t) \rightarrow \theta_{\xi}$ as $t \rightarrow \infty$, each of reduced systems (2), (4) - (7) describes the asymptotic behavior of its original system. The definitions for vector $\underline{\xi}$ and matrix Φ for each system are given in Table 2.6. Here, Φ of (2) is a constant real number, and for other systems, Φ is a time-varying matrix.

2.3.2 Sufficient Conditions for Convergence of $\underline{\xi}(t)$ to θ_{ξ}

For equation (2'), we see that $\xi(t) \rightarrow 0$ as $t \rightarrow \infty$ if and only if $\gamma_1 + \gamma_2 + \gamma_3 > 0$, and $|\xi(t)| \rightarrow \infty$ as $t \rightarrow \infty$ if and only if $\gamma_1 + \gamma_2 + \gamma_3 < 0$. For the remaining cases, the following result in [26] is applicable:

(S.2.1) Consider a time-varying linear system expressed by (2.20) and define

Table 2.6 Differential Equations of Phase Differences $\dot{\xi} = \phi \xi$

	ξ	ϕ
(2)	$\xi = \text{Re}(A_1 A_2^* A_3^*)$	$-(\gamma_1 + \gamma_2 + \gamma_3)$
(3)	$\xi_1 = \text{Re}(A_1 A_2^* A_3^*),$ $\xi_2 = \text{Re}(A_1 A_2),$ $\xi_3 = \text{Im}(A_2^2 A_3),$ $\xi_4 = \text{Im}(A_1^2 A_3^*)$	$\begin{bmatrix} -(\gamma_1 + \gamma_2 + \gamma_3) & 0 & -v_1' v A_0 & -v_2' v A_0 \\ 0 & -(\gamma_1 + \gamma_2) & v_1 & v_2 \\ -2v_2' v A_0 & -(2v_2 A_3 ^2 + v_3 A_2 ^2) & -(2\gamma_2 + \gamma_3) & 0 \\ -2v_1' v A_0 & -(2v_1 A_3 ^2 - v_3 A_1 ^2) & 0 & -(2\gamma_1 + \gamma_3) \end{bmatrix}$
(4)	$\xi_1 = \text{Re}(A_1 A_2^* A_3^*),$ $\xi_2 = \text{Im}(A_2 A_3),$ $\xi_3 = \text{Re}(A_1)$	$\begin{bmatrix} -(\gamma_1 + \gamma_2 + \gamma_3) & -v_1' v A_0^2 & 0 \\ 0 & -(\gamma_2 + \gamma_3) & -(v_2 A_3 ^2 + v_3 A_2 ^2) \\ 0 & v_1 & -\gamma_1 \end{bmatrix}$
(5)	$\xi_1 = \text{Re}(A_1 A_3^*),$ $\xi_2 = \text{Re}(A_1 A_2^2),$ $\xi_3 = \text{Im}(A_2^2 A_3)$	$\begin{bmatrix} -(\gamma_1 + \gamma_3) & 0 & -v_1' \\ 0 & -(\gamma_1 + 2\gamma_2) & v_1 v A_0 \\ 2 A_2 ^2 & -v_3 v A_0 & -(2\gamma_2 + \gamma_3) \end{bmatrix}$

	ξ	ϕ
(6)	$\xi_1 = \text{Re}(A_1^2),$ $\xi_2 = \text{Re}(A_1 A_2^* A_3^*),$ $\xi_3 = \text{Re}(A_2^2 A_3^2),$ $\xi_4 = \text{Im}(A_1 A_2 A_3)$	$\begin{bmatrix} -2\gamma_1 & 0 & 0 & 2\nu_1 \\ 0 & -(\gamma_1 + \gamma_2 + \gamma_3) & 0 & -\nu A_0 \\ 0 & 0 & -2(\gamma_2 + \gamma_3) & 2(\nu_2 A_3 ^2 + \nu_3 A_2 ^2) \\ -(\nu_2 A_3 ^2 + \nu_3 A_2 ^2) & -\nu A_0 & -\nu_1 & -(\gamma_1 + \gamma_2 + \gamma_3) \end{bmatrix}$
(7)	$\xi_1 = \text{Re}(A_1 A_2^*),$ $\xi_2 = \text{Re}(A_1 A_3^*),$ $\xi_3 = \text{Im}(A_1 A_2^* A_3^*),$ $\xi_4 = \text{Re}(A_1 A_3^2),$ $\xi_5 = \text{Im}(A_1^2 A_3^2)$	$\begin{bmatrix} -(\gamma_1 + 2\gamma_2) & 0 & -2\nu_2 \nu A_0 & 0 & 0 \\ 0 & -(\gamma_2 + \gamma_3) & 1 & 0 & 0 \\ \nu_3 \nu A_0 & (A_1 ^2 - \nu_1^2 A_2 ^2) & -(\gamma_1 + \gamma_2 + \gamma_3) & \nu_2 \nu A_0 & 0 \\ 0 & 0 & -2\nu_3 \nu A_0 & -(\gamma_1 + \gamma_2) & \nu_1^2 \\ 0 & 2\nu A_0 (\nu_3 A_2 ^2 - \nu_2 A_3 ^2) & 0 & -2 A_2 ^2 & -2(\gamma_2 + \gamma_3) \end{bmatrix}$

$$\|\xi\|_{\infty} = \max_i |\xi_i|, \quad \mu_{\infty}[\hat{\phi}] = \max_i \{\hat{\phi}_{ii} + \sum_j |\hat{\phi}_{ij}|\},$$

where $\hat{\phi} = (\hat{\phi}_{ij})$. Then,

$$\begin{aligned} \|\underline{\xi}(0)\|_{\infty} \exp\left\{\int_0^t -\mu_{\infty}[-\hat{\phi}(\tau)] d\tau\right\} &< \|\underline{\xi}(t)\|_{\infty} \\ &< \|\underline{\xi}(0)\|_{\infty} \exp\left\{\int_0^t \mu_{\infty}[\hat{\phi}(\tau)] d\tau\right\}, \quad t \geq 0. \end{aligned}$$

The above statement implies that if $\mu_{\infty}[\hat{\phi}(t)] < 0$ for all $t > 0$, then $\|\underline{\xi}(t)\|_{\infty} \rightarrow 0$ as $t \rightarrow \infty$. We derive a modified system

$$\dot{\underline{\xi}}'(t) = \hat{\phi}'(t) \underline{\xi}'(t) \quad (2.22)$$

from (2.20), where $\underline{\xi}' = (p_1' \xi_1, p_2' \xi_2, p_3' \xi_3, p_4' \xi_4)^T$, $p_j' > 0$, $j = 1, 2, 3, 4$. By applying (S.2.1) to (2.22) and since $\|\underline{\xi}'(t)\|_{\infty} \rightarrow 0$ implies $\|\underline{\xi}(t)\|_{\infty} \rightarrow 0$, $\|\underline{\xi}(t)\|_{\infty} \rightarrow 0$ as $t \rightarrow \infty$ if $\mu_{\infty}[\hat{\phi}'(t)] < 0$ for all $t \geq 0$. We consider system (3') as an example. For this case, $\mu_{\infty}[\hat{\phi}'] < 0$ if and only if

$$\left. \begin{aligned} 2v_2|A_3|^2 + v_3|A_2|^2 &< (\gamma_1 + \gamma_2)\{p_3(2\gamma_2 + \gamma_3) - 2|vA_0|\}/(p_3 + p_4), \\ |2v_1|A_3|^2 - v_3|A_1|^2| &< (\gamma_1 + \gamma_2)\{p_4(2\gamma_1 + \gamma_3) - 2|vA_0|\}/(p_3 + p_4), \\ |vA_0| &< (\gamma_1 + \gamma_2 + \gamma_3)/(p_3 + p_4), \end{aligned} \right\} \quad (2.23)$$

where $(1, (\gamma_1 + \gamma_2)/(p_3 + p_4), 1/p_3, 1/p_4) = (p_1', p_2', p_3', p_4')$. Here, we can choose p_i 's to obtain the most convenient forms of the right hand sides of (2.23) for the later uses. Similar conditions for other systems are given in Table 2.7.

2.3.3 Sufficient Conditions for Convergence of $Y(t)$ to Σ

Table 2.7 Sufficient Conditions for Convergence
of $\xi(t)$ to θ_ξ

(2)	$\gamma_1 + \gamma_2 + \gamma_3 > 0$
(3)	$ 2v_2 A_3 ^2 + v_3 A_2 ^2 < (\gamma_1 + \gamma_2)\{(2\gamma_2 + \gamma_3)p_3 - 2 vA_0 \}/(p_3 + p_4),$ $ 2v_1 A_3 ^2 - v_3 A_1 ^2 < (\gamma_1 + \gamma_2)\{(2\gamma_1 + \gamma_3)p_4 - 2 vA_0 \}/(p_3 + p_4),$ $ vA_0 < (\gamma_1 + \gamma_2 + \gamma_3)/(p_3 + p_4),$ $(p'_1, p'_2, p'_3, p'_4) = (1, (\gamma_1 + \gamma_2)/(p_3 + p_4), 1/p_3, 1/p_4)$
(4)	$ v_2 A_3 ^2 + v_3 A_2 ^2 < \gamma_1(\gamma_2 + \gamma_3),$ $ vA_0 < p_2(\gamma_1 + \gamma_2 + \gamma_3),$ $(p'_1, p'_2, p'_3) = (1, p_2 A_0 , p_3\gamma_1 A_0)$
(5)	$ A_2 ^2 < p_3(\gamma_1 + \gamma_3)\{(2\gamma_2 + \gamma_3)/p_3 - vA_0 \}/2,$ $ vA_0 < p_3(\gamma_1 + 2\gamma_2),$ $(p'_1, p'_2, p'_3) = (p_3(\gamma_1 + \gamma_2), 1, p_3)$
(6)	$ v_2 A_3 ^2 + v_3 A_2 ^2 < \min\{p_4(\gamma_2 + \gamma_3)(\gamma_1 + \gamma_2 + \gamma_3),$ $\gamma_1\{(\gamma_1 + \gamma_2 + \gamma_3)(1 - p_4) - (p_4/p_2) vA_0 \}\},$ $ vA_0 < \min\{(p_4/p_2)(\gamma_1 + \gamma_2 + \gamma_3), (p_2/p_4)(1 - p_4)(\gamma_1 + \gamma_2 + \gamma_3)\},$ $(p'_1, p'_2, p'_3, p'_4) = (p_4\gamma_1(\gamma_1 + \gamma_2 + \gamma_3), p_2(\gamma_1 + \gamma_2 + \gamma_3), 1, p_4(\gamma_1 + \gamma_2 + \gamma_3))$
(7)	$ A_1 ^2 - v'_1 A_2 ^2 < (\gamma_2 + \gamma_3)\{(\gamma_1 + \gamma_2 + \gamma_3) - (p_1p_3p_4/(p_1 + p_4)) vA_0 \},$ $ v_3 A_2 ^2 - v_2 A_3 ^2 + (p_2/p_4) A_2 ^2 < vA_0 (\gamma_2 + \gamma_3)/2,$ $ vA_0 < \min\{(p_3/2p_1)(\gamma_1 + 2\gamma_2), (p_3/(p_4(p_2 + p_3)))(\gamma_1 + \gamma_3),$ $(p_1p_4/(p_3(p_1 + p_4)))(\gamma_1 + \gamma_2 + \gamma_3)\},$ $(p'_1, p'_2, p'_3, p'_4, p'_5) = (p_1 vA_0 , p_2 vA_0 ^2, p_3 vA_0 , p_4 vA_0 , 1)$

In this section, we shall show that if $\underline{\xi}(t) \rightarrow \theta_{\underline{\xi}}$ as $t \rightarrow \infty$, then the corresponding $Y(t)$ converges to Σ as $t \rightarrow \infty$. It is sufficient to prove the following statement:

(S.2.2) For any small $\varepsilon > 0$, there is a $\delta > 0$ such that

$$\|\underline{\xi}\| < \delta \Rightarrow \inf_{Y' \in \Sigma} \|Y - Y'\| < \varepsilon \text{ for all } Y \in \{Y : \|\underline{\xi}\| < \delta\}$$

or

$$\tilde{d}(\Sigma, \Sigma_{\delta}) \triangleq \sup_{Y \in \Sigma_{\delta}} \inf_{Y' \in \Sigma} \|Y - Y'\| \rightarrow 0 \text{ as } \delta \rightarrow 0,$$

where $\Sigma_{\delta} = \{Y : \|\underline{\xi}\| = \delta\}$.

The above statement implies that if $\underline{\xi}$ is close to $\theta_{\underline{\xi}}$, the corresponding set Σ_{δ} is also close to Σ in the Y -space.

Here, we give a proof of (S.2.2) only for (2'). The proof for other cases can be established in a similar way. For (2'),

$$\Sigma_{\delta} = \{Y : \xi = y_1 y_2 y_3 + z_1 z_2 y_3 + z_1 y_2 z_3 + y_1 z_2 z_3 = \delta\}.$$

Consider a line parallel to $(1, 0, 0, 0, 0, 0)^T$ and through a point $(0, \hat{z}_1, \hat{y}_2, \hat{z}_2, \hat{y}_3, \hat{z}_3)^T$. This line intersects Σ_{δ} and Σ if $\hat{y}_2 \hat{y}_3 + \hat{z}_2 \hat{z}_3 \neq 0$, since the equations:

$$\left. \begin{aligned} y_1' \hat{y}_2 \hat{y}_3 + \hat{z}_1 \hat{z}_2 \hat{y}_3 + \hat{z}_1 \hat{y}_2 \hat{z}_3 + y_1' \hat{z}_2 \hat{z}_3 &= \delta, \\ y_1 \hat{y}_2 \hat{y}_3 + \hat{z}_1 \hat{z}_2 \hat{y}_3 + \hat{z}_1 \hat{y}_2 \hat{z}_3 + y_1 \hat{z}_2 \hat{z}_3 &= 0, \end{aligned} \right\} \quad (2.24)$$

has a unique solution (y_1, y_1') if $\hat{y}_2 \hat{y}_3 + \hat{z}_2 \hat{z}_3 \neq 0$. From (2.24),

$$(y_1' - y_1)(\hat{y}_2 \hat{y}_3 + \hat{z}_2 \hat{z}_3) = \delta.$$

Hence,

$$\tilde{d}(\Sigma \cap S_1, \Sigma_\delta \cap S_1) < \delta^{\frac{1}{2}}, \quad S_1 \triangleq \{Y : |y_2 y_3 + z_2 z_3| > \delta^{\frac{1}{2}}\},$$

Likewise, by using a line parallel to $(0, 1, 0, 0, 0, 0)^T$ and through a point $(\hat{y}_1, 0, \hat{y}_2, \hat{z}_2, \hat{y}_3, \hat{z}_3)^T$, we have

$$\tilde{d}(\Sigma \cap S_2, \Sigma_\delta \cap S_2) < \delta^{\frac{1}{2}}, \quad S_2 \triangleq \{Y : |z_2 y_3 + y_3 z_2| > \delta^{\frac{1}{2}}\}.$$

Hence,

$$\tilde{d}(\Sigma \cap (S_1 \cup S_2), \Sigma_\delta \cap (S_1 \cup S_2)) < \delta^{\frac{1}{2}}.$$

Consider the sets:

$$\Gamma_0 \triangleq \{Y : y_2 y_3 + z_2 z_3 = 0, \quad z_2 y_3 + y_2 z_3 = 0\},$$

$$\Gamma_2 \triangleq \{Y : |y_2 y_3 + z_2 z_3| = \delta^{\frac{1}{2}}, \quad |z_2 y_3 + y_2 z_3| = \delta^{\frac{1}{2}}\}.$$

A line parallel to $(0, 0, 1, 0, 0, 0)^T$ and through a point $(\hat{y}_1, \hat{z}_1, 0, \hat{z}_2, \hat{y}_3, \hat{z}_3)^T$ intersects Γ_0 and Γ_2 if $\hat{y}_3 \neq 0$, since the equation:

$$y_2 \hat{y}_3 \pm \hat{z}_2 \hat{y}_3 = 0, \quad y_2' \hat{y}_3 \pm \hat{z}_2 \hat{y}_3 = \pm \delta^{\frac{1}{2}}, \quad (2.25)$$

has a unique solution for (y_2, y_2') . From (2.25),

$$(y_2 - y_2') \hat{y}_3 = \pm \delta^{\frac{1}{2}}.$$

Hence,

$$\tilde{d}(\Gamma_0 \cap \Gamma_4, \Sigma_\delta \cap \Gamma_4) < \delta^{\frac{1}{4}}, \quad \Gamma_4 \triangleq \{Y : |y_3| > \delta^{\frac{1}{4}}\}.$$

Since $\Gamma_0 \subset \Sigma$, we have

$$\tilde{d}(\Sigma \cap \Gamma_4, \Sigma_\delta \cap \Gamma_4) < \max\{\delta^{\frac{1}{2}}, \delta^{\frac{1}{4}}\}. \quad (2.26)$$

By repeating the above procedure for different lines, we obtain results similar to (2.26) for $\Gamma_{4i} \triangleq \{Y : |y_i| > \delta^{\frac{1}{2}}\}$ and $\Delta_{4i} \triangleq \{Y : |z_i| > \delta^{\frac{1}{2}}\}$, $i = 1, 2, 3$. To sum up,

$$\tilde{d}(\Sigma \cap (\cup_i (\Gamma_{4i} \cup \Delta_{4i})), \Sigma_\delta \cap (\cup_i (\Gamma_{4i} \cup \Delta_{4i}))) < \max\{\delta^{\frac{1}{2}}, \delta^{\frac{1}{2}}\}.$$

Since $\theta_Y \in \Sigma$, where θ_Y is the zero-vector in the Y -space,

$$\tilde{d}(\Sigma - (\cup_i (\Gamma_{4i} \cup \Delta_{4i})), \Sigma_\delta - (\cup_i (\Gamma_{4i} \cup \Delta_{4i}))) < 6^{\frac{1}{2}} \varepsilon^{\frac{1}{2}}.$$

Hence,

$$\tilde{d}(\Sigma, \Sigma_\delta) < \max\{6^{\frac{1}{2}} \delta^{\frac{1}{2}}, \delta^{\frac{1}{2}}\}.$$

If we choose a δ such that $\max\{6^{\frac{1}{2}} \delta^{\frac{1}{2}}, \delta^{\frac{1}{2}}\} < \varepsilon$, then we have the desired result. Thus, (S.2.2) is proved for (2').

As mentioned earlier for (2'), $\xi(t) \rightarrow 0$ as $t \rightarrow \infty$ for any initial conditions, if $\gamma_1 + \gamma_2 + \gamma_3 > 0$. Hence, by (S.2.2), if $\gamma_1 + \gamma_2 + \gamma_3 > 0$, $Y(t)$ converges to Σ as $t \rightarrow \infty$. For other systems, $Y(t)$ converges to Σ if the wave intensities satisfy the conditions in Table 2.7. We do not know whether the original systems (3') - (7') satisfy these conditions, that is, whether the systems have attractors satisfying these conditions. On the other hand, it is easy to find natural boundaries for some of the reduced equations. If $(v_1, v_2, v_3) = (1, 1, 1)$, $(v'_1, v'_2) = (1, 1)$ and $\gamma_i > 0$, $i = 1, 2, 3$ in (3), then

$$\dot{I} \leq -dI + 9\gamma_3 |vA_0|^2, \quad (2.27)$$

where $I = 2x_1^2 + x_2^2 + (x_3 + 3vA_0)^2$, $d = \min\{2\gamma_1, 2\gamma_2, \gamma_3\}$, and if

$$(v_1, v_2, v_3) = (-1, 1, -1),$$

$$\dot{I} \leq -dI + \gamma_3 |vA_0|^2, \quad (2.28)$$

where $I = x_1^2 + x_2^2 + 2(x_3 + vA_0)^2$, $d = \min\{\gamma_1, \gamma_2, 2\gamma_3\}$. If $(v_1, v_2, v_3) = (1, 1, 1)$ and $\gamma_i > 0$, $i = 1, 2, 3$, in (4), then

$$\dot{I} \leq -dI + |vA_0|^2 / \gamma_1, \quad (2.29)$$

where $I = 2(x_1 - (v_1/\gamma_1)vA_0)^2 + x_2^2 + x_3^2$, $d = \min\{2\gamma_1, \gamma_2, \gamma_3\}$.

Hence, the ellipsoid on which $\dot{I} = 0$ is a natural boundary.

There are no such boundaries for other cases. But, as shown later in the numerical experiments, some pseudo-chaotic solutions of the reduced systems are bounded in certain regions. Therefore, we assume that the reduced systems have attractors in which the trajectories are finally trapped.

Then, a sufficient condition for $Y(t)$ to converge to Σ as $t \rightarrow \infty$ is as follows:

(S.2.3) Assume that a subset Δ of Σ is an attractor of equation (2.10) with the initial condition $Y_0 \in \Sigma$. Also assume that Δ has a smooth boundary $\partial\Delta$ relative to Σ and that at any point $Y_b \in \partial\Delta$, $\hat{F}(Y_b)$ is transverse to $\partial\Delta$. Let Γ be a set in the Y -space such that if $Y(t) \in \Gamma$ for all $t \geq 0$, then $\xi(t) \rightarrow \theta_\xi$ as $t \rightarrow \infty$. Then, if $\Delta \subset \Gamma$, there is a neighborhood O of Δ in the Y -space such that if $Y_0 \in O$, $v^+(Y_0) < 0$ and $Y(t) = v(t, Y_0)$ converges to Σ as $t \rightarrow \infty$.

The sets defined in (S.2.3) are sketched in Figure 2.3.

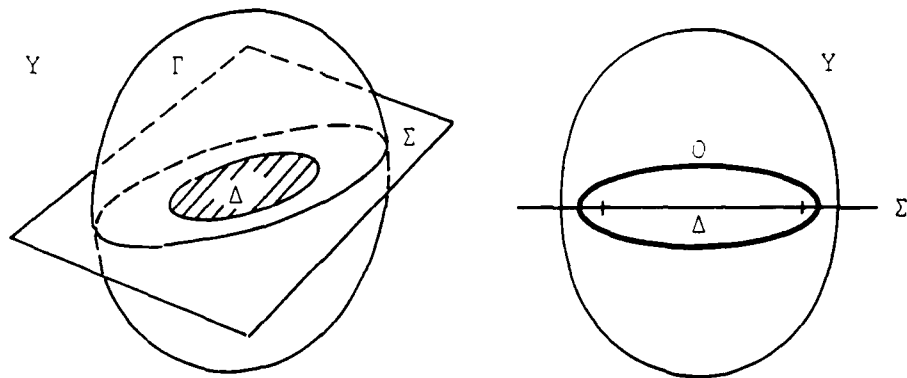


Figure 2.3 Sketches of Sets in (S.2.3)

The validity of statement (S.2.3) can be established as follows. Let Σ and Δ be n -dimensional surfaces. Then, $\partial\Delta$ is a $(n-1)$ -dimensional smooth surface by assumption. Let us consider a set $G_{Y_b} \times \{Y_b\}$ where $Y_b \in \partial\Delta$, and G_{Y_b} is an orthogonal complement of a subspace which is a translated tangent plane of Σ at Y_b to the origin. Then, $G_{Y_b} \times \{Y_b\}$ is $(6-n)$ -dimensional. Since $\partial\Delta$ is smooth, there is a neighborhood $N(\partial\Delta)$ of $\partial\Delta$ such that the set

$$\hat{N}_1(\partial\Delta) \triangleq N(\partial\Delta) \cup \bigcup_{Y_b \in \partial\Delta} G_{Y_b} \times \{Y_b\}$$

is smooth (5-dimensional) and

$$\hat{N}_1(\partial\Delta) \subset \Gamma.$$

Since \hat{F} is C^∞ , there is a neighborhood $\hat{N}_2(\partial\Delta)$ of $\partial\Delta$ relative to $\hat{N}_1(\partial\Delta)$ such that $\hat{F}(Y)$ is transverse to $\hat{N}_2(\partial\Delta)$ at all $Y \in \hat{N}_2(\partial\Delta)$. Let us take a neighborhood $N_\epsilon(\Sigma)$ of Σ with radius ϵ (i.e., $\tilde{d}(\partial N_\epsilon(\Sigma), \Sigma) = \epsilon$) such that

$$(N_\epsilon(\Sigma) \cap \hat{N}_1(\partial\Delta)) \subset \hat{N}_2(\partial\Delta).$$

By (S.2.1), there is a δ_i such that

$$\tilde{d}(\{Y : \xi_i(Y) = 0\}, \{Y : \xi_i(Y) = \delta\}) < \epsilon.$$

Hence, for $\delta < \min_i \{\delta_i\}$,

$$\tilde{N}_\delta(\Sigma) \triangleq \{Y : \|\underline{\xi}(Y)\|_\infty < \delta\} \subset N_\epsilon(\Sigma).$$

Here, $\tilde{N}_\delta(\Sigma)$ is a neighborhood of Σ and

$$(\tilde{N}_\delta(\Sigma) \cap \tilde{N}_1(\partial\Delta)) \subset \hat{N}_2(\partial\Delta).$$

Hence, $V(t, Y_0)$ remains in Γ as long as $V(t, Y_0) \in \tilde{N}_\delta(\Sigma)$. On the other hand, $V(t, Y_0)$ remains in $\tilde{N}_\delta(\Sigma)$ as long as $V(t, Y_0) \in \Gamma$, since $\|\underline{\xi}(t)\|_\infty$ decreases if $Y(t) \in \Gamma$. Consider an open set O containing Δ such that ∂O consists of $\tilde{N}_\delta(\Sigma) \cap \hat{N}_1(\partial\Delta)$ and a part of $\partial\tilde{N}_\delta(\Sigma)$. Then, $O \subset \Gamma$ and if $Y_0 \in O$, then $V^+(Y_0) \subset O$, which is the desired result.

CHAPTER 3

REDUCED EQUATIONS

In this chapter, we shall choose systems from Table 2.4 which may have periodic or chaotic solutions for almost all initial conditions in the X -space. At the present time, sufficient conditions for ensuring the existence of chaotic solution are not known for general three-dimensional ordinary differential equations. Many numerical experiments showed that the existence of more than one unstable equilibrium points could lead to pseudo-chaotic solutions. Here, we shall restrict our attention to those systems whose reduced equations may have periodic or chaotic solutions globally (i.e., for almost all initial conditions) in the X -space. Hence, if we can show that a system has a stable equilibrium point or an open set R_0 such that if $X_0 \in R_0$, $\|X(t)\| \rightarrow \infty$ as $t \rightarrow \infty$, where $X(t) = X(t, X_0)$, then the system is discarded.

In Table 2.4, v_i and v_i' can be ± 1 . The presence of both positive and negative v_i (or v_i') corresponds to the interaction of positive and negative-energy waves. It is known that such a system is explosively unstable, that is, one or more of the wave amplitudes tend to infinity in finite time. The addition of linear damping terms does not suppress such a fast growth. Therefore, we only retain those cases in which all the v_i 's (and v_i' 's) have the same sign. Without loss of generality, we assume that all the v_i 's (and v_i' 's)

are positive, since the sign of each v_i (and v_i') can be altered by changing the signs of the variables.

The procedure for eliminating some of the remaining cases is as follows: (i) We assume that all the γ_i 's are positive; (ii) If there are more than one equilibrium points and all of them are unstable for certain value of parameters, then the case is retained; (iii) If there is only one equilibrium point, or if at least one of the equilibrium points is stable for any values of parameters, we introduce a small linear growth term to the system by changing one of the signs of γ_j 's so that

$$\gamma_1 + \gamma_2 + \gamma_3 > 0; \quad (3.1)$$

(iv) If the condition in (ii) holds for the system having one linear growth term, the system is retained, and if the condition in (iii) holds, the system is discarded. We do not introduce more than one negative γ_j 's, since it is equivalent to an equation with less than two negative γ_j 's by the substitution $t \rightarrow -t$ and by certain variable changes; (v) If there exists an open set R_0 such that $\|X(t)\| \rightarrow \infty$ as $t \rightarrow \infty$ for all $X_0 \in R_0$, where $X(t) = X(t, X_0)$, then the case is discarded.

The reduced systems discarded by the foregoing procedure may have local chaotic solutions. The original systems corresponding to the discarded reduced systems may also have chaotic solutions. Moreover, the remaining systems

may not have chaotic solutions. For the class of three-dimensional ordinary differential equations such that the existence of only one equilibrium point implies the nonexistence of chaotic solutions, we can conclude that if a three-wave interaction system has global periodic or chaotic solutions in the X-space, then it belongs to one of the remaining cases.

3.1 Analysis of Reduced Equations

3.1.1 System (3)

System (3) with positive γ_i 's has been studied by Pikovskii et al. [12]. Here, we present their results along with more detailed analysis. Without loss of generality, we can assume that $vA_0 < 0$, since the substitution $vA_0 \rightarrow -vA_0$ is equivalent to $x_i \rightarrow -x_i$, $i = 1, 3$. Then, the equilibrium points are $P_0 = \{\theta_X\}$ and $P_v = \{X_v\}$, $v = \pm 1$:

$$X_v = (v[(\gamma_3/\gamma_1)(|vA_0|^2 - \gamma_1\gamma_2)^{\frac{1}{2}}\{|vA_0| - (|vA_0|^2 - \gamma_1\gamma_2)^{\frac{1}{2}}\}]^{\frac{1}{2}}, \\ v[\gamma_1\gamma_3(|vA_0|^2 - \gamma_1\gamma_2)^{\frac{1}{2}}/\{|vA_0| - (|vA_0|^2 - \gamma_1\gamma_2)^{\frac{1}{2}}\}]^{\frac{1}{2}}, (|vA_0|^2 - \gamma_1\gamma_2)^{\frac{1}{2}})^T, \quad (3.2)$$

if they exist. At P_0 and P_v , the characteristic equations of dF/dX for (3) are

$$P_0(\lambda) \triangleq (\lambda + \gamma_3)\{\lambda^2 + (\gamma_1 + \gamma_2)\lambda + \gamma_1\gamma_2 - |vA_0|^2\} = 0, \quad (3.3a)$$

$$P_v(\lambda) \triangleq \lambda^3 + (\gamma_1 + \gamma_2 + \gamma_3)\lambda^2 + \lambda[\gamma_2\gamma_3 + \gamma_3\gamma_1|vA_0|/\{|vA_0| - (|vA_0|^2 - \gamma_1\gamma_2)^{\frac{1}{2}}\} \\ - (\gamma_3/\gamma_1)(|vA_0|^2 - \gamma_1\gamma_2)^{\frac{1}{2}}\{|vA_0| - (|vA_0|^2 - \gamma_1\gamma_2)^{\frac{1}{2}}\}]]$$

$$+4\gamma_3(|vA_0|^2 - \gamma_1\gamma_2) = 0, \quad (3.3b)$$

respectively. When $|vA_0|^2 < \gamma_1\gamma_2 \triangleq |\tilde{v}\tilde{A}_0|^2$, P_0 is asymptotically stable and P_v does not exist. At $|vA_0|^2 = |\tilde{v}\tilde{A}_0|^2$, P_v emerges from the origin and (3.3b) has three real roots, one of which is zero and the others are negative. When $A_0^2 = \tilde{A}_0^2 + \epsilon$, where ϵ is positive and sufficiently small, equation (3.3b) has three negative real roots.

We consider the case where $A_0^2 > \tilde{A}_0^2$. Here, equation (3.3a) has two negative and one positive real roots. We assume that (3.3b) has one real root $-c$ and a pair of complex roots $a \pm ib$. Then,

$$\left. \begin{aligned} \gamma_1 + \gamma_2 + \gamma_3 &= c - 2a, \\ \gamma_2\gamma_3 + \gamma_1\gamma_3|vA_0| / \{ |vA_0| - (|vA_0|^2 - \gamma_1\gamma_2)^{1/2} \} \\ &\quad - [(\gamma_3/\gamma_1)(|vA_0|^2 - \gamma_1\gamma_2)^{1/2} \{ |vA_0| - (|vA_0|^2 - \gamma_1\gamma_2)^{1/2} \}] = a^2 + b^2 - 2ac, \\ 4\gamma_3(|vA_0|^2 - \gamma_1\gamma_2) &= c(a^2 + b^2). \end{aligned} \right\} \quad (3.4)$$

Hence, $c > 0$. We assume that at $A_0^2 = \hat{A}_0^2$, the root locus crosses the imaginary axis. Substituting $a = 0$ into (3.4) leads to

$$\begin{aligned} &(|vA_0|^2 - \gamma_1\gamma_2)^{1/2} \{ 2(\gamma_2 + \gamma_3 - \gamma_1)|vA_0|^2 + 4\gamma_1^2\gamma_2 \} \\ &= |vA_0| \{ \gamma_1(\gamma_1 + \gamma_2)(\gamma_1 + \gamma_2 + \gamma_3) + 2(\gamma_2 + \gamma_3 - \gamma_1)(|vA_0|^2 - \gamma_1\gamma_2) \}. \end{aligned} \quad (3.5)$$

Hence,

$$|vA_0|^2 < \min \{ 2\gamma_1^2\gamma_2 / (\gamma_1 - \gamma_2 - \gamma_3), \gamma_1(\gamma_1 + \gamma_2)(\gamma_1 + \gamma_2 + \gamma_3) / \{ 2(\gamma_1 - \gamma_2 - \gamma_3) \} + \gamma_1\gamma_2 \}$$

$$\triangleq |vA_0'|^2, \quad (3.6a)$$

or

$$|vA_0|^2 > \max\{2\gamma_1^2\gamma_2/(\gamma_1-\gamma_2-\gamma_3), \gamma_1(\gamma_1+\gamma_2)(\gamma_1+\gamma_2+\gamma_3)/\{2(\gamma_1-\gamma_2-\gamma_3)\}+\gamma_1\gamma_2\} \\ \triangleq |vA_0''|^2. \quad (3.6b)$$

Now, we consider two subcases :

Case (i) $\gamma_1 < \gamma_2 + \gamma_3$: From (3.5), we obtain an equation for $|vA_0|^2$:

$$s(|vA_0|^2) \triangleq 4\{(\gamma_1-\gamma_2)^2-\gamma_3^2\}(|vA_0|^2)^2 - [(\gamma_1-\gamma_2)^2(\gamma_1+\gamma_2+\gamma_3)^2 \\ + 8\gamma_1\gamma_2\{(\gamma_1-\gamma_2)^2+\gamma_3(\gamma_1+\gamma_2)\}]|vA_0|^2 - 16\gamma_1^3\gamma_2^3 = 0. \quad (3.7)$$

Equation (3.7) has a positive real root if and only if the first term is positive (i.e., $\gamma_1 > \gamma_2 + \gamma_3$ or $\gamma_2 > \gamma_1 + \gamma_3$).

Since $\gamma_1 < \gamma_2 + \gamma_3$ by assumption, equation (3.7) has a positive real root if and only if $\gamma_2 > \gamma_1 + \gamma_3$, and \hat{A}_0^2 is defined by

$$|v\hat{A}_0|^2 = [c_1 + \{c_1^2 + 64(\gamma_1\gamma_2)^3c_2\}^{1/2}]/2c_2, \quad (3.8)$$

where

$$c_1 = (\gamma_1-\gamma_2)^2\{(\gamma_1+\gamma_2+\gamma_3)^2 + 8\gamma_1\gamma_2\} + 8\gamma_1\gamma_2\gamma_3(\gamma_1+\gamma_2), \\ c_2 = 4\{(\gamma_1-\gamma_2)^2 - \gamma_3^2\}.$$

Since $s(\gamma_1\gamma_2) < 0$, $\gamma_1\gamma_2 < |v\hat{A}_0|^2$.

Case (ii) $\gamma_1 > \gamma_2 + \gamma_3$: Since $s(|vA_0'|^2) < 0$ and $s(|vA_0''|^2) > 0$,

the real root of (3.6) does not satisfy (3.5). Thus, if

$\gamma_2 < \gamma_1 + \gamma_3$, the root locus does not cross the imaginary axis.

For sufficiently large $|vA_0|$, equation (3.3b) has one

positive root and a pair of complex roots since the coefficient of λ in (3.3b) is positive and increases monotonically as $|vA_0|$ increases. From (3.4), we obtain an equation for 2a:

$$q(2a) \triangleq (2a)^3 + 2(\gamma_1 + \gamma_2 + \gamma_3)(2a)^2 + (\gamma_1 + \gamma_2 + \gamma_3)(2a) + \{2a + (\gamma_1 + \gamma_2 + \gamma_3)\} \\ [\gamma_2\gamma_3 + \gamma_3\gamma_1|vA_0| / \{|vA_0| - (|vA_0|^2 - \gamma_1\gamma_2)^{\frac{1}{2}}\} - [(\gamma_3/\gamma_1)(|vA_0|^2 - \gamma_1\gamma_2)^{\frac{1}{2}} \\ \{|vA_0| - (|vA_0|^2 - \gamma_1\gamma_2)^{\frac{1}{2}}\}]] - 4\gamma_3(|vA_0|^2 - \gamma_1\gamma_2) = 0, \quad (3.9)$$

which has only a positive (resp., negative) real root for sufficiently large $|vA_0|$ if $\gamma_2 > \gamma_1 + \gamma_3$ (resp., $\gamma_2 < \gamma_1 + \gamma_3$).

From the above results, we obtain the root locus of (3.3b) as shown in Figure 3.1. The origin is asymptotically

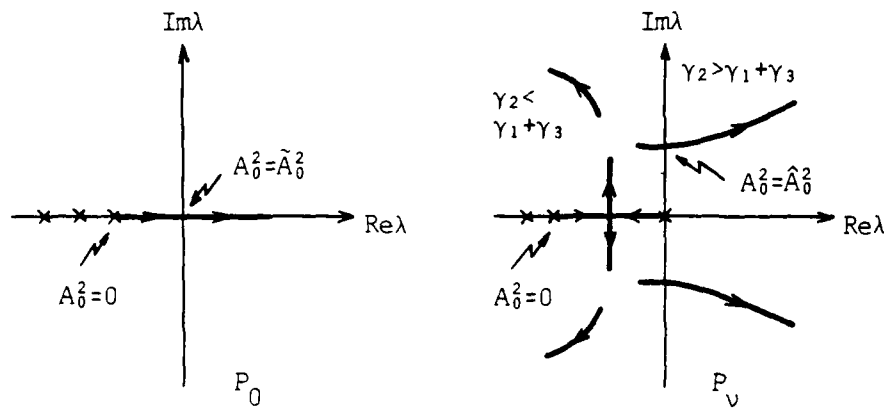


Figure 3.1 Sketches of Root Locus of (3)

stable if $A_0^2 < \tilde{A}_0^2$, and is a stable node in a biunstable plane. If $\gamma_2 < \gamma_1 + \gamma_3$, P_v is asymptotically stable for any value of A_0^2 . If $\gamma_2 > \gamma_1 + \gamma_3$, P_v is asymptotically stable

when $|v\tilde{A}_0|^2 < |vA_0|^2 < |v\hat{A}_0|^2$, and when $|vA_0|^2 > |v\hat{A}_0|^2$, P_v is an unstable focus in a bistable plane. Thus, system (3) with positive γ_j 's may have periodic or chaotic solutions globally if $\gamma_2 > \gamma_1 + \gamma_3$ and $A_0^2 > \hat{A}_0^2$.

3.1.2 System (4)

Without loss of generality, we assume that $v > 0$, since the substitution $v \rightarrow -v$ is equivalent to $x_1 \rightarrow -x_1$ and $x_2 \rightarrow -x_2$. Then, the equilibrium points are $P_0 = \{\theta_X\}$ and $P_{v\mu} = \{X_{v\mu}\}$, $v, \mu = \pm 1$:

$$\begin{aligned} X_{v\mu} = & (v\mu(\gamma_2/\gamma_3))^{\frac{1}{2}} \{ \gamma_2(v\mu A_0^2/(\gamma_2/\gamma_3)^{\frac{1}{2}} - \gamma_1\gamma_3) \}^{\frac{1}{2}}, \quad v(v\mu A_0^2/(\gamma_2/\gamma_3)^{\frac{1}{2}} - \gamma_1\gamma_3)^{\frac{1}{2}}, \\ & \mu(\gamma_2/\gamma_3)^{\frac{1}{2}}(v\mu A_0^2/(\gamma_2/\gamma_3)^{\frac{1}{2}} - \gamma_1\gamma_3)/\gamma_1)^T, \end{aligned} \quad (3.10)$$

if they exist. At P_0 and $P_{v\mu}$, the characteristic equations of dF/dX for (4) are

$$p_0(\lambda) \triangleq (\lambda + \gamma_1) \{ \lambda^2 + (\gamma_2 + \gamma_3)\lambda + \gamma_2\gamma_3 - (vA_0^2/\gamma_1)^2 \} = 0, \quad (3.11a)$$

$$\begin{aligned} p_\mu(\lambda) \triangleq & \lambda^3 + (\gamma_1 + \gamma_2 + \gamma_3)\lambda^2 + \mu(\gamma_3/\gamma_2)^{\frac{1}{2}}(\gamma_2/\gamma_3 + 1)|v|A_0^2 \\ & + 4\gamma_2(\mu|v|A_0^2/(\gamma_2/\gamma_3)^{\frac{1}{2}} - \gamma_1\gamma_3) = 0. \end{aligned} \quad (3.11b)$$

We shall show that if all the γ_i 's are positive, then P_0 or $P_{v\mu}$ is stable. From (3.11a), if $|v|A_0^2 < \gamma_1(\gamma_2\gamma_3)^{\frac{1}{2}}$, P_0 is stable. If $|v|A_0^2 > \gamma_1(\gamma_2\gamma_3)^{\frac{1}{2}}$, there exist two nontrivial equilibrium points P_{11} and P_{-11} (i.e., $\mu = 1$). We shall show that they are stable. Since $|v|A_0^2 > \gamma_1(\gamma_2\gamma_3)^{\frac{1}{2}}$, $p_1^{(i)} > 0$, $i = 0, 1, 2$. Hence, if (3.11b) has three real roots, they are

negative. Assume that (3.11b) has a real root $-c$ and a pair of complex roots $a \pm ib$. Then,

$$\left. \begin{aligned} \gamma_1 + \gamma_2 + \gamma_3 &= c - 2a, \\ \mu(\gamma_2 + \gamma_3) |v| A_0^2 / (\gamma_2 \gamma_3)^{1/2} &= a^2 + b^2 - 2ac, \\ \mu(\gamma_2 \gamma_3)^{1/2} |v| A_0^2 - \gamma_1 \gamma_2 \gamma_3 &= c(a^2 + b^2)/4. \end{aligned} \right\} \quad (3.12)$$

Since $|v| A_0^2 > \gamma_1 (\gamma_2 \gamma_3)^{1/2}$ and $\mu = 1$, c is positive. Furthermore,

$$\gamma_1 \gamma_2 \gamma_3 = \{\gamma_2 \gamma_3 / (\gamma_2 + \gamma_3) - c/4\} (a^2 + b^2) - 2ac \gamma_2 \gamma_3 / (\gamma_2 + \gamma_3),$$

$$4\gamma_1 \gamma_2 / (\gamma_1 + \gamma_2) > c.$$

Hence,

$$c = \gamma_1 + \gamma_2 + \gamma_3 + 2a < 4\gamma_1 \gamma_2 / (\gamma_1 + \gamma_2).$$

This implies that $a < 0$. Thus, (3.11b) has no unstable complex roots. Therefore, P_{v1} is asymptotically stable if all the γ_j 's are positive.

If $\gamma_2 < 0$ or $\gamma_3 < 0$, P_{vu} does not exist. This case is also eliminated in Table 2.5.

Now, we assume that $\gamma_1 < 0$. Equation (3.11a) has one positive and two negative roots if $A_0^2 < \tilde{A}_0^2 \triangleq (\gamma_2 \gamma_3)^{1/2} |\gamma_1 / v|$, and has two positive and one negative roots if $A_0^2 > \tilde{A}_0^2$. Moreover, if $A_0^2 < \tilde{A}_0^2$, there exist four nontrivial equilibrium points $P_{v\mu}$, $v, \mu = \pm 1$, and two equilibrium points P_{11} and P_{-11} if $A_0^2 > \tilde{A}_0^2$.

We first consider P_{11} and P_{-11} (i.e., $\mu = 1$). If

equation (3.11b) has three real roots, then all of them are negative since $p_1^{(i)} > 0$, $i = 0, 1, 2$. When $A_0^2 = 0$ or A_0^2 is sufficiently large, equation (3.11b) has one negative real root and a pair of complex roots. Moreover, the root locus does not cross the origin, since $p_1(0) \neq 0$ for any values of A_0^2 . Suppose that (3.12) holds. Then, c is positive, since $\mu = 1$ and $\gamma_1 < 0$. We consider two subcases to determine when the root locus of (3.11b) crosses the imaginary axis:

Cases (i) $(\gamma_2 - \gamma_3)^2 - |\gamma_1|(\gamma_2 + \gamma_3) > 0$: Let $a = 0$ in (3.12), then

$$A_0^2 = 4(\gamma_2 \gamma_3)^{\frac{1}{2}} |\gamma_1| / \nu \{ (\gamma_2 - \gamma_3)^2 - |\gamma_1|(\gamma_2 + \gamma_3) \} \triangleq \hat{A}_0^2. \quad (3.13)$$

From (3.12), at $A_0^2 = \hat{A}_0^2$,

$$da/dA_0^2 = |\nu| \{ |\gamma_1|(\gamma_2 + \gamma_3) - (\gamma_2 - \gamma_3)^2 \} / \{ 2(\gamma_2 \gamma_3)^{\frac{1}{2}} (\hat{b}^2 + \hat{c}^2) \} < 0, \quad (3.14)$$

where

$$\hat{b}^2 = 4\gamma_2 \gamma_3 |\gamma_1| (\gamma_2 + \gamma_3) / \{ (\gamma_2 - \gamma_3)^2 - |\gamma_1|(\gamma_2 + \gamma_3) \},$$

$$\hat{c} = \gamma_2 + \gamma_3 - |\gamma_1|.$$

Hence, Hopf bifurcation occurs at $A_0^2 = \hat{A}_0^2$.

Case (ii) $(\gamma_2 - \gamma_3)^2 - |\gamma_1|(\gamma_2 + \gamma_3) < 0$: Here, (3.13) does not hold, that is, the root locus of (3.11b) does not cross the imaginary axis. From (3.12), we obtain an equation for $2a$:

$$\begin{aligned} q(2a) &\triangleq (2a)^3 + 2(\gamma_2 + \gamma_3 - |\gamma_1|)(2a)^2 + \{ (\gamma_2 + \gamma_3 - |\gamma_1|)^2 \\ &\quad + \mu(\gamma_3/\gamma_2)^{\frac{1}{2}}(\gamma_2/\gamma_3 + 1) |\nu| A_0^2 \} + \mu(\gamma_3/\gamma_2)^{\frac{1}{2}} |\nu| A_0^2 \{ (\gamma_2 - \gamma_3)^2 - |\gamma_1|(\gamma_2 + \gamma_3) \} / \gamma_3 \\ &\quad - 4|\gamma_1| \gamma_2 \gamma_3 = 0, \end{aligned} \quad (3.15)$$

where $\mu = 1$. Equation (3.15) does not have negative real roots at $A_0^2 = 0$ and for sufficiently large A_0^2 . This means that if (3.11b) has a pair of complex roots, their real parts are positive at $A_0^2 = 0$ and sufficiently large A_0^2 . Thus, equation (3.11b) always has one negative real root and a pair of complex roots whose real parts are positive.

We now consider P_{1-1} and P_{-1-1} (i.e., $\mu = 1$), which exist only if $A_0^2 < \tilde{A}_0^2$. Equation (3.12) with $\mu = -1$ implies that a cannot be zero. Hence, the root locus of (3.11b) does not cross the imaginary axis. Equation (3.12) also implies that the real parts of the complex roots of (3.11b) at $A_0^2 = 0$ are positive. Moreover, at $A_0^2 = \tilde{A}_0^2$, equation (3.11b) has three real roots which are positive, negative and zero. Hence, $b^2 = 0$ in (3.12) for a certain value $A_0^2 < \tilde{A}_0^2$. From (3.12), A_0^2 is uniquely determined:

$$A_0^2 = 2\{18|\gamma_1|\gamma_2\gamma_3 - a(\gamma_2 + \gamma_3 - |\gamma_1|)^2\}(\gamma_2\gamma_3)^{\frac{1}{2}} \\ / [|\gamma| \{ [6a - (\gamma_2 + \gamma_3 - |\gamma_1|)](\gamma_2 + \gamma_3) + 36\gamma_2\gamma_3 \}], \quad (3.16)$$

where a is the positive root of

$$2(\gamma_2 + \gamma_3)a^3 + \{(\gamma_2 + \gamma_3)(\gamma_2 + \gamma_3 - |\gamma_1|) + 12\gamma_2\gamma_3\}a^2 \\ + 8\gamma_2\gamma_3(\gamma_2 + \gamma_3 - |\gamma_1|)a - 4|\gamma_1|\gamma_2\gamma_3(\gamma_2 + \gamma_3) = 0. \quad (3.17)$$

Thus, equation (3.11b) has one negative root and a pair of complex roots whose real parts are positive if $A_0^2 < A_0^2$, and has one negative and two positive real roots if $A_0^2 < A_0^2 < \tilde{A}_0^2$.

From the above results, we have the root loci shown in Figure 3.2. The origin P_0 is a stable node in a biunstable

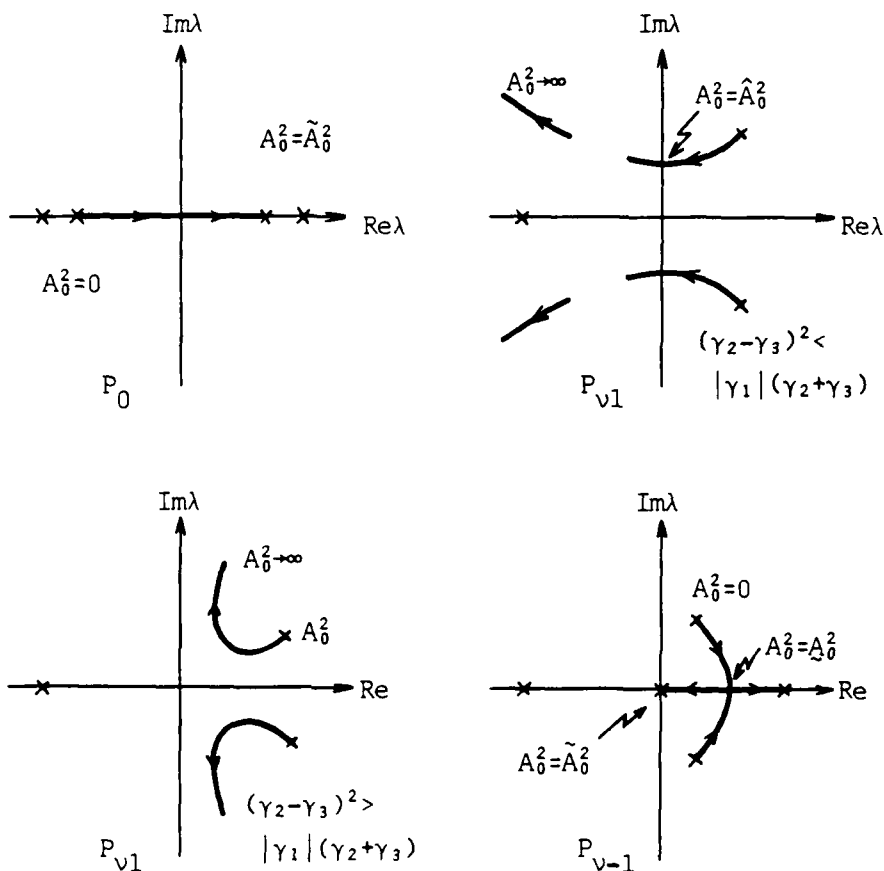


Figure 3.2 Sketches of Root Locus of (4)

plane if $A_0^2 < \tilde{A}_0^2$, and an unstable node in a bistable plane if $A_0^2 > \tilde{A}_0^2$. In case (i), P_{V1} is an unstable focus in a bistable plane if $A_0^2 < \hat{A}_0^2$ and is asymptotically stable if $A_0^2 > \hat{A}_0^2$. In case (ii), P_{V1} is always an unstable foci in a bistable plane. If $A_0^2 < \tilde{A}_0^2$, P_{V-1} is an unstable focus in a

bistable plane and if $A_0^2 < A_0^2 < \tilde{A}_0^2$, P_{v-1} is an unstable node in a bistable plane. Thus, if $A_0^2 < \hat{A}_0^2$, or if $(\gamma_2 - \gamma_3)^2 < |\gamma_1|(\gamma_2 + \gamma_3)$ and $|\gamma_1| < \gamma_2 + \gamma_3$ ((3.1)), all the equilibrium points are unstable and therefore, system (4) may have periodic or chaotic solutions globally.

We shall show that system (4) has an attractor containing P_{vu} . Since equation (4) is invariant to the interchange of subscripts 2 and 3, we can assume that $\gamma_3 \geq \gamma_2$ without loss of generality. We assume that $\gamma_3 > \gamma_2$, since if $\gamma_3 = \gamma_2$, (4) becomes a two-dimensional equation, which has no chaotic solutions. Let $\alpha(t) \triangleq x_3(t)/x_2(t)$, then

$$\dot{\alpha} = (\gamma_3 - \gamma_2)\alpha - (x_1 - vA_0^2/\gamma_1)(1 - \alpha^2). \quad (3.18)$$

At $x_2 = vx_1$, $v = \pm 1$, $\dot{\alpha} = v(\gamma_3 - \gamma_2)$. Since $\gamma_3 > \gamma_2$, then the sets V_+ and V_- defined by

$$V_+ = \{X : x_2 > |x_3|\}, \quad V_- = \{X : x_2 < -|x_3|\}, \quad (3.19)$$

are positive invariant sets (i.e., if $X(\tau, X_0) \in V_+$ (or V_-) for some τ , $X(t, X_0) \in V_+$ (or V_-) for all $t \geq \tau$). Let $V = V_+ \cup V_-$. Then, it is enough to show that if $X(t, X_0) \in -V$ for all $t \in [0, \infty)$, $X(t) = X(t, X_0)$ converges to V as $t \rightarrow \infty$. Let $\beta(t) \triangleq x_2(t)^2 - x_3(t)^2$, then

$$\dot{\beta} = 2(\gamma_3 x_3^2 - \gamma_2 x_2^2) = 2(\gamma_3 - \gamma_2)x_3^2 - \gamma_2 \beta. \quad (3.20)$$

If $X^+(X_0) \in -V$, then $|x_2(t)| < |x_3(t)|$ (or $\beta(t) < 0$) and $|x_2(t)| > (\gamma_3/\gamma_2)^{1/2}|x_3(t)|$ (or $\dot{\beta}(t) > 0$) for $t \geq 0$. Hence,

$\beta(t) \rightarrow 0$ as $t \rightarrow \infty$, that is, $X(t) = X(t, X_0)$ converges to V as $t \rightarrow \infty$. Thus, V is an attractor. Moreover, $P_{v-1} \in V_+$ and $P_{v1} \in V_-$.

3.1.3 System (5)

The equilibrium points are $P_0 = \{\theta_X\}$ and $P_v = \{X_v\}$, $v = \pm 1$:

$$X_v = (\gamma_2, v\{-(\gamma_2/\gamma_3)(\gamma_1\gamma_3 + |vA_0|^2)\}^{\frac{1}{2}}, (\gamma_2/\gamma_3)vA_0)^T, \quad (3.21)$$

if they exist. At P_0 and P_v , the characteristic polynomials of dF/dX for (5) are

$$p_0(\lambda) \triangleq (\lambda + 2\gamma_2)\{\lambda^2 + (\gamma_1 + \gamma_3)\lambda + \gamma_1\gamma_3 + |vA_0|^2\} = 0, \quad (3.22a)$$

$$\begin{aligned} p_v(\lambda) &\triangleq \lambda^3 + (\gamma_1 + \gamma_3)\lambda^2 + (1 - 2\gamma_2/\gamma_3)(\gamma_1\gamma_3 + |vA_0|^2) \\ &\quad - 2\gamma_2(\gamma_1\gamma_3 + |vA_0|^2) = 0, \end{aligned} \quad (3.22b)$$

respectively. We shall show that (5) can be discarded.

Equation (3.22a) implies that P_0 is asymptotically stable if all the γ_i 's are positive.

We assume that $\gamma_2 < 0$. If (3.22b) has three real roots, they are negative since $p_v^{(i)}(0) > 0$, $i = 0, 1, 2$. Assuming that (3.22b) has one real root $-c$ and a pair of complex roots $a \pm ib$,

$$\left. \begin{aligned} \gamma_1 + \gamma_3 &= c - 2a, \\ (1 - 2\gamma_2/\gamma_3)(\gamma_1\gamma_3 + |vA_0|^2) &= a^2 + b^2 - 2ac, \\ -2\gamma_2(\gamma_1\gamma_3 + |vA_0|^2) &= c(a^2 + b^2). \end{aligned} \right\} \quad (3.23)$$

Hence, c is positive, and we have an equation for $2a$:

$$q(2a) \triangleq (2a)^3 + 2(\gamma_1 + \gamma_3)(2a)^2 + \{(\gamma_1 + \gamma_3)^2 + (1 - 2\gamma_2/\gamma_3)(\gamma_1\gamma_3 + |vA_0|^2)\}(2a) + (\gamma_1 - 2\gamma_1\gamma_2/\gamma_3 + \gamma_3)(\gamma_1\gamma_3 + |vA_0|^2) = 0, \quad (3.24)$$

which does not have a positive real root. Therefore, the real parts of the roots of (3.22b) are negative. Thus, P_v is asymptotically stable if $\gamma_1 < 0$.

Now, we assume that $\gamma_1 < 0$. Equilibrium point P_v exists only if $|vA_0|^2 < |\gamma_1|\gamma_3$. Equation (5) is rewritten as

$$\begin{bmatrix} \dot{x}_1 \\ \dot{x}_3 \end{bmatrix} = \begin{bmatrix} -\gamma_1 & -vA_0 \\ vA_0 & -\gamma_3 \end{bmatrix} \begin{bmatrix} x_1 \\ x_3 \end{bmatrix} + \begin{bmatrix} -x_2^2 \\ 0 \end{bmatrix}, \quad (3.25a)$$

$$\dot{x}_2 = -(\gamma_2 - x_1)x_2. \quad (3.25b)$$

The eigenvalues of the square matrix in (3.25a) are positive and negative real numbers if $|vA_0|^2 < |\gamma_1|\gamma_3$. Hence, there is an open set R_0 where $x_1 < 0$ and $|x_2|$ is so small that if $X_0 \in R_0$ and $X(t) = X(t, X_0)$, $|x_1(t)|, |x_3(t)| \rightarrow \infty$ and $|x_2(t)| \rightarrow 0$ as $t \rightarrow \infty$.

Finally, we assume that $\gamma_3 < 0$. If $|vA_0|^2 < \gamma_1|\gamma_3|$, P_v does not exist. If $|vA_0|^2 > \gamma_1|\gamma_3|$ and $|\gamma_3| < \gamma_1$, then P_v is asymptotically stable. If $|vA_0|^2 > \gamma_1|\gamma_3|$ and $|\gamma_3| > \gamma_1$, the eigenvalues of the square matrix of (3.25a) are positive real numbers. Hence, there is an open set similar to R_0 . Thus, system (5) has no periodic or chaotic solutions globally.

3.1.4 System (7)

The equilibrium points are $P_0 = \{\theta_X\}$ and $P_v = \{X_v\}$,
 $v = \pm 1$:

$$\begin{aligned} X_v = & ((\gamma_2\gamma_3 + |vA_0|^2)/\gamma_3, v\{-(\gamma_1/\gamma_3)(\gamma_2\gamma_3 + |vA_0|^2)\}^{1/2}, \\ & -v(vA_0/\gamma_3)\{-(\gamma_1/\gamma_3)(\gamma_2\gamma_3 + |vA_0|^2)\}^{1/2})^T, \end{aligned} \quad (3.26)$$

if they exist. At P_0 and P_v , the characteristic equations of $dF(X)/dX$ of (7) are

$$P_0(\lambda) \triangleq (\lambda + \gamma_1)\{\lambda^2 + (\gamma_2 + \gamma_3)\lambda + \gamma_2\gamma_3 + |vA_0|^2\} = 0, \quad (3.27a)$$

$$\begin{aligned} P_v(\lambda) \triangleq & \lambda^3 + \lambda^2\{(\gamma_1 + \gamma_2 + \gamma_3) - (\gamma_2\gamma_3 + |vA_0|^2)/\gamma_3\} + \lambda\{\gamma_1(\gamma_2 + \gamma_3) \\ & - 3(\gamma_1/\gamma_3)(\gamma_2\gamma_3 + |vA_0|^2)\} - 2\gamma_1(\gamma_2\gamma_3 + |vA_0|^2) = 0, \end{aligned} \quad (3.27b)$$

respectively.

Equation (3.27a) implies that P_0 is asymptotically stable if all γ_i 's are positive.

We assume that $\gamma_2 < 0$. Equilibrium point P_v exists only if $|vA_0|^2 < |\gamma_2|\gamma_3$. If equation (3.27b) has three real roots, they are negative since $p_v^{(i)} > 0$, $i = 0, 1, 2$. Assuming that (3.27b) has one real root $-c$ and a pair of complex roots $a \pm ib$,

$$\left. \begin{aligned} \gamma_1 + \gamma_2 + \gamma_3 - (\gamma_2\gamma_3 + |vA_0|^2)/\gamma_3 &= c - 2a, \\ \gamma_1(\gamma_2 + \gamma_3) - 3\gamma_1(\gamma_2\gamma_3 + |vA_0|^2)/\gamma_3 &= a^2 + b^2 - 2ac, \\ -2\gamma_1(\gamma_2\gamma_3 + |vA_0|^2) &= c(a^2 + b^2). \end{aligned} \right\} \quad (3.28)$$

Hence, c is positive, and we have an equation for $2a$:

$$\begin{aligned}
 q(2a) &\triangleq (2a)^3 + 2\{\gamma_1 + \gamma_2 + \gamma_3 - (\gamma_2\gamma_3 + |vA_0|^2)/\gamma_3\}(2a)^2 \\
 &+ [\{\gamma_1 + \gamma_2 + \gamma_3 - (\gamma_2\gamma_3 + |vA_0|^2)/\gamma_3\}^2 + \gamma_1(\gamma_2 + \gamma_3) - 3\gamma_1(\gamma_2\gamma_3 + |vA_0|^2)/\gamma_3](2a) \\
 &+ \{\gamma_1 + \gamma_2 + \gamma_3 - (\gamma_2\gamma_3 + |vA_0|^2)/\gamma_3\}\{\gamma_1(\gamma_2 + \gamma_3) - 3\gamma_1(\gamma_2\gamma_3 + |vA_0|^2)/\gamma_3\} \\
 &- 2\gamma_1(\gamma_2\gamma_3 + |vA_0|^2) = 0.
 \end{aligned} \tag{3.29}$$

If $|vA_0|^2 < \gamma_3(\gamma_3 - 2\gamma_2)/3$, $q^{(i)} > 0$, $i = 0, 1, 2$. Hence, the real roots of (3.29) are negative, and the real parts of the complex roots of (3.27b) are negative. If $|vA_0|^2 > \gamma_3(\gamma_3 - 2\gamma_2)/3$, a cannot be zero in (3.28). Moreover, $p_v(0) \neq 0$ since $|vA_0|^2 < |\gamma_2|\gamma_3$. Hence, the root locus of (3.27b) does not cross the imaginary axis. Furthermore, when $|vA_0|^2 = \gamma_3(\gamma_3 - 2\gamma_2)/3$, equation (3.27b) has one negative real root and a pair of complex roots, and from (3.29), the real parts of the complex roots are negative. Hence, (3.27b) has three stable roots for $|vA_0|^2 > \gamma_3(\gamma_3 - 2\gamma_2)/3$. Thus, P_v is asymptotically stable if $\gamma_2 < 0$.

Then, we assume that $\gamma_1 < 0$. Rewriting the right hand side of (7),

$$\dot{x}_1 = -\gamma_1 x_1 - x_2^2, \tag{3.30a}$$

$$\begin{bmatrix} \dot{x}_2 \\ \dot{x}_3 \end{bmatrix} = \begin{bmatrix} -\gamma_2 + x_1 & vA_0 \\ -vA_0 & -\gamma_3 \end{bmatrix} \begin{bmatrix} x_2 \\ x_3 \end{bmatrix}. \tag{3.30b}$$

If $x_1(0) < 0$ and $|x_1(0)|$ is sufficiently large and $|x_2(0)|$

and $|x_3(0)|$ are sufficiently small, $x_1(t) \rightarrow -\infty$ and $x_2(t)$, $x_3(t) \rightarrow 0$ as $t \rightarrow \infty$.

Now, we assume that $\gamma_3 < 0$. If $|vA_0|^2 < \gamma_2|\gamma_3|$, P_v does not exist. If $|vA_0|^2 > \gamma_2|\gamma_3|$ and $|\gamma_3| < \gamma_2$, P_0 is stable. If $|vA_0|^2 > \gamma_2|\gamma_3|$ and $|\gamma_3| > \gamma_2$, P_0 is an unstable node in a bistable plane. Equation (3.27b) has at least one positive real root. Hence, system (7) may have a chaotic solution, if $\gamma_3 < 0$, $|\gamma_3| > \gamma_2$ and $|vA_0|^2 > \gamma_2|\gamma_3|$.

3.1.5 System (2) and (6)

Since system (2) can be obtained from (6) by the substitution $\gamma_1 + \sigma v A_0 \rightarrow \gamma_1$, we consider only system (6). Comparing (2') and (6') in Table 2.3, system (6) may have a chaotic solution only if $\gamma_1 + \sigma v A_0 < 0$ and $\gamma_2, \gamma_3 > 0$. Then, the equilibrium points are $P_0 = \{\theta_X\}$ and $P_{\kappa\mu}^v = \{X_{\kappa\mu}^v\}$, $(\kappa, \mu, v) \in K \triangleq \{(1,1,1), (1,-1,-1), (-1,-1,1), (-1,1,-1)\}$:

$$X_{\kappa\mu}^v = (\kappa(\gamma_2\gamma_3)^{\frac{1}{2}}, \mu\{-(\gamma_1 + \sigma v A_0)\gamma_3\}^{\frac{1}{2}}, v\{-(\gamma_1 + \sigma v A_0)\gamma_2\}^{\frac{1}{2}})^T. \quad (3.31)$$

The characteristic equations of dF/dX for (6) are

$$p_0(\lambda) \triangleq (\lambda + \gamma_1 + \sigma v A_0)(\lambda + \gamma_2)(\lambda + \gamma_3) = 0, \quad (3.32a)$$

$$p(\lambda) \triangleq \lambda^3 + \lambda^2(\gamma_2 + \gamma_3 + \gamma_1 + \sigma v A_0) - 4(\gamma_1 + \sigma v A_0)\gamma_2\gamma_3 = 0, \quad (3.32b)$$

at P_0 and $P_{\kappa\mu}^v$, respectively. Since $\gamma_1 + \sigma v A_0 < 0$, equation (3.32b) has one negative real root and a pair of complex roots with positive real parts. Hence, P_0 is a stable node in a biunstable plane and $P_{\kappa\mu}^v$ is an unstable focus in a

bistable plane.

As in the case of system (4), we obtain an attractor $V = V_+ \cup V_-$, where $P_{\kappa-1}^V \in V_-$ and $P_{\kappa 1}^V \in V_+$. In the computer experiments, we did not observe trajectories such that $X^+(X_0) \in -V$ and $X(t) = X(t, X_0)$ converges to ∂V as $t \rightarrow \infty$. We do not prove the nonexistence of such trajectories, but we can show that such trajectories are highly special cases which can be neglected for all practical purposes. Since (6) is invariant to changing the signs of any two of the variables, it is enough to consider the set $\{X: x_3 > 0\}$. Let us define the set $W_{\kappa\mu}$:

$$W_{\kappa\mu} = \{X: |\kappa x_1| = \kappa x_1, |\mu x_2| = \mu x_2, x_3 > 0\} - W, \quad \kappa, \mu \in \{-1, 0, 1\},$$

where

$$W = \left(\bigcup_{(\kappa, \mu, \nu) \in K} \{P_{\kappa\mu}^V\} \right) \cup \{x_1, x_2, x_3\text{-axis}\}.$$

The set W is an invariant set and if $X_0 \notin W$, $X^+(X_0) \cap W = \emptyset$. In the following, the trajectory remaining in W will be neglected. Consider the following sets:

$$S \triangleq \{X: \dot{\alpha} = 0\} \cap (W_{00} - V),$$

$$W_{+(-)} \triangleq \{X: \dot{\alpha} > 0 \ (\dot{\alpha} < 0)\} \cap (W_{00} - V),$$

where $\alpha(t) = x_2(t)/x_3(t)$ and

$$\dot{\alpha} = (\gamma_3 - \gamma_2)\alpha + x_1(1 - \alpha^2). \quad (3.33)$$

The sketches of S and W_{\pm} are shown in Figure 2.3. In $W_{\kappa\mu}$,

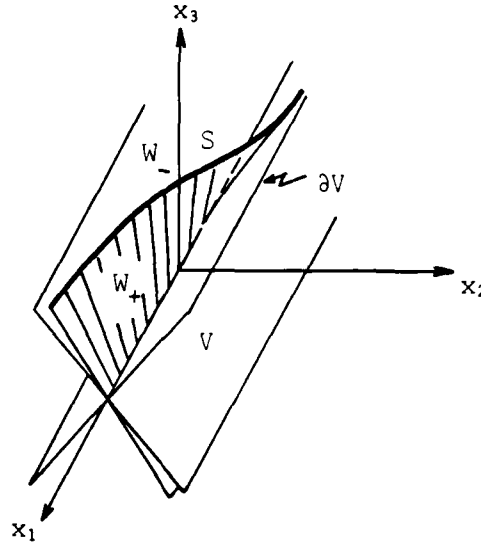


Figure 3.3 Sketches of S and W_{\pm} in (6)

$$(\kappa, \mu) = (1, -1), (-1, 1),$$

$$|\dot{x}_1| = \kappa x_1, \quad |\dot{x}_2| = \kappa x_2, \quad \dot{x}_3 < 0. \quad (3.34)$$

Hence, the trajectory is transverse to S and enters $W_+ \cap W_{1-1}$. In $W_+ \cap W_{1-1}$, $-1 < \alpha < 0$, $\dot{\alpha} > 0$, $x_1 > 0$ and $\dot{x}_1 > 0$. Hence, from (3.33), α increases. Thus, the trajectory enters $W_+ \cap W_{11}$. Let $X(\tau_1, X_0) \in W_{10} \cap (x_1, x_3)$ -plane and $X(\tau_1 + \epsilon, X_0) \in W_+ \cap W_{11}$, where $X(\tau, X_0) \in W_+ \cap W_{11}$ for all $\tau \in [\tau_1, \tau_1 + \epsilon]$. In $W_+ \cap W_{11}$, $0 < \alpha < 1$, $\dot{\alpha} > 0$ and $x_1 > 0$. Hence, from (3.33), if $X(\tau, X_0) \in W_+ \cap W_{11}$ for all $\tau \in [\tau_1 + \epsilon, t]$,

$$\dot{\alpha}(t) \geq (\gamma_3 - \gamma_2)\alpha(t) \geq (\gamma_3 + \gamma_2)\alpha(\tau_1 + \epsilon) > 0. \quad (3.35)$$

This implies that the trajectory enters $W_+ \cap W_{-11}$, since it is transverse to the (x_2, x_3) -plane. Let $X(\tau_2, X_0) \in$

$W_{01} \cap (x_2, x_3)$ -plane and $X(\tau_2 + \epsilon, X_0) \in W_+ \cap W_{-11}$, where $X(\tau, X_0) \in W_+ \cap W_{-11}$ for all $\tau \in [\tau_2, \tau_2 + \epsilon)$. In $W_+ \cap W_{-11}$, $x_1 < 0$, $\dot{x}_1 < 0$, $x_2 > 0$, $\dot{x}_2 < 0$, $x_3 > 0$ and $\dot{x}_3 < 0$. Hence, if $X(\tau, X_0) \in W_+ \cap W_{-11}$ for all $\tau \in [\tau_2 + \epsilon, t]$,

$$\left. \begin{aligned} \dot{x}_1(t) &< -(\gamma_1 + \sigma v A_0) x_1(\tau_2 + \epsilon) < 0, \\ \dot{x}_i(t) &\leq -\gamma_i x_i(t), \quad i = 2, 3. \end{aligned} \right\} \quad (3.36)$$

Consequently, if $X(t, X_0) \in W_+ \cap W_{-11}$ for all $t \geq 0$, then $x_1(t) \rightarrow -\infty$, $x_2(t) \rightarrow 0$ and $x_3(t) \rightarrow 0$ as $t \rightarrow \infty$. Otherwise, the trajectory enters $S \cap W_{10}$. Similarly, if $X(\tau_0, X_0) \in S \cap W_{-10}$ at some τ_0 , the trajectory converges to the x_1 -axis (where $x_1(t) \rightarrow \infty$) as $t \rightarrow \infty$ or enters $S \cap W_{10}$. Thus, if $X^+(X_0) \in W_{00} - V$, then as $t \rightarrow \infty$, the trajectory converges to the x_1 -axis monotonically after some or no oscillations about the x_3 -axis, or oscillates about the x_3 -axis for all $t \geq 0$.

Let us see roughly how a trajectory oscillating about the x_3 -axis for all $t \geq 0$ behaves. Rewriting (3.20) for (6),

$$\dot{\beta} = 2(\gamma_3 x_3^2 - \gamma_2 x_2^2) = 2(\gamma_3 - \gamma_2) x_3^2 - 2\gamma_2 \beta. \quad (3.37)$$

Integrating (3.37),

$$\begin{aligned} 0 < \int_0^t x_3(\tau)^2 d\tau &= (\beta(t) - \beta(0) + 2\gamma_2 \int_0^t \beta(\tau) d\tau) / 2(\gamma_3 - \gamma_2) \\ &< -\beta(0) / 2(\gamma_3 - \gamma_2), \end{aligned} \quad (3.38)$$

for all t since $\beta(t) < 0$ for all t . By studying $F(X)$ of (6) carefully, we know that $x_2(t)$ takes a larger value than

$\{-(\gamma_1 + \sigma v A_0) \gamma_3\}^{\frac{1}{2}}$ at each time when the trajectory encircles the x_3 -axis. Therefore, for any small $\epsilon > 0$, the time duration for which $x_2(t)^2 > \epsilon$ converges to zero as $t \rightarrow \infty$. Thus, $x_2(t)^2$ behaves as a train of pulses whose heights are larger than $\{-(\gamma_1 + \sigma v A_0) \gamma_3\}^{\frac{1}{2}}$ and whose widths converge to zero as $t \rightarrow \infty$. The above arguments also hold for x_3 .

A trajectory, which lies in $W_+ \cap W_{-11}$ or $W_- \cap W_{1-1}$ for all $t \geq \tau_1$ for some τ_1 and converges to the x_1 -axis monotonically, is unstable in the sense that a small perturbation of α can shift $X(t, X_0)$ into V or cause $X(t, X_0)$ to oscillate about the x_3 -axis. For, $\dot{\alpha} = \mu(\gamma_3 - \gamma_2)$ on ∂V ($|y| = \mu y$) and the trajectory is transverse to S , and ∂V and S approach to each other as $|x_1| \rightarrow \infty$. A trajectory which oscillates about the x_3 -axis for all $t \geq 0$ is also unstable in the sense that $X(t, X_0)$ is shifted into V by small perturbation of α . For, $|x_i(t)|$ is larger than $\{-(\gamma_1 + \sigma v A_0) \gamma_i\}^{\frac{1}{2}}$, $i = 2, 3$, at each turn around the x_3 -axis, and $X(t) = X(t, X_0)$ converges to ∂V as $t \rightarrow \infty$. Hence, the trajectories which remain in $-(W \cup V)$ for all $t \geq 0$ can be neglected for all practical purposes. In fact, such trajectories were not observed in computer experiments.

We note that (6) is the only system which explicitly includes $\sigma = \sin(\theta_1(0) + \theta_2(0))$. If $|v A_0| < |\gamma_1|$, $P_{\kappa\mu}^V$ exists and is unstable when $\gamma_1 < 0$, and P_0 is stable when $\gamma_1 > 0$. If $|v A_0| > |\gamma_1|$, $P_{\kappa\mu}^V$ exists and unstable when $\text{sgn}(\sigma v A_0) = -1$, and P_0 is stable when $\text{sgn}(\sigma v A_0) = 1$. We assume that $v A_0 > |\gamma_1|$

and that the trajectories converge to Σ as $t \rightarrow \infty$. The question is which of the reduced equations with $\sigma = 1$ or -1 describes the asymptotic behavior of (6') in the limit $t \rightarrow \infty$. Obviously, the equation with $\sigma = 1$ is not the one, since the origin of the Y-space is unstable if $vA_0 > |\gamma_1|$. It is possible that either one of them does not describe the asymptotic behavior of (6') in the limit $t \rightarrow \infty$, but the trajectory of the original system approaches in turn either of the subsets of Σ corresponding to the X-spaces of the systems with $\sigma = 1$ and -1 .

3.2 Physical Interpretation for Reduced Systems

In this section, we shall try to give some physical interpretation for the results presented in the previous section. The equations for frequency matching and their corresponding decay diagrams are shown in Table 3.1.

3.2.1 System (2)

In the decay process of (2), wave 1 decays into waves 2 and 3. Let us define $I = 2x_1^2 + x_2^2 + x_3^2$. For convenience, we call I the energy of (2), though it is not exactly the wave energy of (2). Taking the time derivative of I gives:

$$\dot{I} = -2(\gamma_1 x_1^2 + \gamma_2 x_2^2 + \gamma_3 x_3^2). \quad (3.39)$$

We assume that $\gamma_1 < 0$. The constant I and $\dot{I} = 0$ surfaces are sketched in Figure 3.4, where they correspond to the ellipsoid E and the elliptic cone C , respectively. If $X(t)$

Table 3.1 Frequency Matching and Decay Diagrams

	Frequency Matching	Decay Diagram
(1)	$\omega_1 = 2\omega_2$	
(2)	$\omega_1 = \omega_2 + \omega_3$	
(3)	$\omega_0 = \omega_1 + \omega_2,$ $\omega_1 = \omega_2 + \omega_3$	
(4)	$2\omega_0 = \omega_1,$ $\omega_1 = \omega_2 + \omega_3$	
(5)	$\omega_3 = \omega_0 + \omega_1,$ $\omega_1 = 2\omega_2$	
	$\omega_1 = \omega_0 + \omega_3,$ $\omega_1 = 2\omega_2$	
(6)	$\omega_0 = 2\omega_1,$ $\omega_1 = \omega_2 + \omega_3$	
(7)	$\omega_1 = 2\omega_2,$ $\omega_2 = \omega_0 + \omega_3$	
	$\omega_1 = 2\omega_2,$ $\omega_3 = \omega_0 + \omega_2$	

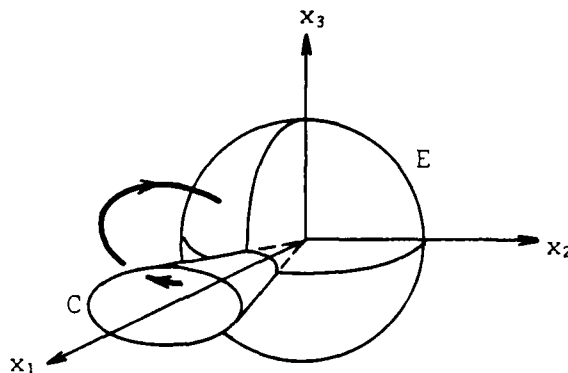


Figure 3.4 Dynamics of Energy of (2)

is inside (resp., outside) C , I increases (resp., decreases). That is, when the amplitude of wave 1 is large, the linear growth of wave 1 is dominant so that the energy of the whole system increases. When the amplitude of wave 2 or 3 is large, the linear damping of 2 or 3 is dominant so that the energy of the whole system decreases. Thus, the energy of the waves are not balanced in a static manner, but may oscillate in a chaotic manner.

As mentioned in Section 2.1, if $\gamma_2 < 0$ (or $\gamma_3 > 0$), there is no chaotic solution. For, if $\gamma_2 < 0$,

$$\left. \begin{aligned} (d/dt)(|A_1|^2 + |A_3|^2) &= -\gamma_1 |A_1|^2 - \gamma_3 |A_3|^2, \\ (d/dt)(|A_1|^2 - |A_2|^2) &= -\gamma_1 |A_1|^2 - |\gamma_2| |A_2|^2, \end{aligned} \right\} \quad (3.40)$$

and therefore, $|A_1(t)|$ and $|A_3(t)| \rightarrow 0$ and $|A_2(t)| \rightarrow \infty$ as $t \rightarrow \infty$. This phenomenon does not depend on the magnitude of γ_i 's, since they are normalized by the substitution

$|\gamma_i|t \rightarrow t$, $i = 1, 2$ or 3 . From the physical view point, these results seem to be peculiar. For, system (2) describes a three-wave interaction including both decay and fusion processes, and it could be expected that the energy of the linearly growing and damped waves are balanced as in the case where $\gamma_1 < 0$. The above results show that when the decaying wave 1 is linearly growing ($\gamma_1 < 0$), its energy is transferred to the damped waves 2 and 3. On the other hand, when wave 2 is linearly growing ($\gamma_2 < 0$), its energy is not transferred to other waves. It is suggested that when the linearly damping or growth terms are introduced, even if the damping or growth rates are very small, system (2) describes only the irreversible decay process. It should be noted that the nonlinear coupling terms in (2) does not possess any mechanisms for such an irreversible process.

3.2.2 System (3)

As mentioned earlier, in the decay process of (3), an external wave with constant amplitude decays into waves 1 and 2 which have another resonant wave 3. When the external wave is weak ($|vA_0|^2 < \gamma_1\gamma_2$), the linear damping of three waves is dominant. Therefore, the energy supplied by the external wave is dissipated through the linearly damped waves. If the external wave is strong ($|vA_0|^2 > \gamma_1\gamma_2$), the input energy is supplied at a higher rate than the dissipation rate when the amplitudes of damped waves are small. External energy and energy dissipation are finally balanced

when the amplitudes of waves are large. When wave 2 is highly damped linearly ($\gamma_2 > \gamma_1 + \gamma_3$), the external energy supply and energy dissipation are balanced in a static manner regardless of the magnitude of the external energy. That is, the energy of each wave reaches a constant value. When wave 2 is damped slowly ($\gamma_2 < \gamma_1 + \gamma_3$) and the external wave is not strong ($A_0^2 < \hat{A}_0^2$), the wave energy is also balanced in a static manner. When the external wave is strong ($A_0^2 > \hat{A}_0^2$), the energy of the waves may oscillate in a chaotic manner.

3.2.3 System (4)

In the decay process of (4), the external wave generates a harmonic wave 1 which decays into waves 2 and 3. If all the waves are linearly damped and the external wave is weak ($|v|A_0^2 < \gamma_1(\gamma_2\gamma_3)^{\frac{1}{2}}$), the energy is dissipated more rapidly than supplied. When the external wave is strong ($|v|A_0^2 > \gamma_1(\gamma_2\gamma_3)^{\frac{1}{2}}$), the energy supply is at a higher (resp., lower) rate than the dissipation if the wave amplitudes are small (resp., large). Thus, the wave energy is balanced in a static manner at certain values of amplitudes. If wave 2 (or 3) is linearly growing, wave 2 (or 3) grows to infinity as $t \rightarrow \infty$ regardless of the magnitudes of the growth or damping rates. This phenomenon is similar to that of (2) discussed in Section 3.2.1.

If wave 1 linearly growing and if there is no external wave, the system is identical to (2). When wave 1 grows

rapidly ($|\gamma_1|(\gamma_2 + \gamma_3) > (\gamma_2 - \gamma_3)^2$) or the external wave is weak ($A_0^2 < \hat{A}_0^2$), the system behaves in a similar manner as (2). If wave 1 grows slowly ($|\gamma_1|(\gamma_2 + \gamma_3) > (\gamma_2 - \gamma_3)^2$) and the external wave is strong ($A_0^2 > \hat{A}_0^2$), the energy supply is dominated by the external wave and the wave energy is balanced in a static manner.

3.2.4 System (5)

As shown in Table 3.1, we have two cases. In the decay process of the first case, the external wave generates wave 3 by interacting with 1 which is a harmonic wave of wave 2. In the decay process of the second case, the external wave generates wave 1 by interacting with wave 3, and wave 1 generates a subharmonic wave 2. If all the waves are linearly damped, the energy of the whole system is dissipated regardless of the external wave. If wave 2 is linearly growing, the wave energy is balanced in a static manner regardless of the amplitude of the external wave. If wave 3 is slowly growing linearly ($|\gamma_3| < \gamma_2$) and the external wave is weak ($|vA_0|^2 < \gamma_1|\gamma_3|$), wave 1 and 3 grows to infinity and wave 2 dies away. If the external wave is strong ($|vA_0|^2 > \gamma_1|\gamma_3|$), wave 3 is strongly coupled with linearly damped waves 1 and 2 and consequently, all waves die away. If wave 1 is growing rapidly ($|\gamma_3| < \gamma_1$), wave 1 and 3 grow to infinity and wave 2 dies away regardless of the amplitude of the external wave. If wave 1 is growing slowly ($|\gamma_1| < \gamma_3$) and the external wave is strong

($|vA_0|^2 > |\gamma_1|\gamma_3$), all waves die away. If the external wave is weak ($|vA_0|^2 < |\gamma_1|\gamma_3$), the wave energy is balanced in a static manner, or wave 1 and 3 grows to infinity and wave 2 dies away. The mode of the actual behavior depends on the initial conditions if wave 2 is highly damped ($2\gamma_2 > \gamma_3$), and if $2\gamma_2 < \gamma_3$, it depends on the γ_i 's and vA_0 in a more complicated way.

3.2.5 System (6)

In the decay process of (6), the external wave generates a subharmonic wave 1 which decays into waves 2 and 3. We can make the same argument as we used for (2) by replacing γ_1 with $\gamma_1 + \sigma vA_0$. If $\gamma_1 > 0$, and the external wave is weak ($|vA_0| < \gamma_1$), all waves die away. If $\gamma_1 > 0$ and the external wave is strong ($|vA_0| > \gamma_1$), there may be a chaotic solution. If $\gamma_1 < 0$, there may be a chaotic solution regardless of the external wave.

3.2.6 System (7)

Here, we have two distinct cases. In the decay process of the first case, the external wave generates wave 2 by interacting with wave 3 and wave 2 generates a harmonic wave 1. In the decay process of the second case, the external wave generates wave 3 by interacting with wave 2 which is a subharmonic wave of wave 1. If all the waves are linearly damped, the energy of the system is dissipated regardless of the external wave. If wave 2 is linearly

growing and the external wave is weak ($|vA_0|^2 < \min\{\gamma_2|\gamma_3, \gamma_3(\gamma_1+\gamma_3)\}$), the wave energy is balanced in a static manner. If the external wave is strong ($|vA_0|^2 > |\gamma_2|\gamma_3$), all waves die away since wave 2 is coupled well with the linearly damped wave 3 through the external wave. If wave 1 is linearly growing, wave 1 tends to infinity and wave 2 and 3 die away regardless of the external wave amplitude. If wave 3 grows rapidly ($|\gamma_3| > \gamma_2$) and the external wave is strong ($|vA_0|^2 > \gamma_2|\gamma_3|$), the wave energy may oscillate in a chaotic manner.

3.3 Systems with Parametric Instability

Now, we have six reduced systems which have periodic or chaotic solutions for almost all initial conditions. These systems are listed in Table 3.2, where all the γ_i 's are positive except for (6). The parameters of each system satisfy the following condition:

$$(3) \quad \gamma_2 > \gamma_1 + \gamma_3, \quad A_0^2 > \hat{A}_0^2 \quad ((3.8)), \quad (3.41)$$

$$(4) \quad \left. \begin{aligned} A_0^2 < \hat{A}_0^2 \quad ((3.13)), \\ (\gamma_2 - \gamma_3)^2 < \gamma_1(\gamma_2 + \gamma_3), \quad \gamma_1 < \gamma_2 + \gamma_3, \end{aligned} \right\} \quad (3.42)$$

$$(6) \quad \gamma_1 > 0, \quad \sigma v A_0 < -\gamma_1, \quad \text{or} \quad (3.43a)$$

$$\gamma_1 < 0, \quad \sigma v A_0 > 0, \quad (3.43b)$$

$$(7) \quad |vA_0|^2 > \gamma_2\gamma_3, \quad \gamma_3 > \gamma_2. \quad (3.44)$$

Table 3.2 Systems for Chaotic Solutions

(1')	$\dot{A}_1 - \gamma_1 A_1 = -i\{A_2^2 + A_1(v_{111} A_1 ^2 + v_{122} A_2 ^2)\},$ $\dot{A}_2 + \gamma_2 A_2 = -i\{A_1 A_2^* + A_2(v_{211} A_1 ^2 + v_{222} A_2 ^2)\},$
(1)	$\dot{x}_1 = \gamma_1 x_1 - \delta x_2 + 2x_1 x_2 - x_2 \{(v_{111} - 2v_{211})(x_1^2 + x_2^2) + (v_{122} - 2v_{222})x_3\},$ $\dot{x}_2 = \gamma_1 x_2 + \delta x_1 + x_3 - 2x_1^2 + x_1 \{(v_{111} - 2v_{211})(x_1^2 + x_2^2) + (v_{122} - 2v_{222})x_3\},$ $\dot{x}_3 = -2\gamma_2 x_3 - 2x_2 x_3, \quad x_3 \geq 0$
(2')	<div style="display: flex; justify-content: space-between;"> <div style="width: 48%;"> $\dot{A}_1 = \gamma_1 A_1 - iA_2 A_3,$ $\dot{A}_2 = -\gamma_2 A_2 - iA_1 A_3^*,$ $\dot{A}_3 = -\gamma_3 A_3 - iA_1 A_2^*$ </div> <div style="width: 48%;"> $(2) \quad \begin{aligned} \dot{x}_1 &= \gamma_1 x_1 - x_2 x_3, \\ \dot{x}_2 &= -\gamma_2 x_2 + x_1 x_3, \\ \dot{x}_3 &= -\gamma_3 x_3 + x_1 x_2 \end{aligned}$ </div> </div>
(3')	<div style="display: flex; justify-content: space-between;"> <div style="width: 48%;"> $\dot{A}_1 = -\gamma_1 A_1 - i(A_2 A_3 + vA_0 A_2^*),$ $\dot{A}_2 = -\gamma_2 A_2 - i(A_1 A_3^* + vA_0 A_1^*),$ $\dot{A}_3 = -\gamma_3 A_3 - iA_1 A_2$ </div> <div style="width: 48%;"> $(3) \quad \begin{aligned} \dot{x}_1 &= -\gamma_1 x_1 - x_2 x_3 - vA_0 x_2, \\ \dot{x}_2 &= -\gamma_2 x_2 + x_1 x_3 - vA_0 x_1, \\ \dot{x}_3 &= -\gamma_3 x_3 + x_1 x_2 \end{aligned}$ </div> </div>
(4')	<div style="display: flex; justify-content: space-between;"> <div style="width: 48%;"> $\dot{A}_1 = \gamma_1 A_1 - i(A_2 A_3 + vA_0^2),$ $\dot{A}_2 = -\gamma_2 A_2 - iA_1 A_3^*,$ $\dot{A}_3 = -\gamma_3 A_3 - iA_1 A_2^*$ </div> <div style="width: 48%;"> $(4) \quad \begin{aligned} \dot{x}_1 &= \gamma_1 x_1 + x_2 x_3, \\ \dot{x}_2 &= -\gamma_2 x_2 - x_1 x_3 + (vA_0^2/\gamma_1)x_3, \\ \dot{x}_3 &= -\gamma_3 x_3 - x_1 x_2 + (vA_0^2/\gamma_1)x_2 \end{aligned}$ </div> </div>
(6')	<div style="display: flex; justify-content: space-between;"> <div style="width: 48%;"> $\dot{A}_1 = -\gamma_1 A_1 - i(A_2 A_3 + vA_0 A_1^*),$ $\dot{A}_2 = -\gamma_2 A_2 - iA_1 A_3^*,$ $\dot{A}_3 = -\gamma_3 A_3 - iA_1 A_2^*$ </div> <div style="width: 48%;"> $(6) \quad \begin{aligned} \dot{x}_1 &= (-\gamma_1 - \sigma vA_0)x_1 - x_2 x_3, \\ \dot{x}_2 &= -\gamma_2 x_2 + x_1 x_3, \\ \dot{x}_3 &= -\gamma_3 x_3 + x_1 x_2 \end{aligned}$ </div> </div>
(7')	<div style="display: flex; justify-content: space-between;"> <div style="width: 48%;"> $\dot{A}_1 = -\gamma_1 A_1 - iA_2^2,$ $\dot{A}_2 = -\gamma_2 A_2 - i(A_1 A_2^* + vA_0 A_3),$ $\dot{A}_3 = \gamma_3 A_3 - ivA_0 A_2$ </div> <div style="width: 48%;"> $(7) \quad \begin{aligned} \dot{x}_1 &= -\gamma_1 x_1 - x_2^2, \\ \dot{x}_2 &= -\gamma_2 x_2 + x_1 x_2 + vA_0 x_3, \\ \dot{x}_3 &= \gamma_3 x_3 - vA_0 x_2 \end{aligned}$ </div> </div>

The systems given in Table 3.2 except for (7) have an unstable focus in a bistable plane. All three-dimensional ordinary differential equations having pseudo-chaotic solutions so far have this type of equilibrium point. Actually, we did not observe any pseudo-chaotic solutions of (7).

Systems (1), (2), (4) and (7) have linear growth terms which cause the equilibrium points to be unstable. Such models are not widely accepted, since the linear growth terms cannot be readily derived from the fundamental equations describing wave-wave interactions in plasmas. On the other hand, introducing linear damping terms is natural since any collective motion of plasmas is damped by particle collisions. System (3) has only damping terms, and so does system (6) if $\gamma_1 > 0$ ((3.43a)). Hence, in what follows, we consider only these two cases where the instability is due to an external wave (parametric instability).

Now, we combine the sufficient conditions for the convergence of the trajectories to Σ (Table 2.7 and (S.2.3)) with the conditions for the existence of global periodic or chaotic solutions in the X-space ((3.41), (3.43a)).

3.3.1 Sufficient Conditions for Convergence of $\xi(t)$ to θ_ξ

We now recall the sufficient conditions for $\xi(t)$ to converges to θ_ξ as $t \rightarrow \infty$. Rewriting the equation (3) in Table 2.7,

$$\left. \begin{aligned} |A_2|^2 + 2|A_3|^2 &< (\gamma_1 + \gamma_2) \{ (2\gamma_2 + \gamma_3) p_3 - 2|vA_0| \} / (p_3 + p_4), \\ |A_1|^2 - 2|A_3|^2 &< (\gamma_1 + \gamma_2) \{ (2\gamma_1 + \gamma_3) p_4 - 2|vA_0| \} / (p_3 + p_4), \\ |vA_0| &< (\gamma_1 + \gamma_2 + \gamma_3) / (p_3 + p_4). \end{aligned} \right\} \quad (3.45)$$

For system (6), by choosing p_2 and p_4 satisfying

$$p_4/p_2 = |vA_0| / (\gamma_1 + \gamma_2 + \gamma_3),$$

the right hand side of (6) in Table 2.7 is maximized:

$$|A_2|^2 + |A_3|^2 < \gamma_1(\gamma_2 + \gamma_3) \{ 1 - |vA_0|^2 / (\gamma_1 + \gamma_2 + \gamma_3)^2 \}. \quad (3.46)$$

We denote the set whose elements satisfy (3.45) (or (3.46)) by $\hat{\Gamma}$. Equation (3.45) and (3.46) implies that the volume of $\hat{\Gamma}$ decreases as $|vA_0|^2$ increases to its maximum value if all the γ_i 's are fixed. We also know that as γ_i , $i = 1, 2, 3$, becomes large, the maximum value of $|vA_0|^2$ and the volume of $\hat{\Gamma}$ increase. As $\gamma_i \rightarrow \infty$, $i = 1, 2$ or 3 , and $\max_i \{\gamma_i\} / |vA_0| \rightarrow \infty$, $\hat{\Gamma}$ is extended to the whole Y-space.

3.3.2 Attractor in X-space

We obtain an attractor of (3) smaller than that described by (2.27) in a manner similar to that given by Treve [27] for the Lorenz system. Equation (2.27) was obtained as follows:

$$\begin{aligned} (d/dt) \{ 2x_1^2 + x_2^2 + (x_3 + 3vA_0)^2 \} &= -4\gamma_1 x_1^2 - 2\gamma_2 x_2^2 - \gamma_3 (2x_3^2 + 6vA_0 x_3) \\ &\leq -2\gamma_1 (2x_1^2) - 2\gamma_2 x_2^2 - \gamma_3 (x_3 + 3vA_0)^2 + 9\gamma_3 |vA_0|^2 \end{aligned}$$

$$\leq -d\{2x_1^2 + x_2^2 + (x_3 + 3vA_0)^2\} + 9\gamma_3|vA_0|^2, \quad d \triangleq \min\{2\gamma_1, 2\gamma_2, \gamma_3\}. \quad (3.47)$$

Hence, the set Ω_0 :

$$\Omega_0 \triangleq \{X : 2x_1^2 + x_2^2 + (x_3 + 3vA_0)^2 < 9(\gamma_3/d)|vA_0|^2\} \quad (3.48)$$

is an attractor. Suppose that $\gamma_3 = d$, and let γ_1 and γ_2 increase while $|vA_0|$ is fixed. Then, from (3.45) and (3.48), $\Omega_0 \subset \hat{\Gamma}$ is satisfied for sufficiently large γ_1 and γ_2 . Hence, by (S.2.3), there exists a set O . Likewise, for sufficiently large γ_3 and fixed γ_1, γ_2 and $|vA_0|$, or for sufficiently small $|vA_0|$ and fixed γ_1, γ_2 and γ_3 , there exists a set O .

Taking the time derivative of $I_1 \triangleq x_1^2 + (x_3 + vA_0)^2$ and $I_2 \triangleq x_2^2 - (x_3 - vA_0)^2$,

$$\dot{I}_1 \leq -d_1 I_1 + \gamma_3 |vA_0|^2, \quad d_1 \triangleq \min\{2\gamma_1, \gamma_3\}, \quad (3.49a)$$

$$\dot{I}_2 \geq \begin{cases} -2\gamma_2 x_2^2 + \gamma_2 (x_3 - vA_0)^2 - \gamma_3 |vA_0|^2, & \text{if } 2\gamma_2 > \gamma_3, \\ -\gamma_3 I_2 - \gamma_3 |vA_0|^2, & \text{if } 2\gamma_2 \leq \gamma_3. \end{cases} \quad (3.49b)$$

Thus, the sets Ω_1 and Ω_2 :

$$\Omega_1 \triangleq \{X : x_1^2 + (x_3 + vA_0)^2 \leq (\gamma_3/d_1)|vA_0|^2\}, \quad (3.50a)$$

$$\Omega_2 \triangleq \{X : -x_2^2 + (x_3 - vA_0)^2 \leq |vA_0|^2\}, \quad (3.50b)$$

are attractors (it was assumed that $2\gamma_2 < \gamma_3$ for Ω_2). Hence, $\hat{\Delta} \triangleq \Omega_0 \cap \Omega_1$ is an attractor, and $\tilde{\Delta} \triangleq \Omega_0 \cap \Omega_1 \cap \Omega_2$ is an attractor if $2\gamma_2 < \gamma_3$. Figure 3.5 gives sketches of $\hat{\Delta}$ and $\tilde{\Delta}$. Here,

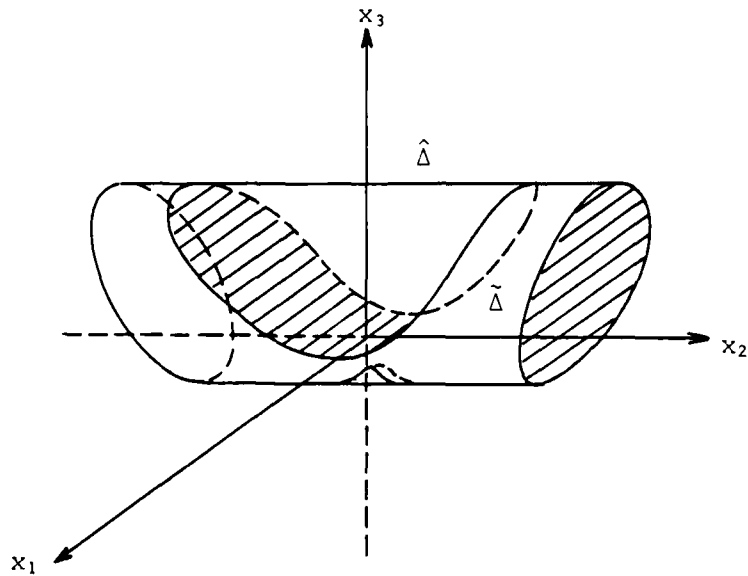


Figure 3.5 Attractors $\hat{\Delta}$ and $\tilde{\Delta}$ of (3)

if $2\gamma_2 \leq \gamma_3$, the dint at the bottom appears when $(\gamma_3/d_1) > 9$.

3.3.3 Phase Locking and Chaotic Solutions

Here, we combine equation (3.45) with Figure 3.5 to see when $\hat{\Delta} \subset \hat{\Gamma}$ is satisfied. If $\hat{\Delta} \subset \hat{\Gamma}$, then by (S.2.3), there exists a set O . If $\hat{\Delta} \subset \hat{\Gamma}$ is not satisfied, the sufficient condition $\hat{\Delta} \subset \hat{\Gamma}$ for the existence of O is too strong or there exists no O .

Suppose that all the γ_i 's are fixed. As mentioned in the previous section, $\hat{\Delta} \subset \hat{\Gamma}$ is satisfied and there exists a set O for sufficiently small $|vA_0|$. In this case, phase locking is of no importance, since the trajectory converges to θ_Y as $t \rightarrow \infty$.

We consider under what conditions $\hat{\Delta} \subset \hat{\Gamma}$ is not satisfied. From (3.45),

$$|A_2|^2 + 2|A_3|^2 < (2\gamma_2 + \gamma_3)(\gamma_1 + \gamma_2), \quad (3.51a)$$

$$||A_1|^2 - 2|A_3|^2| < (2\gamma_1 + \gamma_3)(\gamma_1 + \gamma_2), \quad (3.51b)$$

$$|vA_0|^2 < (2\min\{\gamma_1, \gamma_2\} + \gamma_3)(\gamma_1 + \gamma_2 + \gamma_3). \quad (3.51c)$$

Hence, a necessary condition for $\hat{\Delta} \subset \hat{\Gamma}$ is as shown in Figure 3.6. Here, the projection of $\hat{\Delta}$ onto the (x_2, x_3) -plane and

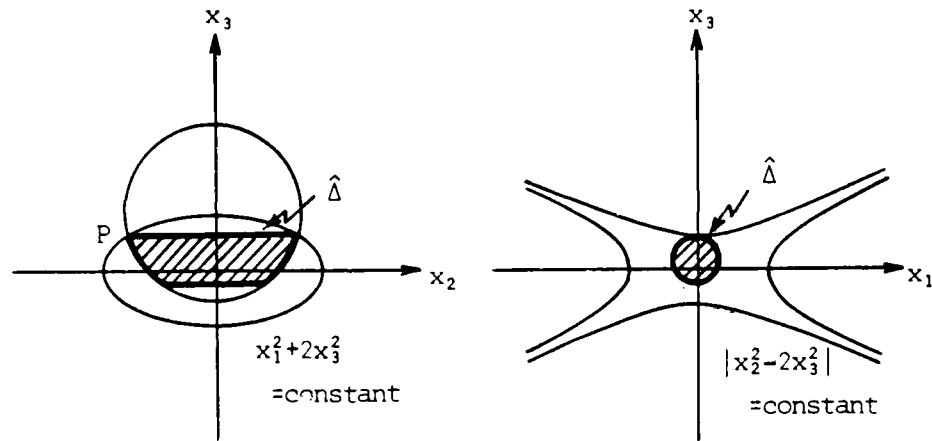


Figure 3.6 Necessary Conditions for $\hat{\Delta} \subset \hat{\Gamma}$

the (x_1, x_3) -plane satisfy (3.51a) and (3.51b), respectively. Then, from (3.48) and (3.51),

$$|vA_0|^2 < (2\gamma_2 + \gamma_3)(\gamma_1 + \gamma_2) / 2 \{ 9(\gamma_3/d) + (\gamma_3/d_1) \} / 2 - \{ 1 - 4(\gamma_3/d)^{1/2} \}^2, \quad (3.52a)$$

$$|vA_0|^2 < (2\gamma_1 + \gamma_3)(\gamma_1 + \gamma_2) / \{ 1 + (\gamma_3/d_1)^{1/2} \}^2. \quad (3.52b)$$

Since $d < d_1$, from (3.52),

$$|vA_0|^2 < (2\gamma_2 + \gamma_3)(\gamma_1 + \gamma_2)/16. \quad (3.53)$$

As mentioned in Section 3.3.1, equation (3) has two nontrivial equilibrium points P_v 's if $A_0^2 > \tilde{A}_0^2$. If $\gamma_2 > \gamma_1 + \gamma_3$,

$$|vA_0|^2 = \gamma_1\gamma_2 > (2\gamma_2 + \gamma_3)(\gamma_1 + \gamma_2)/16. \quad (3.54)$$

Hence, if $\gamma_2 > \gamma_1 + \gamma_3$, (3.52) does not hold for $A_0^2 > \tilde{A}_0^2$. In other words, when system (3) has periodic or chaotic solutions globally ($A_0^2 > \hat{A}_0^2$), the sufficient condition $\hat{\Delta} < \hat{\Gamma}$ is too strong so that we cannot determine whether there exists a set O .

It is likely that there may exist an attractor smaller than $\hat{\Delta}$, since equation (3.52) is determined at points P and Q in Figure 3.6. Equation (3.49) is derived by the method similar to that in (3.47). The inequality corresponding to the second inequality in (3.47) used to derive (3.49a) holds with a large margin at P . Furthermore, since $\gamma_2 > \gamma_1 + \gamma_3$, the inequality corresponding to the second inequality in (3.47) used to derive (3.49b) also holds with a large margin. Later, we shall evaluate the size of attractor by direct integration of equation (3). On the other hand, the sufficient condition (3.45) for the convergence of $\xi(t)$ to θ_ξ is obviously too strong. The maximum value of $|vA_0|$ satisfying (3.45) is

$$|vA_0|_{\max}^2 = (2\gamma_1 + \gamma_3)(2\gamma_2 + \gamma_3)/4,$$

when $p_3 = |vA_0|/(2\gamma_2 + \gamma_3)$ and $p_4 = |vA_0|/(2\gamma_1 + \gamma_3)$. Since $s(|vA_0|_{\max}) < 0$ ((3.7)), $|vA_0|_{\max} < |\hat{vA}_0|$. Hence, if $A_0^2 > \hat{A}_0^2$, the set $\hat{\Gamma}$ is empty.

Equation (6) has a solution which goes to infinity as $t \rightarrow \infty$ on the x_1 -axis. Hence, there is no natural boundary of the trajectories of (6) as in the case of equation (3). On the other hand, the numerical results in the next chapter suggest that the pseudo-chaotic solutions of (6) are bounded for certain values of parameters. If such trajectories are contained in $\hat{\Gamma}$ ((3.46)), there exists a set O . For other values of parameters, the limit set of the pseudo-chaotic solutions appears to be unbounded. If the limit set is unbounded, it is not contained in $\hat{\Gamma}$ in the Y -space. Then, the sufficient condition in (S.2.3) for the existence of O is too strong, or there does not exist a set O .

3.3.4 Local Properties of Original Systems

In the previous sections, we did not prove the existence of O for system (3') or (6'). In this section, we study the local properties of these systems about certain sets and the stability of $\bar{\Sigma}_0$, which will provide some insight on the convergence of the trajectories to Σ .

If $\hat{e} \triangleq |vA_0|^2 - \gamma_1\gamma_2 > 0$ in (3'), then the equilibrium set consists of $P_{0Y} = \{\theta_Y\}$ and

$$EQ_3 = \{Y: (r_1, r_2, r_3) = ((\gamma_3/\gamma_1)\hat{e}^{1/2}(|vA| - \hat{e}^{1/2}))^{1/2}, \{\gamma_1\gamma_3\hat{e}^{1/2}/(|vA_0| - \hat{e}^{1/2})\}^{1/2}, \hat{e}^{1/2}\},$$

$$\sin(\theta_1 + \theta_2) = \sin(\theta_1 - \theta_2 - \theta_3) = 1\}, \quad (3.55)$$

where $vA_0 < 0$ is assumed. The characteristic equation of $d\hat{F}/dY$ for (3') at any point P_Y EQ_3 is $\hat{p}(\lambda) \triangleq p_Y(\lambda)\tilde{p}(\lambda) = 0$, where

$$\begin{aligned} \tilde{p}(\lambda) = & \lambda\{\lambda^2 + (\gamma_1 + \gamma_2 + \gamma_3)\lambda + \gamma_3(\gamma_1 + \gamma_2)|vA_0| \\ & / (|vA_0|e^{\hat{e}_2} - 2(\gamma_3/\gamma_1)|vA_0|e^{\hat{e}_2})\}, \end{aligned} \quad (3.56)$$

and P_Y is defined in (3.3b). If $\gamma_2 > \gamma_1 + \gamma_3$ and $A_0^2 > \hat{A}_0^2$, equation (3.56) has a zero root and two stable roots. As mentioned earlier, equation (3.3b) has a pair of complex roots with positive real parts if $\gamma_2 > \gamma_1 + \gamma_3$ and $A_0^2 > \hat{A}_0^2$. Hence, all the eigenvectors corresponding to the unstable roots of (3.5b) lie on $\bar{\Sigma}_\theta$ at P_Y where $\theta_3 = \theta$. Thus, there is no unstable manifold which is transverse to $\bar{\Sigma}_\theta$ at its corresponding P_Y .

For system (3'), the intersection of all the $\bar{\Sigma}_\theta$'s is the origin P_{0Y} . The characteristic equation of $d\hat{F}/dY$ at P_{0Y} is $\hat{p}_0(\lambda) \triangleq p_0(\lambda)^2 = 0$, where p_0 is defined in (3.3a). We know that (3.3a) has one positive and two negative real roots if $|vA_0|^2 > \gamma_1\gamma_2$. Hence, there is a two-dimensional space ES_{Y+} spanned by the eigenvectors corresponding to the unstable eigenvalues at P_{0Y} . As mentioned in Section 3.1.1, the eigenspace in $\bar{\Sigma}_\theta$ corresponding to the unstable eigenvalues of dF/dX at θ_X is one dimensional. Therefore, ES_{Y+} is transverse to all the $\bar{\Sigma}_\theta$'s at P_{0Y} .

We shall show that ES_{Y+} lies in Σ at P_{0Y} , which

implies that the trajectories tend to approach Σ about P_{0Y} .

The positive root of (3.3a) is

$$\lambda_{Y+} = [\{(\gamma_1 - \gamma_2)^2 + 4|vA_0|^2\}^{1/2} - (\gamma_1 + \gamma_2)]/2,$$

and

$$ES_{Y+} = \{Y: Y = (-vA_0\eta_1, -vA_0\eta_2, \lambda_{Y+}\eta_2, \lambda_{Y+}\eta_1, 0, 0)^T; \eta_1, \eta_2 \in \mathbb{R}\}.$$

On the other hand, in Σ ,

$$y_1y_2 - z_1z_2 = 0, \quad (y_1y_2 + z_1z_2)y_3 + (z_1y_2 - y_1z_2)z_3 = 0. \quad (3.57)$$

If $Y \in ES_{Y+}$, Y satisfies (3.57) for any (η_1, η_2) . Hence, $ES_{Y+} \subset \Sigma$.

The matrix $d\hat{F}/dY$ at P_{0Y} has a block diagonal representation. The submatrix corresponding to the (y_3, z_3) -space is diagonal and has a repeated eigenvalue $-\gamma_3$. This implies that $\theta_3(t)$ tends to a constant about P_{0Y} . On the other hand, $\theta_1(t)$ and $\theta_2(t)$ tend to vary about P_{0Y} , since ES_{Y+} does not coincide with the (y_1, z_1) or (y_2, z_2) -space. In the above sense, $\bar{\Sigma}_0$ is unstable about P_{0Y} .

Finally, we examine the extent of the unstable manifolds tangent to ES_{Y+} at the origin, along the (y_3, z_3) -direction. The characteristic equation of the linearized vector field about Σ_0 ($\hat{=} \{Y: r_1 = r_2 = 0\}$) is

$$p(\lambda) \hat{=} \{\lambda^2 + (\gamma_1 + \gamma_2)\lambda + (\gamma_1\gamma_2 - |vA_0|^2) + r_3^2\}^2 = 0. \quad (3.58)$$

Suppose that $|vA_0|^2 > \gamma_1\gamma_2$, then (3.58) has unstable roots for $r_3^2 < |vA_0|^2 - \gamma_1\gamma_2$, and has only stable roots for

$$r_3^2 > |vA_0|^2 - \gamma_1 \gamma_2.$$

If $|vA_0| > \gamma_1$ in (6'), the equilibrium set consists of P_{0Y} and

$$EQ_6 = \{Y : (r_1, r_2, r_3) = ((\gamma_2 \gamma_3)^{\frac{1}{2}}, \{(|vA_0| - \gamma_1) \gamma_3\}^{\frac{1}{2}}, \{(|vA_0| - \gamma_1) \gamma_2\}^{\frac{1}{2}}),$$

$$\sin(2\theta_1) = \sin(\theta_1 - \theta_2 - \theta_3) = 1\}, \quad (3.59)$$

where $vA_0 < 0$ is assumed. The characteristic equation of $d\hat{F}/dY$ for (6') at any point P_Y in EQ_6 is $\hat{p}(\lambda) = p(\lambda)\tilde{p}(\lambda) = 0$, where

$$\tilde{p}(\lambda) \triangleq \lambda\{\lambda^2 + \lambda(\gamma_1 + \gamma_2 + \gamma_3 + |vA_0|) + 2(\gamma_2 + \gamma_3)|vA_0|\} = 0, \quad (3.60)$$

and p is defined in (3.32b). Equation (3.60) does not have unstable roots. Hence, the eigenvectors corresponding to the unstable roots of (3.32b) lie in $\bar{\Sigma}_\theta$ at P_Y where $\theta_3 = \theta$. Thus, there is no unstable manifold which is transverse to $\bar{\Sigma}_\theta$ at its corresponding P_Y . At the origin, the characteristic equation of $d\hat{F}/dY$ has only one unstable root. The eigenspace corresponding to this root coincides with the one-dimensional space $S_1 = \{Y : r_2 = r_3 = 0, \cos(2\theta_1) = 0, \sin(2\theta_1) = 1\}$, which lies in Σ_θ for all θ .

For system (6'), the intersection of all the $\bar{\Sigma}_\theta$'s is the surface $S_2 = \{Y : r_2 = r_3 = 0\}$. The characteristic equation of the linearized vector field about S_2 is

$$\hat{p}(\lambda) \triangleq \{\lambda^2 + (\gamma_2 + \gamma_3)\lambda + \gamma_2 \gamma_3 - r_1^2\}^2 = 0. \quad (3.61)$$

The above equation has a repeated unstable root:

$$\lambda_{Y+} = [\{(\gamma_2 - \gamma_3)^2 + 4r_1^2\}^{1/2} - (\gamma_2 + \gamma_3)]/2,$$

if $r_1^2 > \gamma_2 \gamma_3$. Hence, if $r_1^2 > \gamma_2 \gamma_3$, S_2 is unstable.

Moreover, $\theta_2(t)$ and $\theta_3(t)$ tend to vary about S_2 , since the submatrix of the linearized vector field corresponding to the (y_2, z_2, y_3, z_3) -space is not diagonal except for the origin. In this sense, $\bar{\Sigma}_\theta$ is unstable about S_2 .

We have proved that for (3'), $\bar{\Sigma}_\theta$ is unstable about the origin and for (6'), $\bar{\Sigma}_\theta$ is unstable about S_2 . In (6'), the trajectories always approach the origin before approaching S_2 . Hence, the trajectories of (3') and (6') may not converge to one of $\bar{\Sigma}_\theta$'s if the trajectories get arbitrarily close to the origin without converging to the origin as $t \rightarrow \infty$, that is,

$$\left. \begin{aligned} \limsup_{t \rightarrow \infty} \sup_{\tau < t} \|Y(\tau)\| &> 0, \\ \liminf_{t \rightarrow \infty} \inf_{\tau < t} \|Y(\tau)\| &= 0, \end{aligned} \right\} \quad (3.62)$$

where $Y(t) = Y(t, Y_0)$. The question is whether the nonconvergence of the trajectories to one of $\bar{\Sigma}_\theta$'s implies the nonconvergence of the trajectories to Σ . Intuitively, it is less likely that there exists a trajectory which converges to the union of more than one $\bar{\Sigma}_\theta$'s as $t \rightarrow \infty$, but it is difficult to prove it.

3.3.5 Energy of Original Systems

Let $I \triangleq \{2|A_1|^2 + |A_2|^2 + |A_3|^2\}/2$ in system (3'). We call

I an energy function of (3') for convenience. We shall see the difference between the behaviors of I for the original and reduced systems. Taking the time derivative of I,

$$\begin{aligned} \dot{I} = & -[2\gamma_1\{|A_1| - (3\nu/4\gamma_1)|vA_0||\sin(\theta_1+\theta_2)||A_2|\}^2 \\ & + \{\gamma_2 - (3\nu|vA_0||\sin(\theta_1+\theta_2)|)^2/(8\gamma_1)\}|A_2|^2 + \gamma_3|A_3|^2], \end{aligned} \quad (3.63)$$

where $\nu = \text{sgn}\{vA_0\sin(\theta_1+\theta_2)\}$. Equation (3.63) is sketched in Figure 3.7, where E is a constant I surface. Since $|vA_0|^2 > \gamma_1\gamma_2$, the second term of the right hand side of (3.62) can

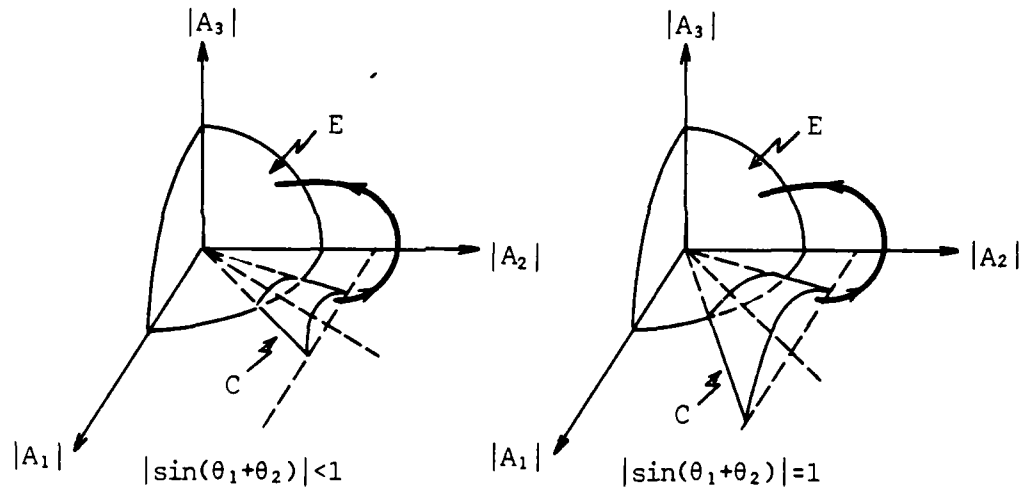


Figure 3.7 Dynamics of Energy of (3')

be negative. Hence, we have an elliptic cone $C: \dot{I} = 0$, in which the energy I increases, and outside which I decreases. The line of foci and the radii of the cone vary as $\theta_1+\theta_2$ varies. We assume that $vA_0 < 0$. Then, if

$$\sin(\theta_1 + \theta_2) < (8^{1/2}/3)(\gamma_1 \gamma_2)^{1/2}/|vA_0|,$$

cone C does not exist and the energy I decreases. For (3) or on Σ , $\sin(\theta_1 + \theta_2) = \pm 1$ and the cone C is fixed.

Taking the time derivative of I for (6'),

$$\dot{I} = -\{2(\gamma_1 - v|vA_0||\sin 2\theta_1|)|A_1|^2 + \gamma_2|A_2|^2 + \gamma_3|A_3|^2\}, \quad (3.64)$$

where $v = -\text{sgn}(vA_0 \sin 2\theta_1)$. Since $|vA_0| > \gamma_1$ for chaotic motion, the first term of the right hand side of (3.64) can be negative. Hence, we also have an elliptic cone C as in the case of (3'). The line of foci is fixed at the $|A_1|$ -axis, and the radii of cone vary as θ_1 varies. If $\sin 2\theta_1 < \gamma_1/|vA_0|$, I always decreases. For (6') or on Σ , $\sin 2\theta_1 = \pm 1$ and the cone C fixed.

CHAPTER 4

NUMERICAL EXPERIMENTS

In this chapter, we present some numerical results for equations (3'), (3), (6') and (6). An attempt will be made to correlate some of the numerical results with the analytical results given in the previous chapters. Equation (3) has already been studied numerically by Pikovskii et al. [12]. In the calculations, we use the normalized time γt , where $\gamma = \max\{\gamma_1, \gamma_2, \gamma_3\}$ for (3') and (3), and $\gamma = \max\{\gamma_2, \gamma_3\}$ for (6') and (6). In what follows, we denote the normalized time by t also. By the substitutions:

$$\left. \begin{aligned} A_i/\gamma &\rightarrow A_i, \quad i = 0, 1, 2, 3, \\ x_i/\gamma &\rightarrow x_i, \quad \gamma_i/\gamma \rightarrow \gamma_i, \quad i = 1, 2, 3, \end{aligned} \right\} \quad (4.1)$$

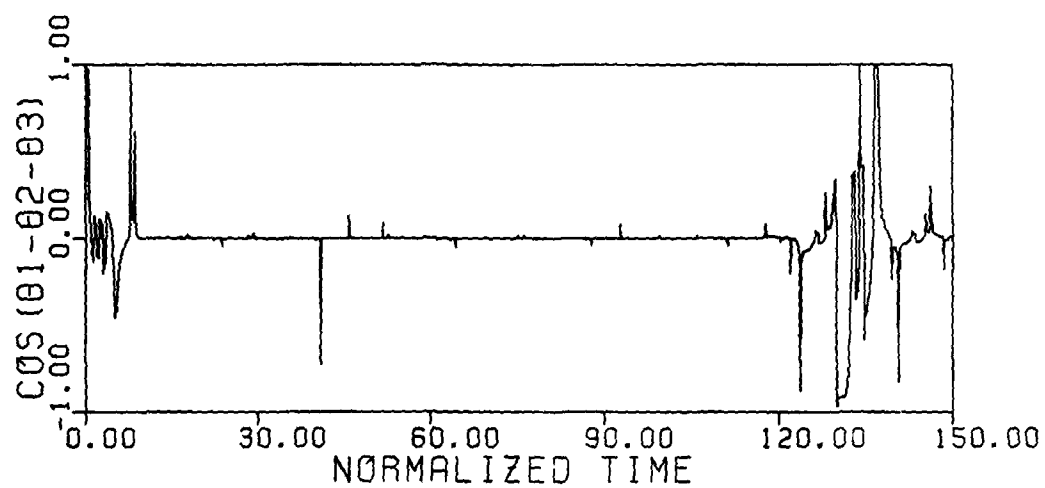
we obtain a system described by the same equation except for $\gamma = 1$. Any equations derived in the previous chapters are not changed by this substitution.

4.1 Behavior of Original Systems (3') and (6')

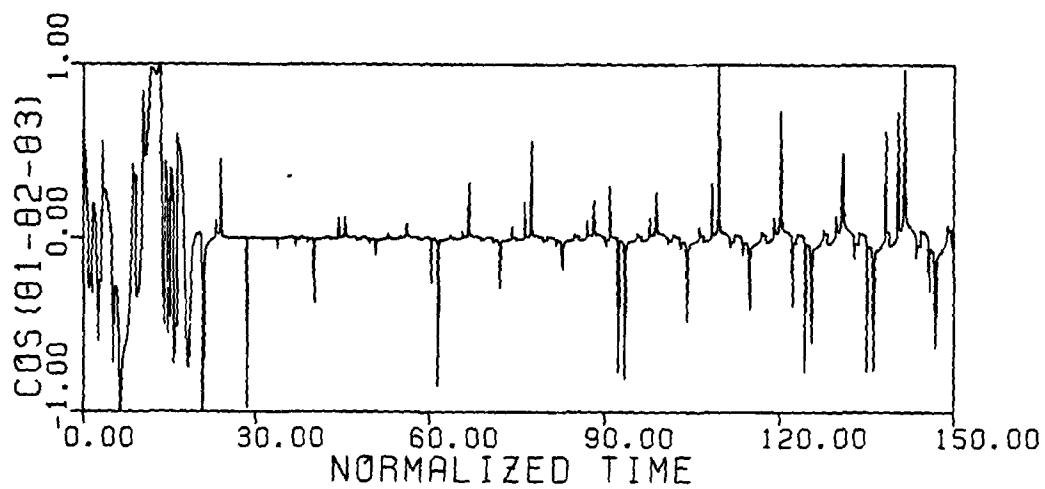
We fix the values of parameters as follows: $\gamma_1 = \gamma_3 = 0.25$, $\gamma_2 = 1$. These are the values used by Pikovskii et al. [12] for the model (1.4) describing the parametric interaction of a whistler with ion sound and plasma oscillations near the lower hybrid resonance combined with the three-wave

interaction involving another plasma wave synchronous to the parametrically excited pair. For these values, the condition $\gamma_2 > \gamma_1 + \gamma_3$ is satisfied. Hence, the stability of the equilibrium points is as follows: For $|vA_0| < |\tilde{vA}_0| = 0.5$, P_0 is stable and P_v does not exist; for $0.5 < |vA_0| < |\hat{vA}_0| = 1.259$, P_0 is unstable and P_v is stable; and for $|vA_0| > 1.259$, P_0 and P_v are unstable.

The condition (3.45) is violated for $|vA_0| > 1.259$. On the other hand, numerical results show that the phases are nearly locked for $|vA_0| < 3.0$ at least for 150 time units. The plots of $\cos(\theta_1(t) - \theta_2(t) - \theta_3(t))$ and $(\text{Re}(A_1(t))/|vA_0|, \text{Im}(A_1(t))/|vA_0|)$ are shown in Figures 4.1 and 4.2, respectively. As $|vA_0|$ increases from 3.0, the nearly phase-locked state appears to be unstable. At $|vA_0| = 3.2$, an abrupt phase change occurs occasionally in an unpredictable manner (Fig. 4.1(a), 4.2(a), (a')). In Figure 4.2(a'), we do not observe any abrupt phase change for 150 time units, while in (a) (corresponding to Fig. 4.1(a)), it is observed twice. From this observation, it seems to be difficult to determine numerically the critical value of $|vA_0|$ at which such a phase change takes place. For, even if no abrupt phase change is observed over a long time interval, we do not know whether it will occur at the next moment. At $|vA_0| = 3.5$, the abrupt phase change occurs more often (Fig. 4.1(b), 4.2(b)). At $|vA_0| = 4.0$, the phase varies in a complicated manner most of the time (Fig. 4.1(c), 4.2(c)). At $|vA_0| = 8.0$,

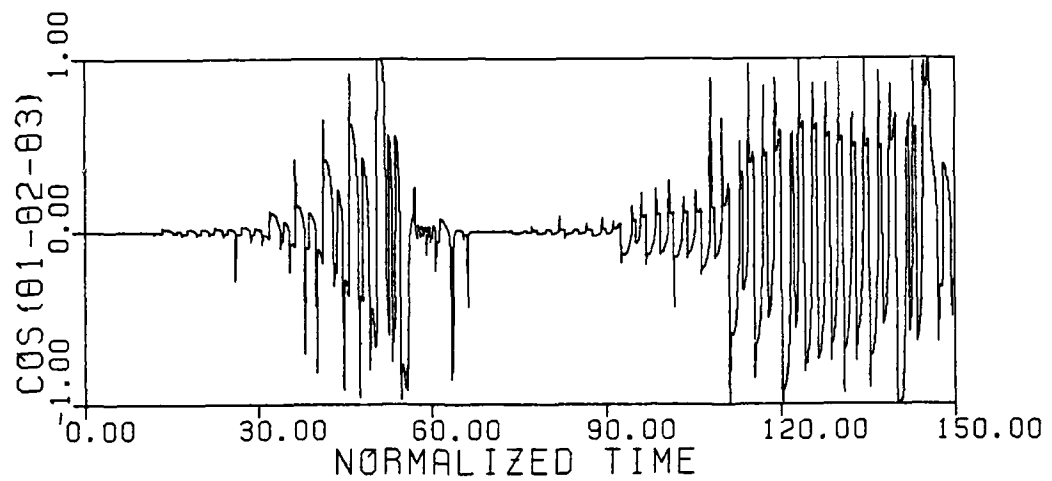


(a)

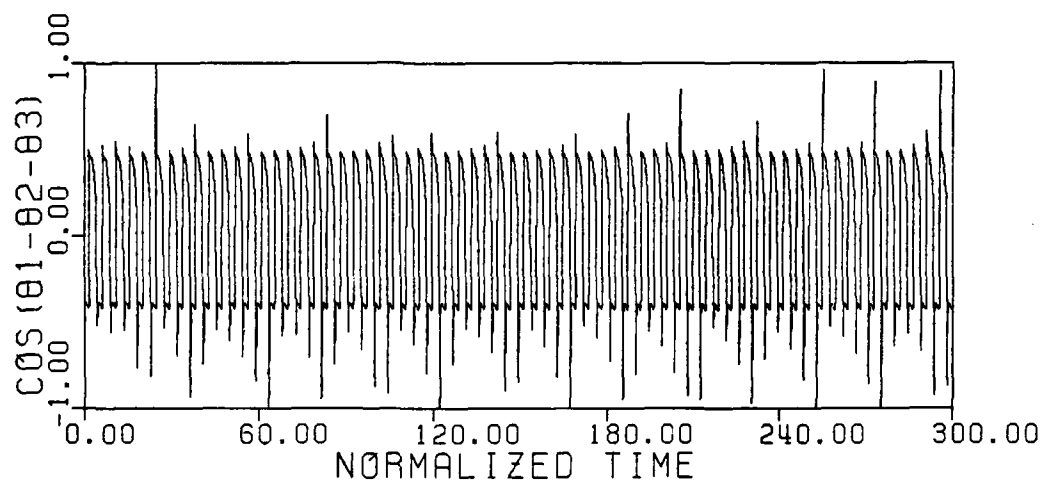


(b)

Figure 4.1 Time Variations of Phase Difference
of (3')



(c)



(d)

Figure 4.1 Time Variations of Phase Difference
of (3')

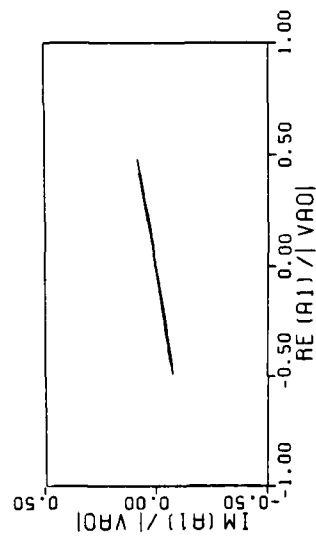
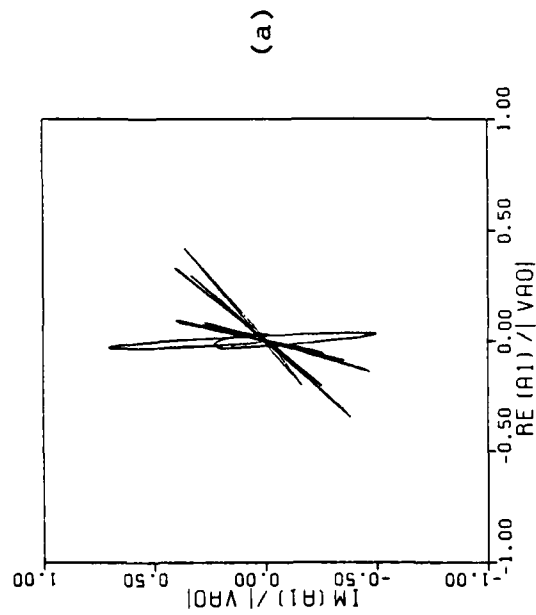
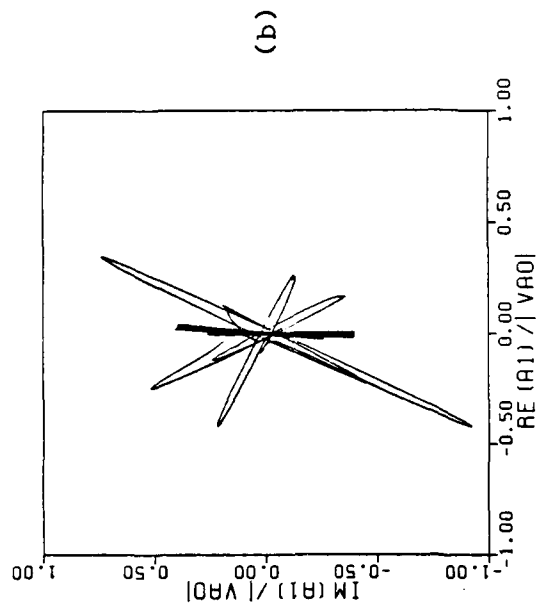


Figure 4.2 Plots of Wave Amplitude
of (3')

AD-A094 628

CALIFORNIA UNIV LOS ANGELES SCHOOL OF ENGINEERING A--ETC F/6 20/9
CHAOTIC SOLUTIONS OF NONLINEAR WAVE-WAVE INTERACTING SYSTEMS IN--ETC(U)
JUN 80 K MASUI AFOSR-79-0050

UNCLASSIFIED

UCLA-ENG-8026

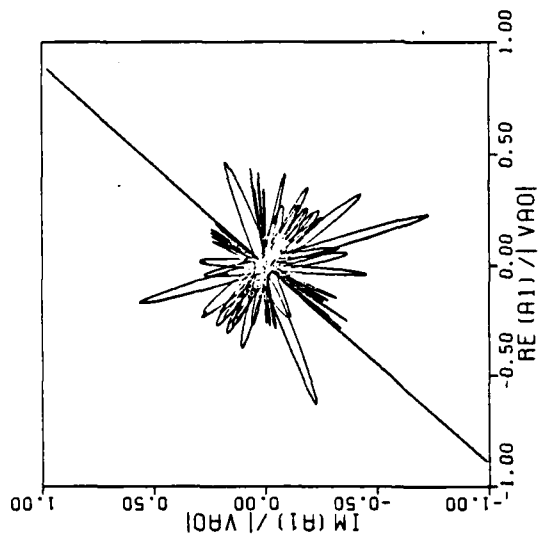
AFOSR-TR-81-0074

NL

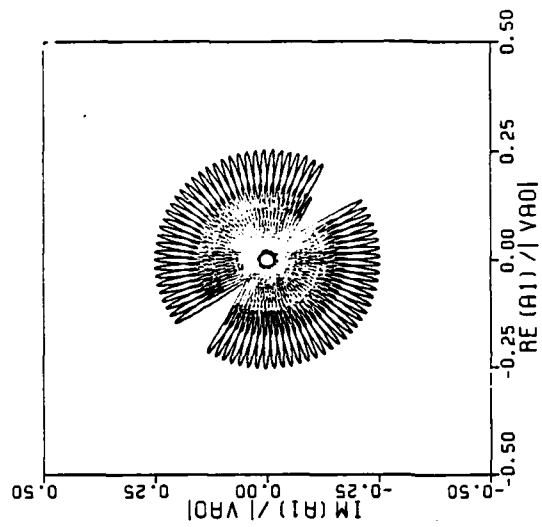
2 OF 2
MICROFILMED



END
DATE
FILMED
3 81
DTIC



(c)



(d)

Figure 4.2 Plots of Wave Amplitude of (3')

the phase varies periodically with time (Fig.4.1(d),4.2(d)). Thus, for $|vA_0| \geq 3.5$, the reduced system (3) does not represent the original system (3') most of the time. For $|vA_0| \leq 3.2$, system (3) may represent (3') most of the time, but not asymptotically.

It is observed that the abrupt phase changes occur only about Σ_0 near the origin. This is consistent with the result in Section 3.3.4 where it was shown that there exists an unstable manifold at Σ_0 if $r_3^2 < |vA_0|^2 - \gamma_1\gamma_2$. The extent of this manifold is increased as $|vA_0|$ increases, which may be one of the reasons why the abrupt phase changes occur more often as $|vA_0|$ increases. According to the observation, the hypothesis (3.62) appears to be satisfied, that is, the trajectories always return to an arbitrary neighborhood of the origin. Furthermore, the numerical results show that as A_0^2 decreases to \hat{A}_0^2 ((3.8)), the trajectories are trapped in a smaller neighborhood of Σ , but they do not converge to Σ as $t \rightarrow \infty$.

For system (6'), we fix the values of parameters as follows: $\gamma_1 = \gamma_2 = 0.4$ and $\gamma_3 = 1$. These values are reasonable for the model such that plasma wave 1 generated by an external wave decays into another plasma wave 2 and an ion acoustic wave 3. The numerical results show that for a wide range of parameter values, the phase becomes locked rapidly and remain locked (within the accuracy of computation). The phase is locked even when condition (3.47) is not

satisfied.

As mentioned in Section 3.3.4, the trajectories approach the origin before approaching S_2 . From the observation, equation (3.62) appears to be satisfied for certain values of $|vA_0|$. Therefore, the trajectories may return to an arbitrary neighborhood of S_2 repeatedly. According to the analysis in Section 3.3.4, $\bar{\Sigma}_\theta$ is unstable about S_2 . Hence, the abrupt phase changes may occur about S_2 . But, actually, we did not observe any abrupt phase changes for (3') for a wide range of parameter values. This result may be explained as follows. Since the trajectories approach Σ exponentially about the origin (Section 2.3), therefore as a trajectory gets closer to S_2 , it is closer to Σ . From the continuity of the vector field, the vector $\hat{F}(Y)$ tends to parallel to $\bar{\Sigma}_\theta$ as Y approaches Σ except in the neighborhood of a certain set containing S_2 and EQ_6 . The volume of such a neighborhood is smaller, as a smaller neighborhood of Σ is considered. Hence, it is less likely that the trajectory moves transverse to $\bar{\Sigma}_\theta$ as it gets closer to Σ . That is, it is less likely that about S_2 , the trajectory moves across $\bar{\Sigma}_\theta$'s and the abrupt phase change occurs.

4.2 Behavior of Reduced Systems (3) and (6)

In what follows, we consider only the reduced system (3) and (6). For (3), we assume that $1.259 \leq |vA_0| \leq 3.2$ for which the system may have a chaotic solution, and describes

(3') approximately most of the time, but not asymptotically as $t \rightarrow \infty$. For (6), we assume that $|vA_0| > 0.4$ for which (6) may have a chaotic solution and describes the asymptotic behavior of (6').

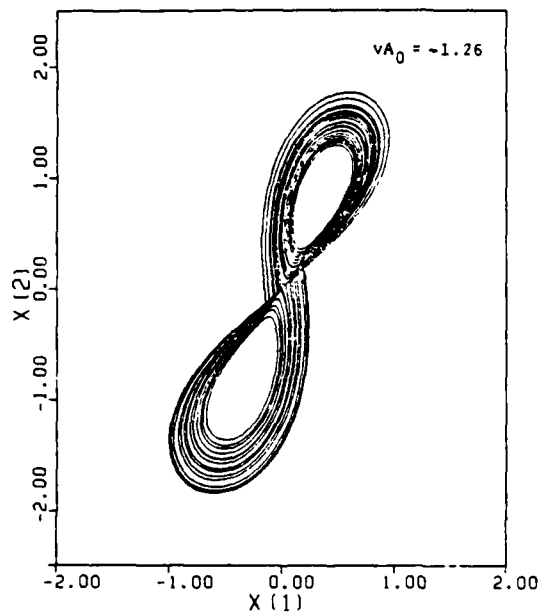
4.2.1 System (3)

The projection of the trajectory onto the (x_1, x_3) -plane is shown in Figure 4.3. At each value of vA_0 , there appears a pseudo-chaotic attractor. According to Pikovskii et al. [12], periodic solutions appear for $|vA_0| \geq 3.35$. But, as mentioned earlier, equation (3) does not describe equation (3') approximately most of the time for such values of $|vA_0|$.

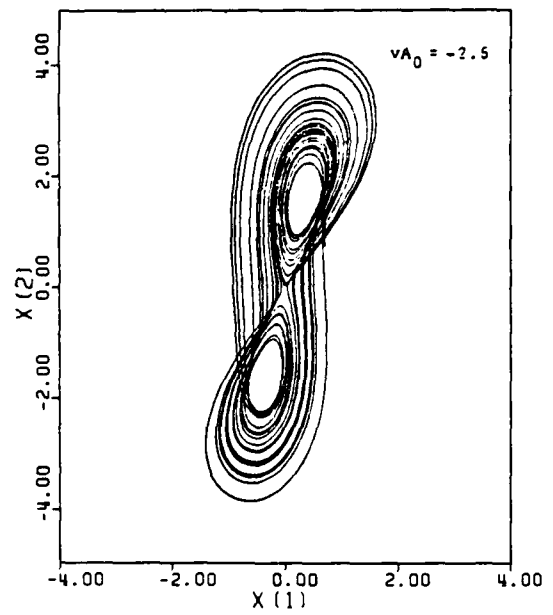
The attractors in the Figure 4.3 resemble two-dimensional surfaces. But, their cross sections have a complicated structure. Let us consider a connected set Q on a plane PL which is transverse to the trajectories as shown in Figure 4.4. In equation (3), the phase volume shrinks uniformly, since

$$\frac{\partial \dot{x}_1}{\partial x_1} + \frac{\partial \dot{x}_2}{\partial x_2} + \frac{\partial \dot{x}_3}{\partial x_3} = -(\gamma_1 + \gamma_2 + \gamma_3) < 0. \quad (4.1)$$

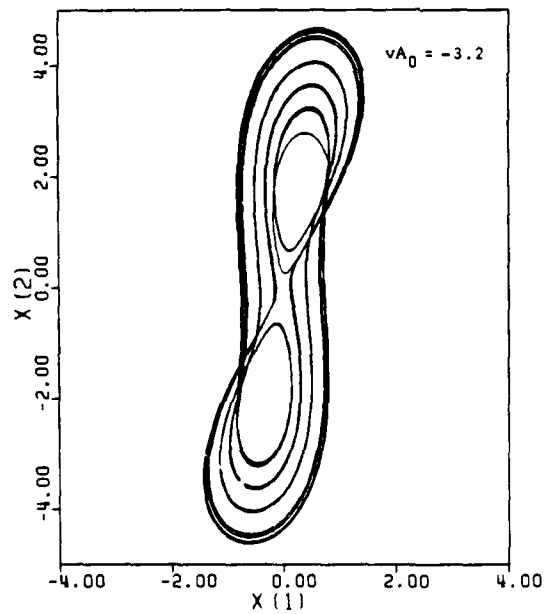
Hence, the area of Q shrinks exponentially to zero as $t \rightarrow \infty$. Simultaneously, as shown in Figure 4.3, Q is stretched in one direction while moving around the nontrivial equilibrium point P_v (Fig. 4.3(a)). Hence, compression of Q must take place along another direction. In Figure 4.3(a), Q is split



(a)



(b)



(c)

Figure 4.3 Projections of Trajectories of (3)

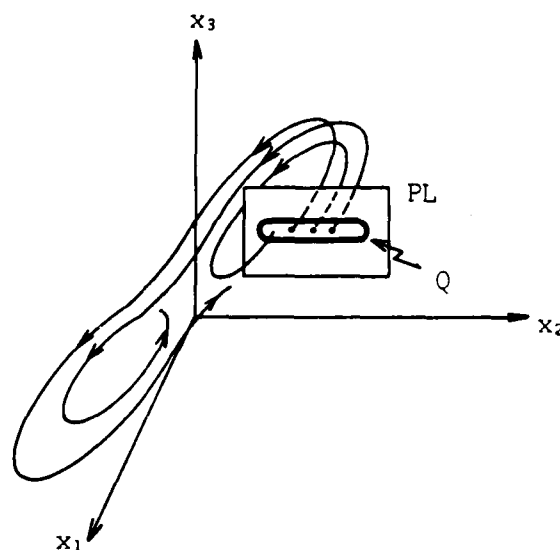


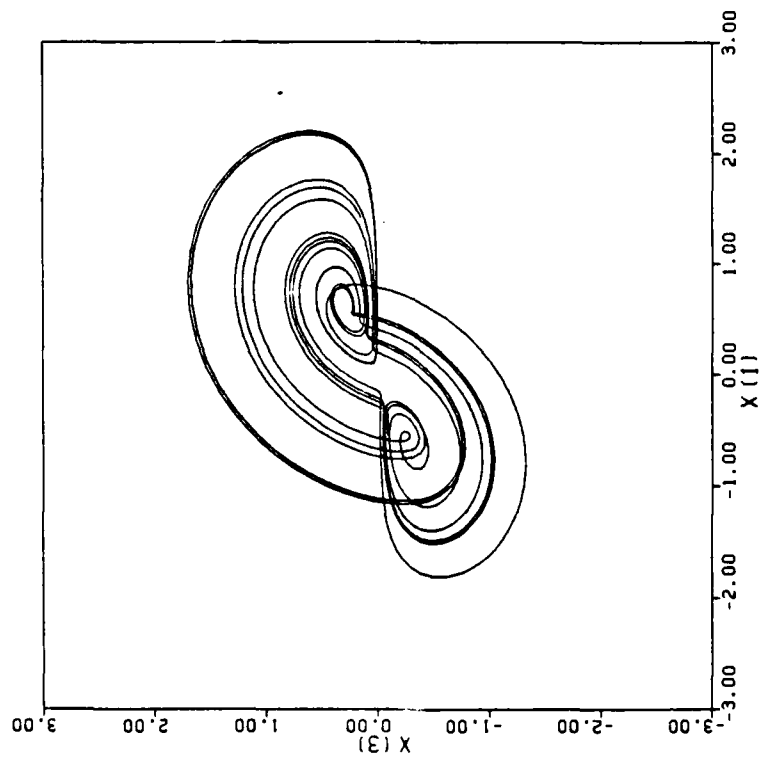
Figure 4.4 First Return Mapping

into two parts at the origin and then folded. In (b), Q is also bent along those portions of the trajectories which are close to P_v . If we consider a first return mapping from PL into PL , Q is finally mapped into a set exhibiting a Cantor-set like structure after stretching, splitting and bending infinitely many times.

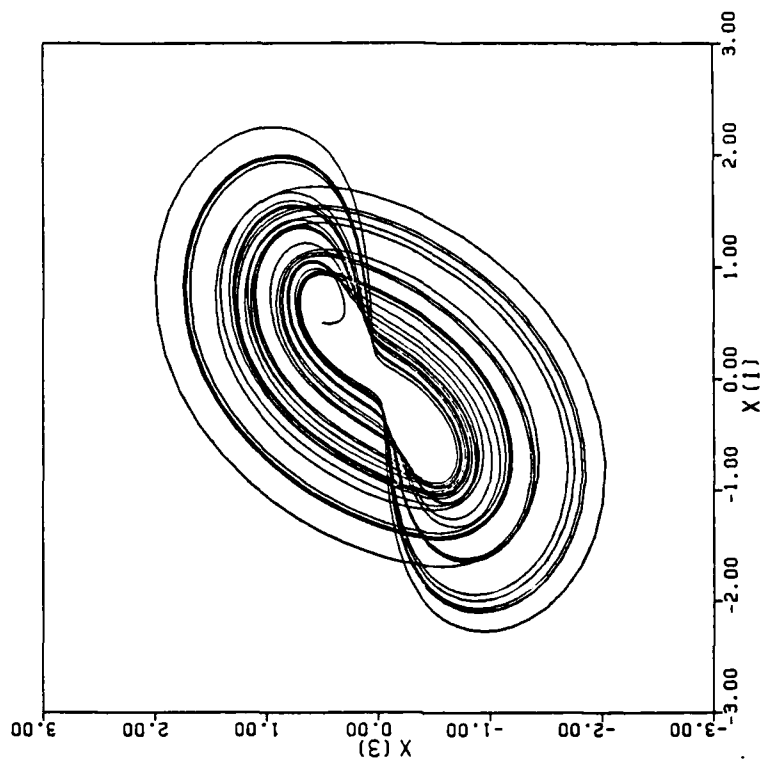
4.2.2 System (6)

Here, a detailed numerical study for system (6) is made. The projection of the trajectories onto the (x_1, x_3) -plane is shown in Figure 4.5. In equation (6), the phase volume also shrinks uniformly if $|vA_0| < \gamma_1 + \gamma_2 + \gamma_3 = 1.8$, since

$$\frac{\partial \dot{x}_1}{\partial x_1} + \frac{\partial \dot{x}_2}{\partial x_2} + \frac{\partial \dot{x}_3}{\partial x_3} = |vA_0| - (\gamma_1 + \gamma_2 + \gamma_3) < 0. \quad (4.2)$$

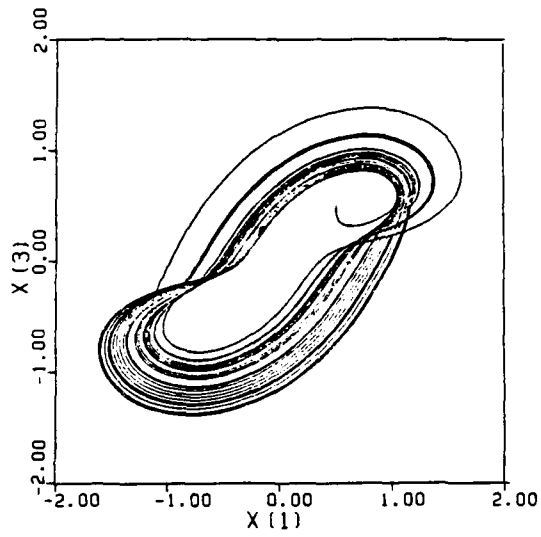


(a)

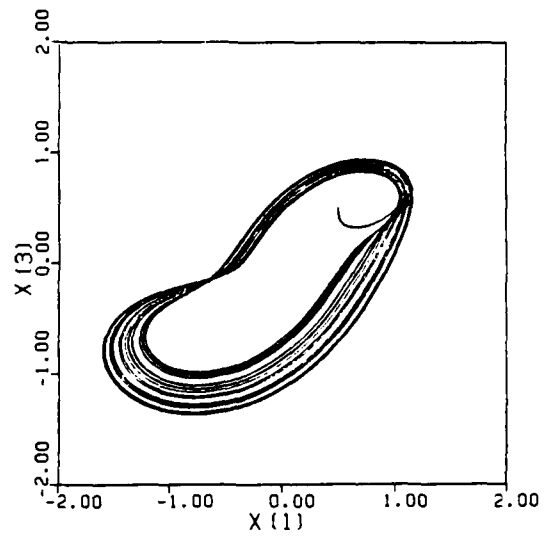


(b)

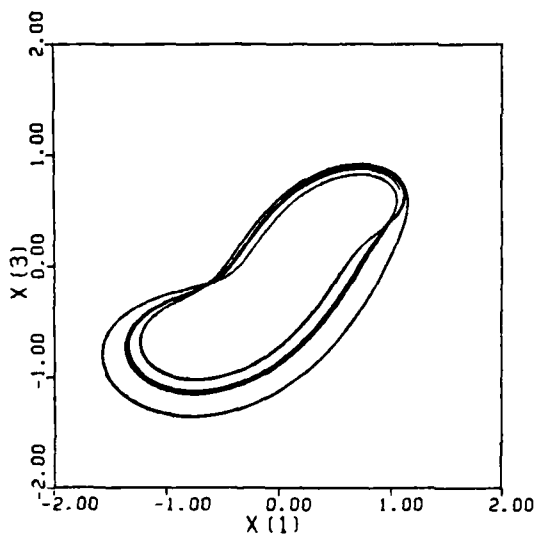
Figure 4.5 Projections of Trajectories of (6)



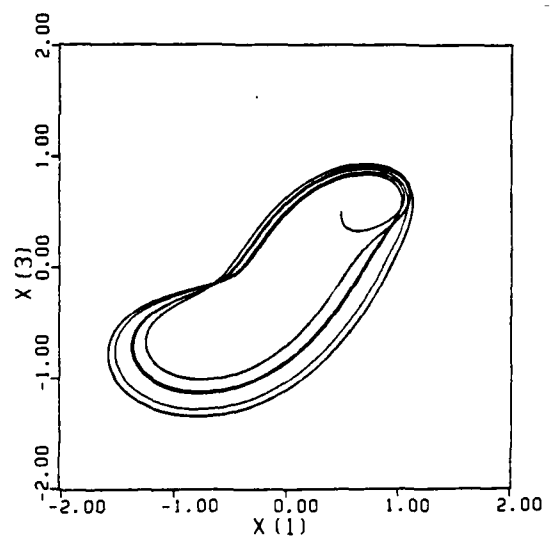
(c)



(d)

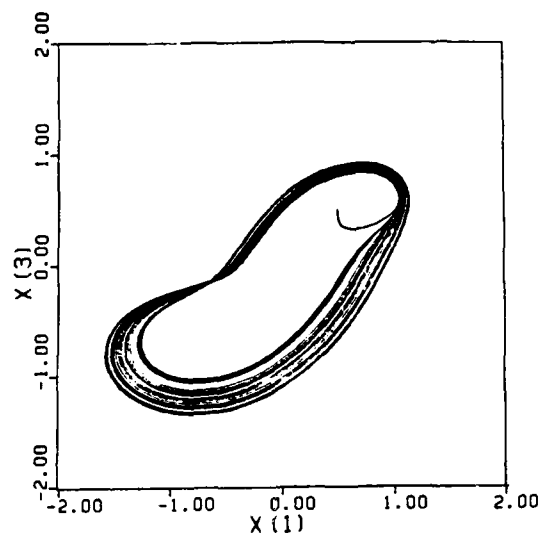


(e)

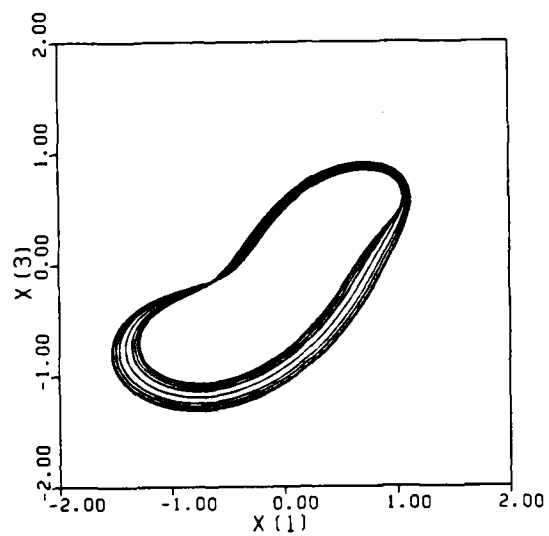


(f)

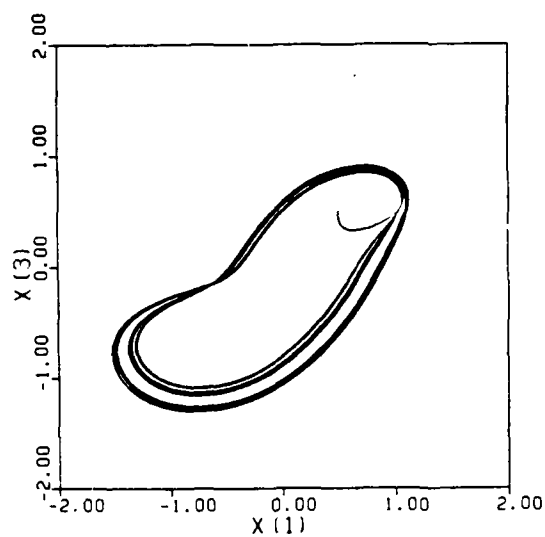
Figure 4.5 Projections of Trajectories of (6)



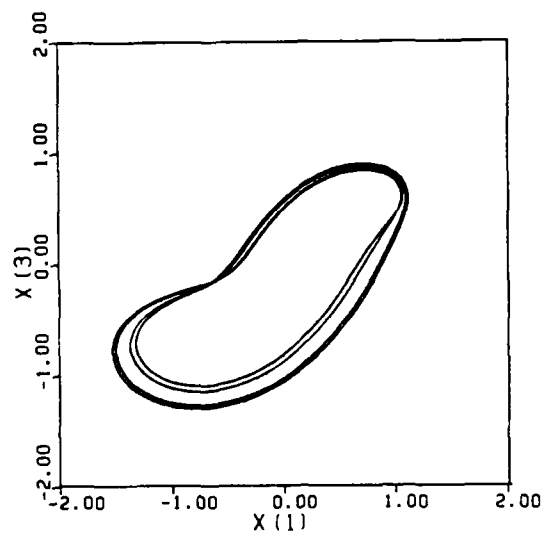
(g)



(h)

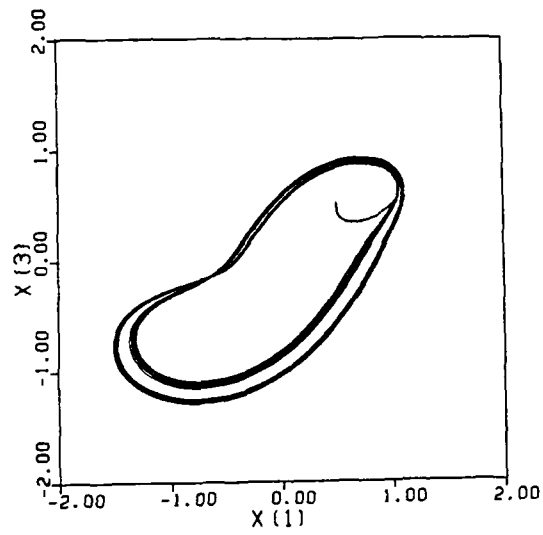


(i)

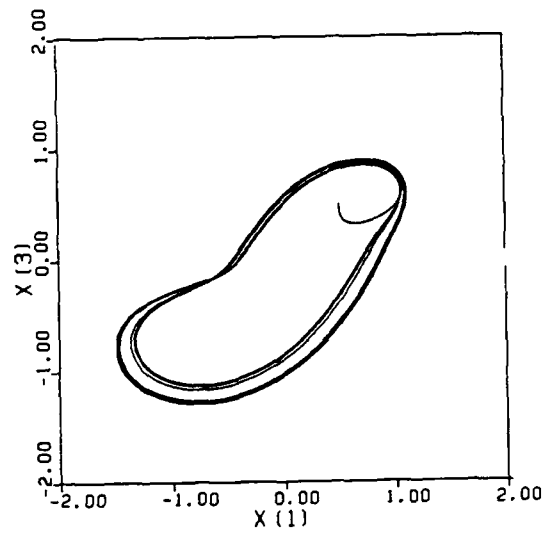


(j)

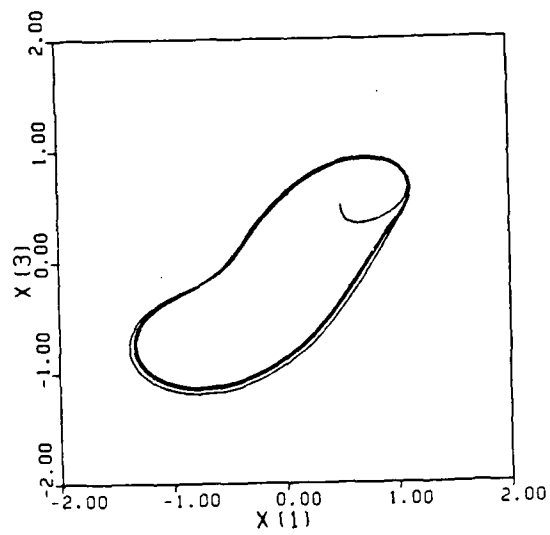
Figure 4.5 Projections of Trajectories of (6)



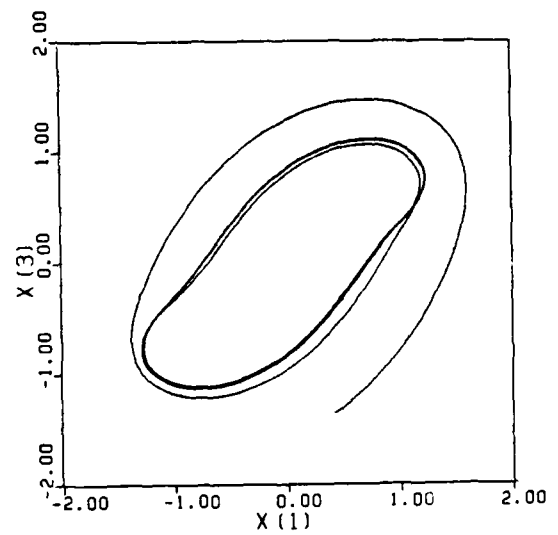
(k)



(l)



(m)



(n)

Figure 4.5 Projections of Trajectories of (6)

As $\gamma_1' \triangleq |vA_0| - \gamma_1 = 0.2$, the solution is pseudo-chaotic (see Fig.4.5(a)). A set Q as defined in the previous section is split at the origin and is bent along the closest trajectory to $P_{\kappa\mu}^v$. The closure of the attractor seems to contain the x_1 -axis, which means that the attractor is unbounded. As $|vA_0|$ increases, the trajectory tends to leave $P_{\kappa\mu}^v$ more rapidly in a spiral manner. Actually, the ratio r of the frequency and the growth rate of the spiral trajectory at $P_{\kappa-1}^v$ decreases as $|vA_0|$ increases, since from equation (3.33b),

$$\frac{dr^2}{d|vA_0|} = - \frac{(r^2-3)^2(r^2+9)(\gamma_1+\gamma_2+\gamma_3-|vA_0|)^2\{2(|vA_0|-\gamma_1)+\gamma_2+\gamma_3\}}{4(1+r^2)(|vA_0|-\gamma_1)^2\gamma_2\gamma_3} < 0. \quad (4.3)$$

Thus, at $\gamma_1' \approx 0.4$, the pseudo-chaotic attractor is far from the origin (Fig.4.5(b)). Hence, the set Q is only bent along the trajectory closest to $P_{\kappa 1}^v$. At $\gamma_1' \approx 0.488 \sim 0.4896$ (Fig. 4.5(d)), two pseudo-chaotic attractors appear. They are linked, but disconnected with each other. In the figure, one of them is omitted. The omitted one is symmetric to the given one with respect to a 180° rotation around the x_2 -axis. At $\gamma_1' \approx 0.4875$, these two pseudo-chaotic attractors have a small intersection so that the trajectory moves from one to the other infrequently as shown in Figure 4.5(c). At $\gamma_1' \approx 0.4896 \sim 0.4899$, a three-loop pseudo-chaotic solution appears (Fig.4.5(e)). At $\gamma_1' \approx 0.49$, we have a three-loop periodic solution (Fig.4.5(f)), where the trajectory in a transient

state should be neglected. At $\gamma_1' \approx 0.491 \sim 0.495$, a pseudo-chaotic attractor of the type in Figure 4.5(d) appears again (Fig.4.5(g)). At $\gamma_1' \approx 0.4955$, an eight-loop solution appears (Fig.4.5(h)). At $\gamma_1' \approx 0.496 \sim 0.497$ and 0.498 , we have a four-loop pseudo-chaotic attractor (Fig.4.5(i)) and a stable four-loop periodic solution (Fig.4.5(j)), respectively. Furthermore, at $\gamma_1' \approx 0.498 \sim 0.5$ and 0.51 , we have a two-loop pseudo-chaotic attractor (Fig.4.5(k)) and a two-loop periodic solution (Fig.4.5(l)), respectively. At $\gamma_1' \approx 0.52 \sim 0.56$, there is a single-loop periodic solution (Fig.4.5(m)). This solution is not accompanied by a single-loop pseudo-chaotic solution. As γ_1' increases, this asymmetrical single-loop periodic solution gradually shifts, and finally, a symmetrical one appears at $\gamma_1' \geq 0.6$.

4.2.3 Sizes of Attractors

In Figure 3.6, $P = (0, -8^{\frac{1}{2}}vA_0, -2vA_0)$. Hence, for the values of vA_0 given in Figures 4.3(a),(b) and (c), $P = (0, 2.53, 3.56), (0, 7.07, 5.0)$ and $(0, 9.05, 6.4)$, respectively. From the numerical experiments, the maximum values of $|x_2(t)|$ and $x_3(t)$ with respect to t are approximately $(2.0, 2.0), (4.0, 4.0)$ and $(4.5, 5.0)$, respectively. Hence, the sizes of attractors are smaller than $\hat{\Delta}$ as predicted in Section 3.3.3.

Rewriting equation (3.46) for $\gamma_2 = 0.4, \gamma_3 = 1$,

$$|A_2|^2 + |A_3|^2 < 1.4\gamma_1 \{1 - |vA_0|^2 / (\gamma_1 + 1.4)^2\}. \quad (4.4)$$

Hence, for fixed $\gamma_1' = |vA_0| - \gamma_1$, the size of \hat{r} depends on γ_1 .

Assume that $\gamma_1' = 0.489$, for instance. Then, from Figure 4.5 (d), the maximum value of $|A_2|^2 + |A_3|^2$ is approximately 5.49. The right hand side of (4.4) has a maximum value of 2.546 in the limit $\gamma_1 \rightarrow \infty$. Hence, equation (4.4) is not satisfied. This result implies that the sufficient condition (3.46) for the convergence of $\xi(t)$ to θ_ξ is not applicable.

4.2.4 Periodic Solutions and Bifurcations

The asymmetric periodic solution in Figure 4.5(m) successively bifurcates as γ_1' decreases. The observed transition for $\gamma_1' \in [0.489, 0.5)$ resembles that of the well known one-dimensional mapping [21,22]

$$x(k+1) = G(x(k)) \triangleq rx(k)(1-x(k)) \quad (4.5)$$

which has properties shared by more general models [28]. Actually, we obtain a first return mapping of the trajectory for $\gamma_1' = 0.489$ in Figure 5.1(d), which seems to satisfy the conditions for the models in reference [28].

Figure 4.6 is a schematic diagram of bifurcation phenomena of system (6). Here, the circles represent actually observed periodic solutions, but the branching is conjectured from that of (4.5). The broken lines are unstable closed orbits and the solid lines are stable closed orbits. From Figure 4.6, the bifurcation phenomena of (6) for $\gamma_1' \in [0.489, 0.55)$ seem to be explainable by a one-dimensional mapping of type (4.5), although it is a rough approximation.

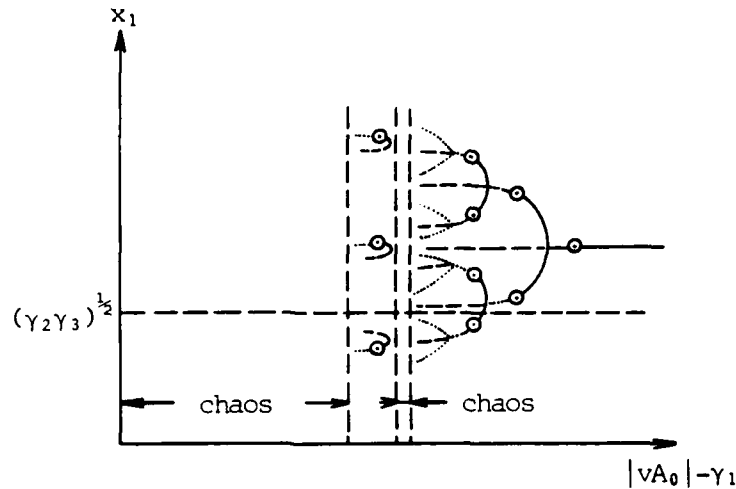


Figure 4.6 Schematic Diagram of Bifurcation of (6)

According to [21,22,28], the "chaos" appears when the bifurcation parameter exceeds an accumulation point of the sequences of bifurcation values, which correspond to Figures 4.5(d) and (g). For other values of parameters, stable periodic orbits appear. Hence, the three-loop pseudo-chaotic solutions for $\gamma_1' \approx 0.4896 \sim 0.4899$ seem to be 3×2^n time-loop stable periodic orbits, and the two and four-loop pseudo-chaotic solutions in Figures 4.5(i) and (k) seem to be converging to a stable periodic orbit.

4.3 Simple Models Describing Attractors

In this section, we consider the existence and the transition of the attractors shown in Figures 4.3 and 4.5. We consider only the attractors in which there occurs the splitting and bending mentioned earlier, since such mechan-

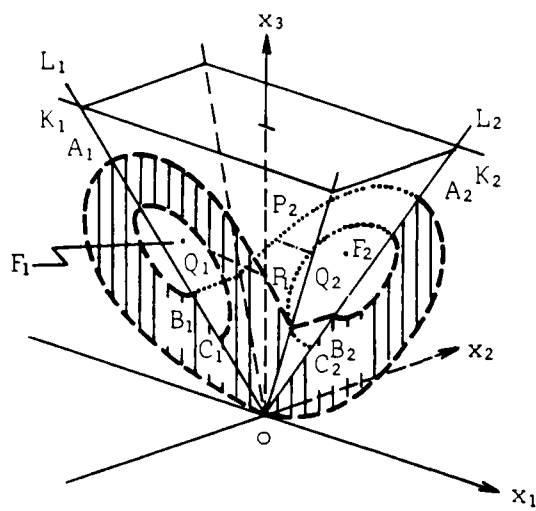
isms may lead to chaotic behavior. It is too difficult to verify mathematically the existence and transition of the attractors. Therefore, we introduce a simple two-dimensional model whose behavior is similar to that of (3) and (6). This model is only a schematic one, but is useful to explain the behavior of the attractors and to understand the relation between the trajectories in Figures 4.3 and 4.5 and the first return mappings shown in Chapter 5.

We consider half planes K_1 and K_2 containing the unstable foci F_1 and F_2 , respectively (Fig. 4.7 and 4.8). The trajectories move away from F_1 (resp., F_2) in a spiral manner on K_1 (resp., K_2) and jump to the line L_2 (resp., L_1) parallel to the x_2 -axis in Figure 4.7 and to the x_3 -axis in Figure 4.8. The basic assumptions are as follows:

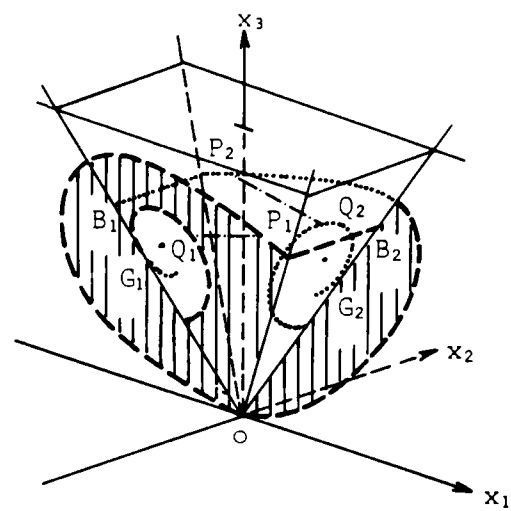
(A.4.1) Foci F_1 and F_2 move upward slowly as $|vA_0|$ increases so that it crosses L_1 and L_2 , respectively;

(A.4.2) The ratio r of the frequency and the growth rate of the spiral trajectory about the nontrivial equilibrium points decreases rapidly as $|vA_0|$ increases;

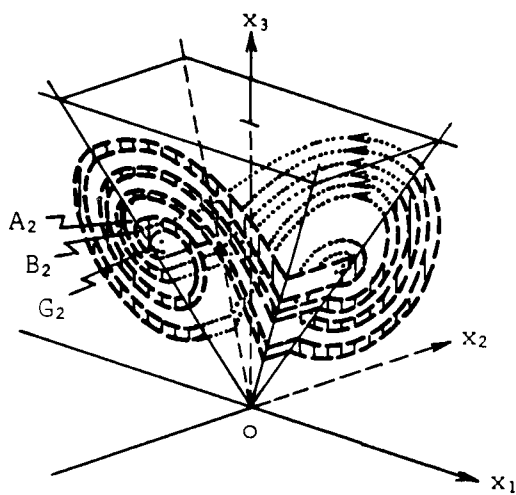
(A.4.3) Suppose that $t_1 < t_2$, $X_i = X(t_i) \in L_i$, $i = 1, 2$ and $X(t) \notin L_1, L_2$ for all $t \in (t_1, t_2)$. Then, $\|X_2\|/\|X_1\|$ decreases monotonically as $\|X_1\|$ increases, and if $\|X_2\|/\|X_1\| > 1$ for sufficiently small $\|X_1\|$, $\|X_2\|/\|X_1\| = 1$ for a certain value of $\|X_1\|$. Here, suffices 1 and 2 can be exchanged.



(a)

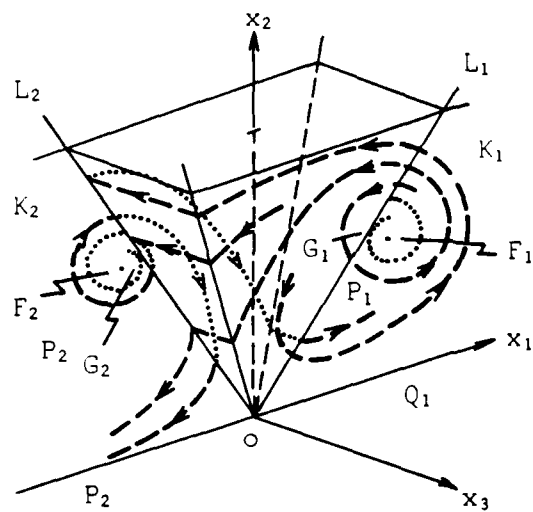


(b)

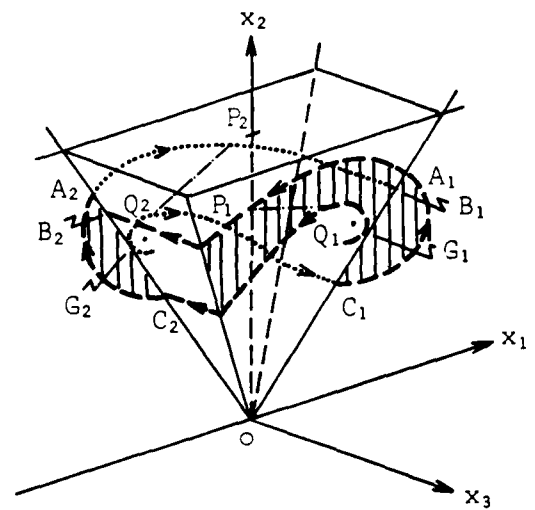


(c)

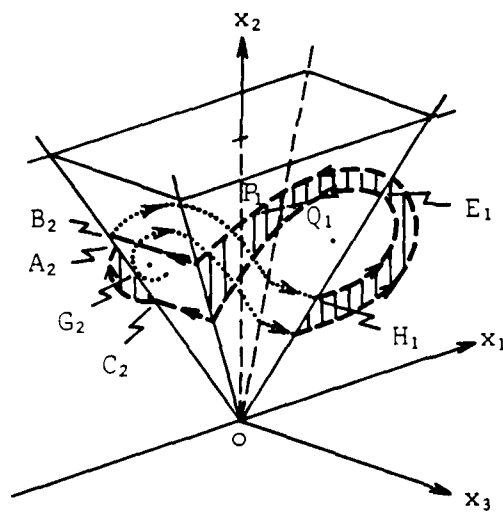
Figure 4.7 Simple Models for (3)



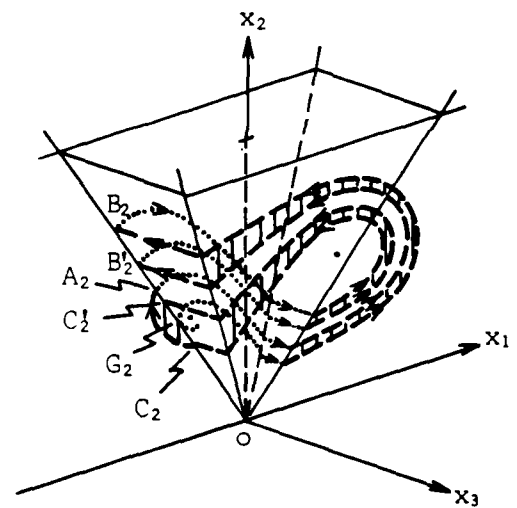
(a)



(b)

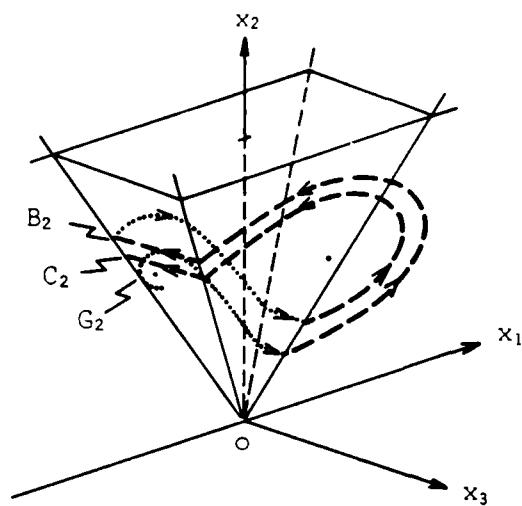


(c)

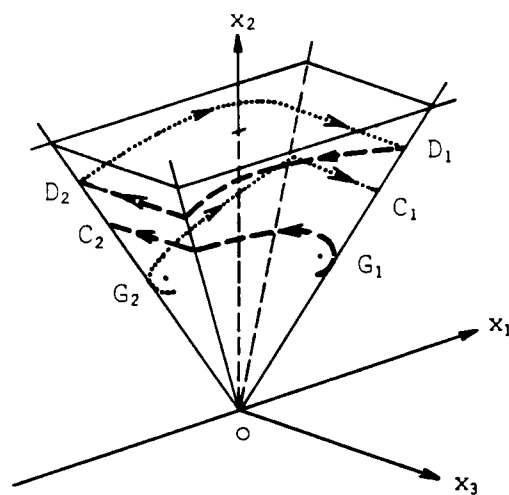


(d)

Figure 4.8 Simple Models for (6)



(e)



(f)

Figure 4.8 Simple Models for (6)

Actually for (6), the x_2 and x_3 components of $P_{\kappa 1}^1$ increase perpendicularly to the x_1 -axis as $|vA_0|$ increases. For (3), P_1 behaves in a similar way for sufficiently large $|vA_0|$. Numerical results and equation (4.3) show that (A.4.2) is reasonable for the models describing (3) and (6).

Assumption (A.4.3) implies that the trajectory does not diverge as it bounces between L_1 and L_2 without passing through $F_1 0$ or $F_2 0$. We shall introduce other assumptions for each of (3) and (6) later.

This model resembles a "universal circuit" used in reference [29], but is not obtained by taking limits or choosing specific values of parameters in (3) or (6). That is, introducing such a model is not justified mathematically or from the physical point of view. We use this model to avoid the difficulties in studying equations (3) and (6) directly.

For the model describing (3), we assume that the trajectory converging to the origin as $t \rightarrow -\infty$ encircles F_1 (resp., F_2) and hits L_2 (resp., L_1) at B_2 (resp., B_1) near F_2 (resp., F_1). Then, by decreasing r according to assumption (A.4.2), we obtain the transition as shown in Figure 4.7. Here, the broken and dotted lines are trajectories, and at G_1 (resp., G_2), they are tangent to L_1 (resp., L_2). The shadowed regions in Figure 4.7 are obviously local attractors. In (a) and (b), they are also global attractors by assumption (A.4.3). Figures 4.7(a)-(c) correspond to

Figures 4.3(a)-(c), respectively. In Figure 4.7(a), the line segment P_1Q_1 (corresponding to the set Q in Fig.4.4) is split at the origin. In (b), P_1Q_1 is also bent at G_1 and G_2 .

By assumption (A.4.1) and (A.4.2), as $|vA_0|$ increases, points A_i and B_i in (a) move upward more rapidly than G_i , and C_i moves downward first, hits the origin and then moves upward. We assume that C_i hits the origin after B_i and G_i coincide at some value of $|vA_0|$. When B_i coincides with G_i , the attractor of type (a) disappears. When B_i is above G_i , there appears as an attractor of type (b) or a multi-loop attractor of type (c). After C_i hits the origin, the situation is the same as that of the model describing (6).

The model describing (6) is shown in Figure 4.8. We assume that the x_1 -axis is a trajectory and $x_1(t) = x_1(0)\exp(\gamma_1' t)$, $\gamma_1' > 0$. Hence, in (a), the attractor is unbounded and there exist various types of trajectory behavior as shown in the figure. The line segment P_1Q_1 is split at the origin and bent at G_1 and G_2 . This case corresponds to Figure 4.5(a).

As $|vA_0|$ increases, F_i moves upward and C_i moves downward, hits the origin and then moves upward. Assume that all the points are located as shown in (b). Such an attractor corresponds to that in Figure 4.5(b). The attractor is bounded, and the line segment P_1Q_1 is bent at G_i .

As $|vA_0|$ increases further, A_i , B_i and C_i approach G_i .

Assume that A_i and C_i approach G_i more rapidly than B_i . Then, A_i and B_i exchange their positions at a certain value of $|vA_0|$, before A_i and C_i hit G_i . Then, we have an attractor of type (c), where another attractor obtained by 180° rotation about the x_2 -axis is omitted. Hence, the line segment E_1H_1 contains B_1C_1 (which is omitted in the figure), i.e., the attractors are interlinked and disconnected. When A_i is slightly above B_i , we have an attractor of type (b) corresponding to Figure 4.5(c).

When A_i is slightly above G_i , we have a two-loop attractor as shown in (d). Moreover, in the attractor of type (c), we may have multi-loop attractors. Assume that the attractor is n_p -loop and encircles G_2 n_e times on K_2 . Obviously, for the existence of an attractor in which there occurs a bending, A'_2 is above B'_2 if $n_p - n_e$ is odd, and A'_2 is below if $n_p - n_e$ is even (Figure 4.9). Practically, it is

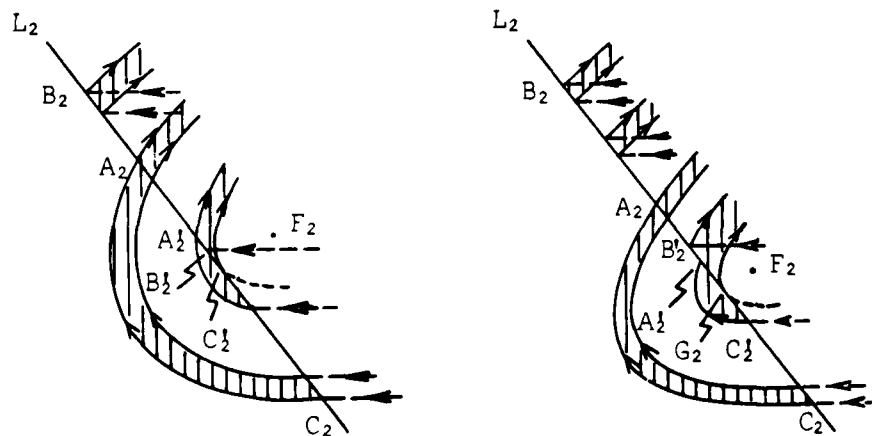


Figure 4.9 Multi-loop Attractors

likely that there exists a stable periodic solution in such a small-width multi-loop attractor. In the numerical experiment, we did not find any evidence for the existence of such a multi-loop attractor.

If C_2 is above G_2 for certain value of $|vA_0|$ as shown in (e), the attractor of type (c) does not exist. Finally, assume that C_1 is above G_1 as shown in (f). From assumption (A.4.3), there exists a point D_1 where $\|X_2\|/\|X_1\| = 1$. Then, the mapping of C_2D_2 (resp., C_1D_1) into C_1D_1 (resp., C_2D_2) is a contraction mapping and we have a single-loop symmetric stable periodic solution corresponding to Figure 4.5(1).

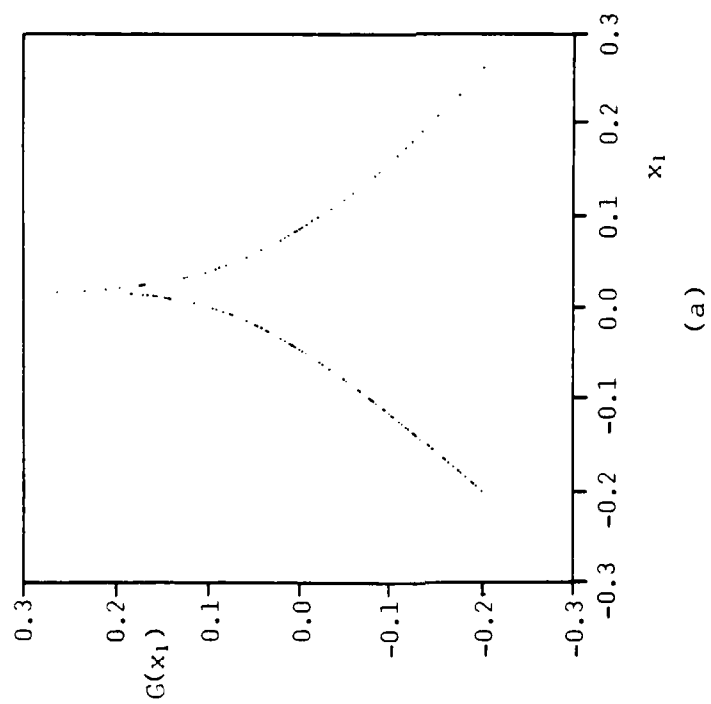
CHAPTER 5

FIRST RETURN MAPPINGS AND STATISTICAL PROPERTIES

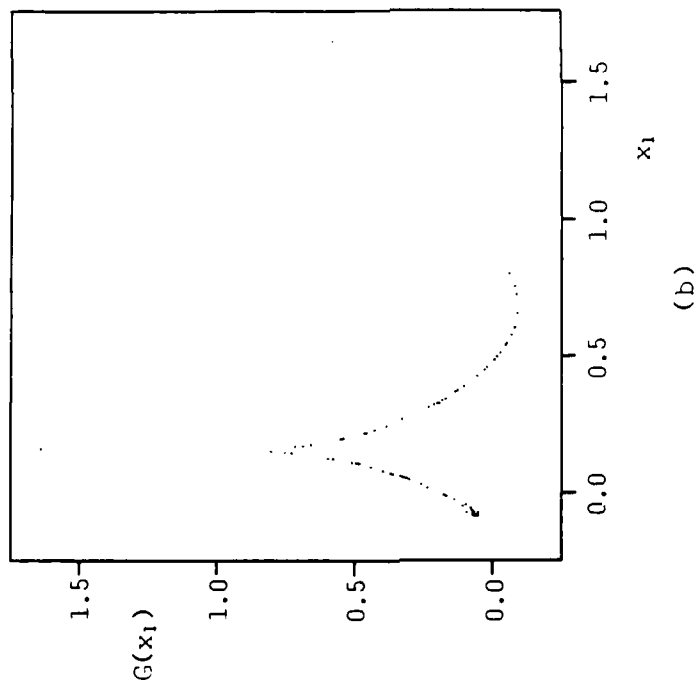
Most of the analytical works on the chaotic solutions of nonlinear systems have been devoted primarily to discrete-time systems [21,22,28,30-32]. For continuous-time systems with dimension greater than two, an analytical approach to the problem of existence of chaotic solutions appears to be quite formidable. Up to the present time, most of the works on such systems resort to numerical experimentation. The numerical results show that many three-dimensional continuous-time systems have pseudo-chaotic solutions lying in sets resembling two-dimensional surfaces in the system's state space. For such cases, we obtain a quasi one-dimensional mapping by taking a first return mapping (Fig. 4.4). In this chapter, we study such a quasi one-dimensional mapping for simplicity.

5.1 First Return Mappings of (3) and (6)

First return mappings of the trajectories in Figures 4.3(a),(b) and 4.5(a),(b),(d) are given in Figures 5.1(a)-(e), respectively. For the trajectories in Figures 4.3(a) and (b), we consider mappings from $T_+ = \{X : x_2 = x_{2e}^+, x_3 > x_{3e}\}$ or $T_- = \{X : x_2 = x_{2e}^-, x_3 > x_{3e}\}$ to T_+ or T_- , where $(x_{1e}^\pm, x_{2e}^\pm, x_{3e}^\pm)$ are equilibrium points defined in (3.2) and $x_{ie}^+ > 0$, $x_{ie}^- < 0$, $i = 1, 2$. Such a mapping is the first return mapping of the

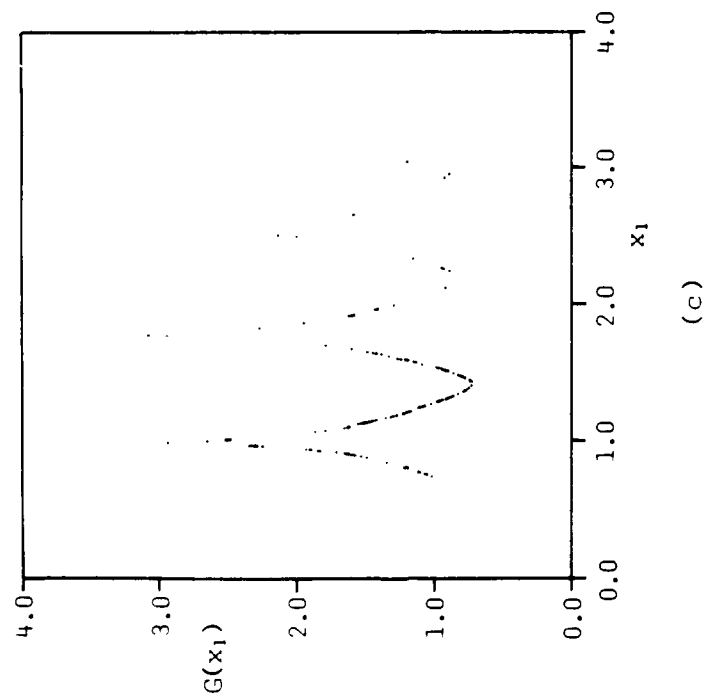


(a)

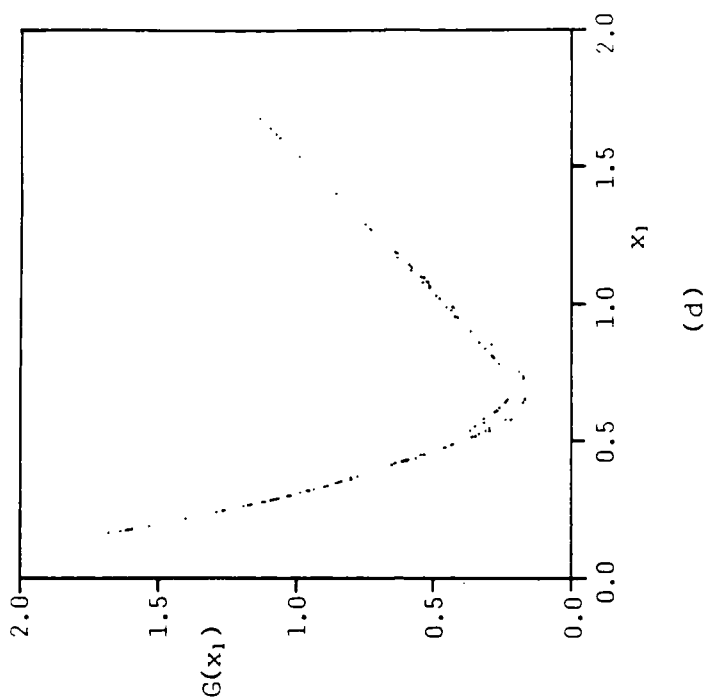


(b)

Figure 5.1 First Return Mappings of x_1

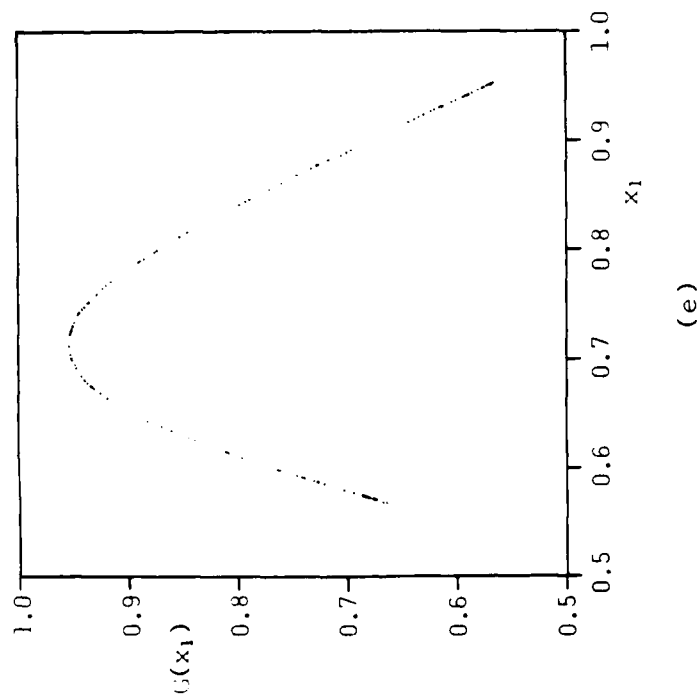


(c)

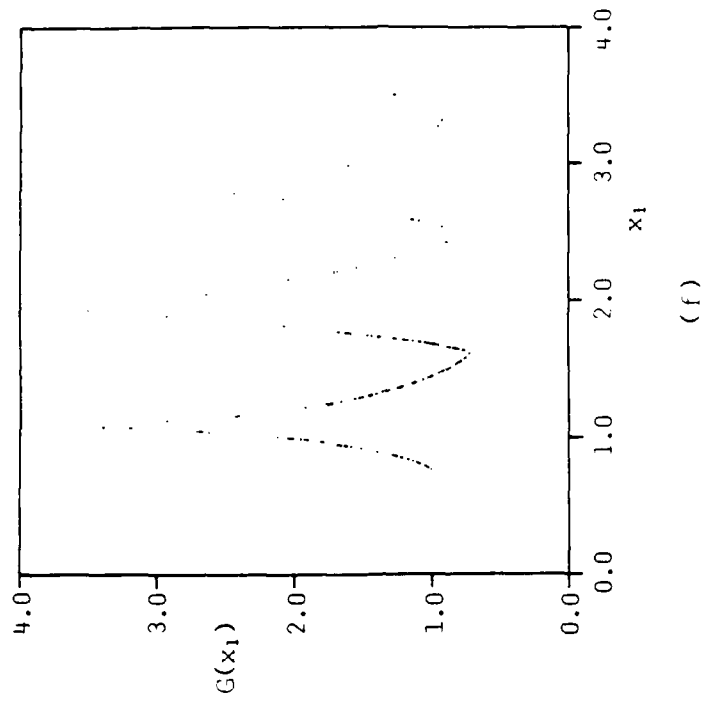


(d)

Figure 5.1 First Return Mappings of x_1

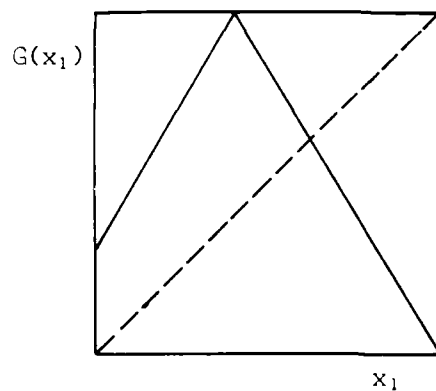


(e)

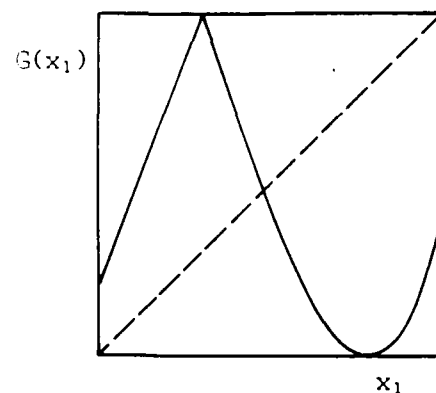


(f)

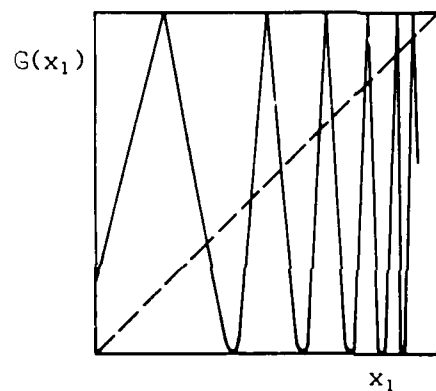
Figure 5.1 First Return Mappings of x_1



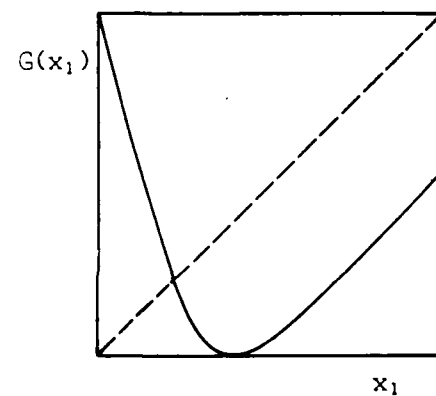
(a')



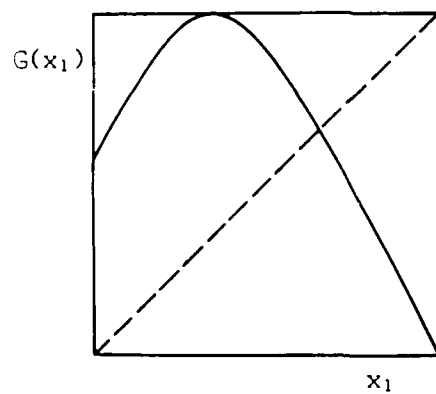
(b')



(c')



(d')



(e')

Figure 5.1 First Return
Mappings of x_1

trajectories $\tilde{X} = (|x_1(t)|, |x_2(t)|, x_3(t))$. The behaviors of the modified trajectories are identical to those of the original ones because of the system's symmetry around the x_3 -axis. For Figure 5.1(c), we choose $T_+ = \{X : x_2 = (x_1 - x_{1e}^+) \times x_{2e} / (x_{1e}^+ - 4), x_{1e}^+ < x_1 < 4\}$ and $T_- = \{X : x_2 = (x_1 - x_{1e}^-) x_{2e} / (x_{1e}^- + 4), -4 < x_1 < x_{1e}^-\}$, where $(x_{1e}^\pm, x_{2e}^\pm, x_{3e}^\pm)$ are defined in (3.31) and $x_{ie}^+ > 0, x_{ie}^- < 0, i = 1, 3$. In (d), $T_+ = \{X : x_3 = 0, x_1 > 0\}$ and $T_- = \{X : x_3 = 0, x_1 < 0\}$. In (e), we choose a mapping from $T_+ = \{X : x_3 = 0, x_1 > 0\}$ into itself. We should note that T_\pm are transverse to the trajectories. The intersection of the trajectories with T_\pm corresponds to those on $P_i Q_i, i = 1, 2$ in Figures 4.7 and 4.8.

The mappings given in Figures 5.1(a), (c) and (e) resemble one-dimensional mappings. In (b) and (d), we observe that the mappings are more complicated. For (b) and (d), there exist no simple planes like T_\pm on which we have a first return mapping resembling an one-dimensional mapping. This is due to the fact that the bent Q (Fig.4.4) is not completely folded after Q encircles the origin from T_+ (or T_-) to T_- (or T_+).

In Figures 5.1(a)-(c), the whole interval of x_1 contains the points which describe the trajectories converging to the origin as $t \rightarrow \infty$. Near the origin, the velocity can be arbitrarily small. Hence, for these cases, the continuous-time systems (3) and (6) cannot be replaced by discrete-time systems. In (d) and (e), there are no such

points so that there is a supremum for the time in which the trajectories return to T_{\pm} .

In Figures 5.1(a')-(e'), we show one-dimensional mappings of simple models in Figures 4.7 and 4.8. The half planes T_{+} and T_{-} correspond to P_1Q_1 and P_2Q_2 in Figures 4.7 and 4.8, respectively. These mappings are useful in conjecturing the behavior of the first return mappings of (3) and (6) at those points which are not observed in the experiment.

5.2 One-Dimensional Mappings

We regard the first return mappings in Figures 5.1(a), (c) and (e) as one-dimensional discrete-time systems. As mentioned in the previous section, this means that for (a) and (c), the temporal behaviors of the continuous-time versions of systems (3) and (6) are not considered.

One-dimensional discrete-time systems having chaotic solutions have been studied extensively in mathematics [28, 30-32] and other areas [21,22]. Here, we present some of the known results and discuss their applicability to the systems under consideration.

5.2.1 Period Three Implies Chaos

The following theorem is due to Li and Yorke [31]:

(S.5.1) Let J be an interval and let $G: J \rightarrow J$ be continuous. Assume that there is a point $a \in J$ for

which the points $b = G(a)$, $c = G^2(a)$ and $d = G^3(a)$ satisfy

$$d \leq a < b < c \text{ (or } d \geq a > b > c \text{)}.$$

Then,

T1: for every $k = 1, 2, \dots$, there is a periodic point in J having period k .

Furthermore,

T2: there is an uncountable set $S \subset J$ (contains no periodic points), which satisfies the following conditions:

(A) For every $p, q \in S$ with $p \neq q$,

$$(T2.1) \quad \limsup_{n \rightarrow \infty} |G^n(p) - G^n(q)| > 0$$

and

$$(T2.2) \quad \liminf_{n \rightarrow \infty} |G^n(p) - G^n(q)| = 0$$

(B) For every $p \in S$ and periodic point $q \in J$,

$$(T2.3) \quad \limsup_{n \rightarrow \infty} |G^n(p) - G^n(q)| = 0$$

If there is a periodic point with period 3, then the hypothesis of the theorem are satisfied. Statement (A) means two sequences $\{G^n(p)\}$ and $\{G^n(q)\}$, $p, q \in S$ can be made arbitrarily close to each other for sufficiently large n , but they do not converge to each other as $n \rightarrow \infty$. Statement (B) implies that a sequence $\{G^n(p)\}$, $p \in S$ does not converge to any periodic points. If S is an attractor, it is obviously a strange attractor.

The mappings in Figures 5.1(a),(c),(e) and (a')-(e') satisfy the hypotheses of (S.5.1), and therefore, there exists a S for each of them. Theorem (S.5.1) does not give any information about the size of S . If there is a stable periodic point $p_S \in J$, then there is a neighborhood $N(p_S)$ of p_S such that $G^N(p) \in N(p_S)$ implies $G^n(p) \in N(p_S)$ for all $n \geq N$. At the present time, it is not known whether the following statement is true or false:

(S.5.2) The existence of a stable periodic point $p_S \in V$, where V is an attractor, implies that the sequence $\{G^n(p)\}$ converges to p_S as $n \rightarrow \infty$ for almost all $p \in V$.

If this statement is true, then even if the trajectories in the transient state appears to be very complicated, there is no strange attractor.

Many examples of one-dimensional mappings derived from actual systems have points \tilde{p}_S at which $dG(p)/dp = 0$ as that in Figure 5.1(e). There may exist a stable periodic solution p_S near \tilde{p}_S . Experimental results show that there exists a complicated solution which is not periodic (within the accuracy of computation). This does not necessarily mean the nonexistence of p_S or that (S.5.2) is false. For, even if there exists a p_S and (S.5.2) is true, a small perturbation in the system may shift the trajectory out of $N(p_S)$ if the size of $N(p_S)$ is very small. In other words,

from the practical standpoint, the existence of p_S may be ignored for certain cases.

We consider the mappings in Figures 5.1(b),(d). In these cases, the mapping cannot be approximated by an one-dimensional mapping especially about \tilde{p}_S . We do not know how such a structure about \tilde{p}_S affect the existence or nonexistence of stable periodic orbits in the three-dimensional space. It should be noted that the mapping in (e) also has such a structure about \tilde{p}_S which is not so explicit as those of (b) and (d).

5.2.2 Statistical Properties of $\{G^n(p)\}$

We consider the following theorem given in [31]:

(S.5.3) Let $G: J \rightarrow J$ satisfy the following conditions:

(A) G is continuous.

(B) Except at one point $\hat{p} \in J$, F is twice continuously differentiable.

(C) $\inf_{q \in J, p \neq \hat{p}} |dG(q)/dq| > 1$.

Then, there is a unique function $g: J \rightarrow [0, \infty)$, such that for almost all $p \in J$, g is the density of p .

Here, g is defined to be a density of p if

$$\phi(p, [p_1, p_2]) = \lim_{N \rightarrow \infty} \phi(p, N, [p_1, p_2]) = \int_{p_1}^{p_2} g(q) dq$$

for all $p_1, p_2 \in J$, $p_1 < p_2$, where $\phi(p, N, [p_1, p_2])$ is the fraction of the iterates $\{p, \dots, G^{N-1}(p)\}$ of $p \in [p_1, p_2]$.

Moreover, the set $J_\infty = \{q: g(q) > 0\}$ is an interval, and

J_∞ is the positive limit set of almost all initial point $p \in J$.

The mapping in Figure 5.1(a') satisfies the hypotheses of (S.5.3). From (S.5.3), the behavior of $\{G^n(p)\}$ is described schematically as follows. Choose an arbitrary $p \in J$. As $n \rightarrow \infty$, $G^n(p)$ wanders around in J and finally, $\{G^n(p)\}$ fills an interval J_∞ . The density $g(p)$ of points in the limit $n \rightarrow \infty$ is unique and independent of almost all initial points $p \in J$, and is mapped to the same $g(q)$ by G . We can predict the behavior of the system in the limit $n \rightarrow \infty$ only in some probabilistic sense although the system is deterministic. For example, we know that the probability for the point to be in $[p_1, p_2]$ in the limit $n \rightarrow \infty$ is $\int_{p_1}^{p_2} g(q) dq$. Very little is known for other mappings which do not satisfy the hypotheses of (S.5.3).

The mapping in Figure 5.1(c') is peculiar, since it has a countably infinite number of discontinuities. If we choose $T_+ = \{X : x_1 > x_{1e}^+, x_2 = x_{2e}\}$ and $T_- = \{X : x_1 < x_{1e}^-, x_2 = x_{2e}\}$, then we have a one-dimensional mapping in Figure 5.1(f) and its corresponding mapping (f') for the simple model. Here, the domain of mapping is an unbounded interval. We assume that a density $g(p)$ of p exists for this system, then $g(p) \rightarrow 0$ as $p \rightarrow 0$. We know that the magnitude of any physical parameter must be finite. Here, p can be infinite, but with zero probability. Hence, there seems to be no contradiction to the requirement as a physical model. Such

an interpretation may provide new types of physical models. For, the magnitude of variables have been conventionally classified only two cases, that is, bounded or diverging to infinity, and no concept of probability has been involved for such a simple deterministic model.

5.3 Statistical Properties of (3) and (6)

Quasi one-dimensional mappings obtained experimentally from (3) and (6) are useful to understand the behavior of (3) and (6). But, as mentioned in the previous sections, it is difficult to study their statistical properties analytically. The only one-dimensional mapping whose statistical property is well-known [22] is given by

$$G(p) = \begin{cases} 2p, & 0 \leq p \leq 1/2, \\ 2(1-p), & 1/2 < p \leq 1. \end{cases} \quad (5.1)$$

It is known that if $p \in [0,1]$ is described by a binary sequence $\{b_n\}$, the map G acts on $\{b_n\}$ like a shift map which shifts terms of the sequence to the left (Bernoulli shifts). A Bernoulli shift is a stochastic system (i.e., the system behavior is completely unpredictable in a certain sense [33]). For other maps, very little is known. Here, we try to obtain the statistical properties of (3) and (6) numerically.

5.3.1 Mixing Property

If there is an attractor Λ which is ergodic and $\mu(X)$ is a defined measure on Λ , then for any smooth function u ,

$$\bar{u} \triangleq \int_{\Lambda} u(X') d\mu(X') = \lim_{T \rightarrow \infty} (1/T) \int_0^T dt u(X(t, X_0))$$

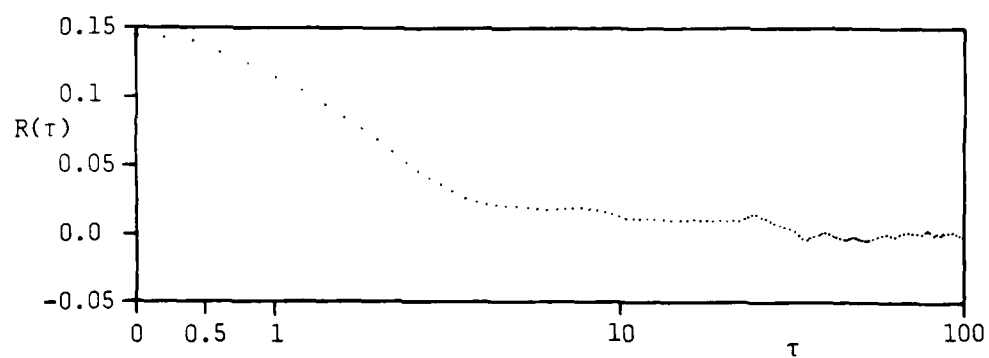
for almost all initial conditions X_0 . The system has a mixing property, if for any smooth functions u and v ,

$$\begin{aligned} R(\tau) &\triangleq \bar{u}\bar{v} - \int_{\Lambda} u(X(\tau, X')) v(X') d\mu(X') \\ &= \bar{u}\bar{v} - \lim_{T \rightarrow \infty} (1/T) \int_0^T dt u(X(\tau+t, X_0)) v(X(t, X_0)) \end{aligned}$$

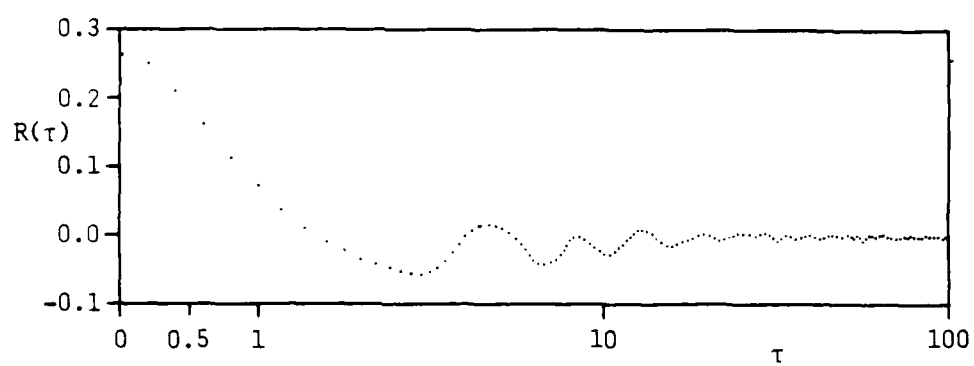
for almost all X_0 and $R(\tau) \rightarrow 0$ as $\tau \rightarrow \infty$. As mentioned in Chapter 1, this property implies that the time evolution of the trajectories is highly sensitive to the initial condition, which is an important property of the turbulent solutions. The system having a mixing property is a stochastic system in a weaker sense than a Bernoulli shift. We examined numerically $R(\tau)$ with $u(X) \equiv v(X) \equiv x_1$. The results for Figures 5.1(a)-(e) are shown in Figures 5.2(a)-(e), respectively. We can not try all smooth functions u and v , but the results in Figure 5.2 suggest that the systems have the mixing properties for certain values of parameters.

5.3.2 Unbounded Solutions of System (6)

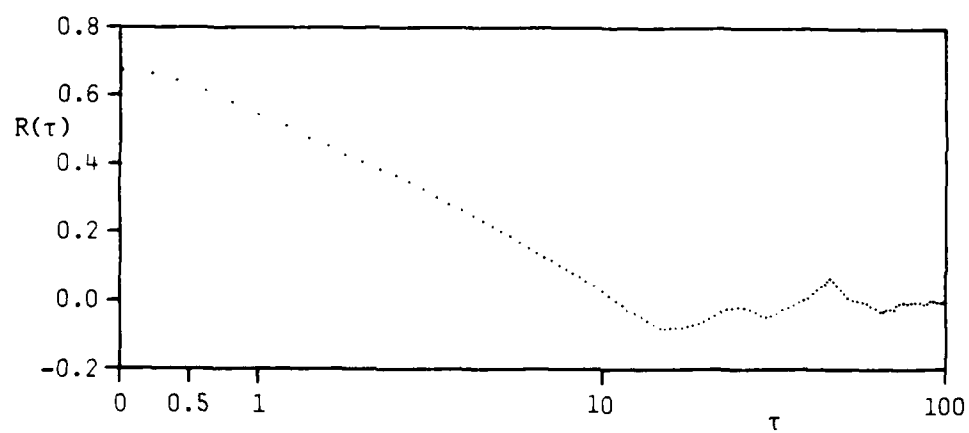
As mentioned earlier, system (6) with $\gamma_1' = 0.2$ has an unbounded solution. If its first return mapping as a discrete-time system has a density $g(p)$ of p , $g(p) \rightarrow 0$ as



(a)

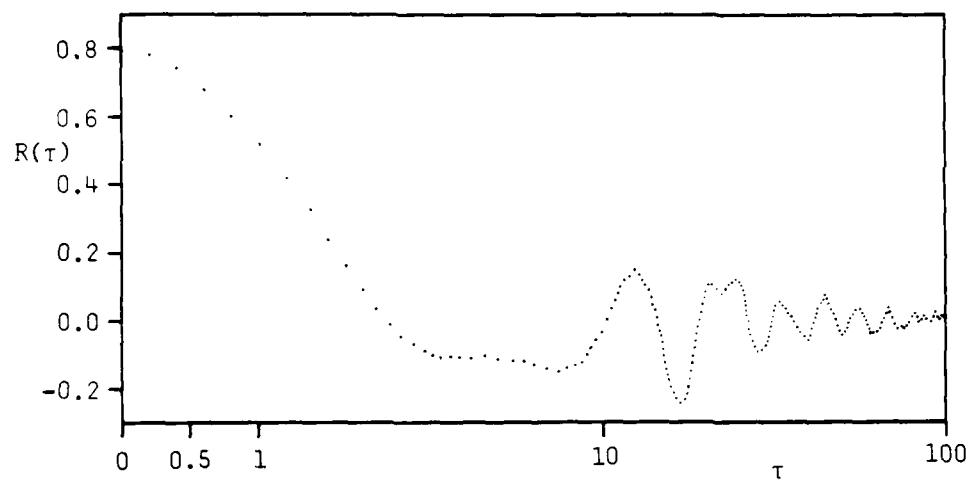


(b)

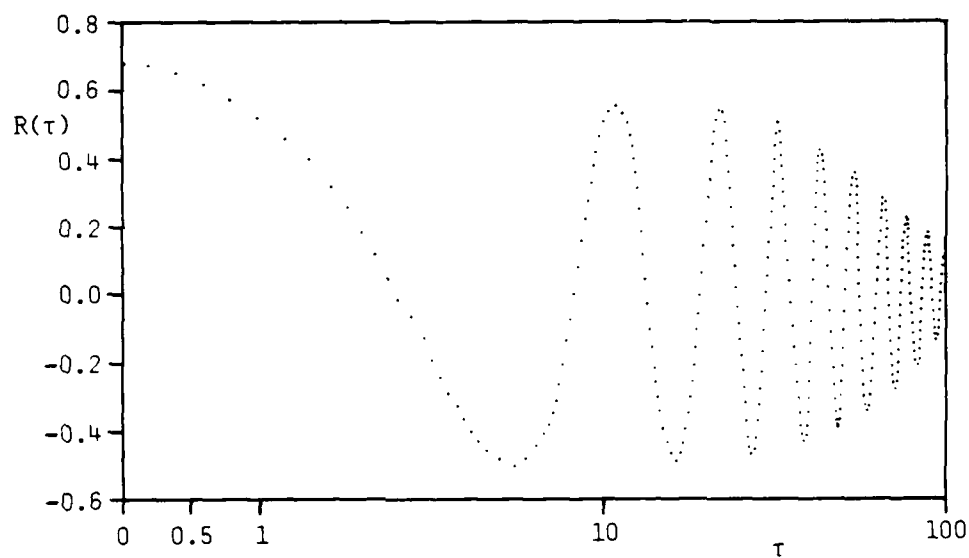


(c)

Figure 5.2 Autocovariances $R(\tau)$ of x_1



(d)



(e)

Figure 5.2 Autocovariances $R(\tau)$ of x_1

$p \rightarrow 0$. As a continuous-time system, system (6) must satisfy the physical requirement that the time-averaged energy is finite. We consider the ratio:

$$P_T(\chi) \triangleq \text{measure}\{t : x_1(t) \geq \chi, 0 \leq t \leq T\} / T.$$

In Figure 5.3, we have plotted those values of χ for which P_T is insensitive to the initial conditions. As T increases, the interval of such values of χ also increases in size. Hence, it is likely that as $T \rightarrow \infty$, P_T approaches P_∞ which is independent of the initial conditions and goes to zero as $|\chi| \rightarrow \infty$.

If P_∞ exists and decays more rapidly than $1/\chi^3$, and if

$$E_1 \triangleq \lim_{T \rightarrow \infty} (1/T) \int_0^T x_1(t)^2 dt = \int_0^\infty \chi^2 P_\infty(\chi) d\chi$$

is satisfied, then from the physical point of view, we can state as follows: the energy of wave 1 of system (6) can be arbitrarily large over a finite time interval, but its time duration is so short that the time-averaged energy E_1 is finite.

Equation (6) is obtained by neglecting higher order terms with small coupling coefficients. Hence, if $\|X(t)\|$ is sufficiently large, model (6) is not valid. From the above argument, the time duration for which $x_1(t) > \chi$ becomes smaller in the ratio $P_T(\chi)$ as χ becomes large. Hence, if the range for the approximation is large, we can state that model (6) is valid most of the time.

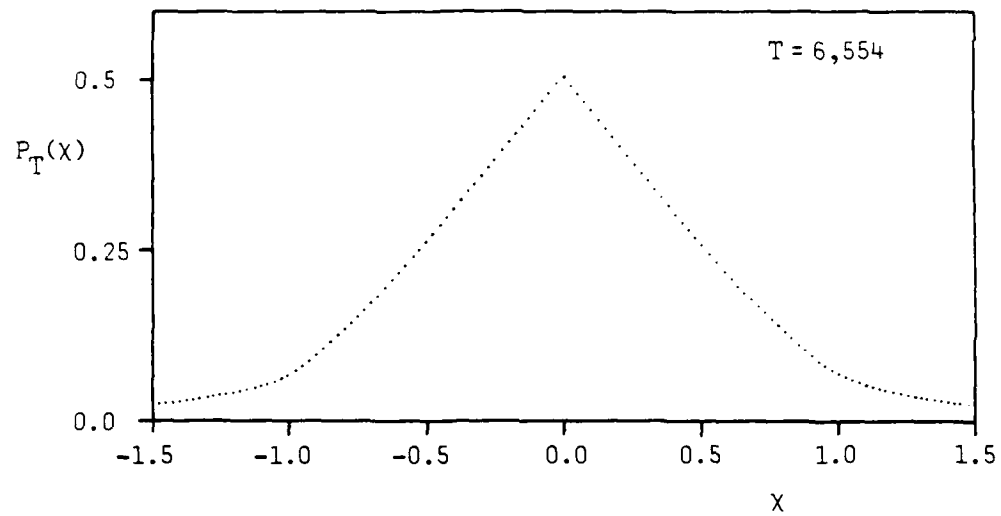


Figure 5.3 Density $P_T(x)$ of Distribution of x_1

CHAPTER 6

CONCLUSIONS

6.1 Summary of Results

In this work, we have studied the chaotic behaviors of wave-wave interacting systems involving at most four waves (Table 2.2). These systems can be described by a real three-dimensional equation on a certain set in the state space, where the phases of the waves are locked for (2')-(7') (Sec. 2.2). We have found that there remained only six systems of positive-energy waves (Table 3.2), if we discard the cases which have the following property: The corresponding reduced equations have only one equilibrium point or a stable equilibrium point, or they have an open set R_0 in the state space such that if $X_0 \in R_0$, $X(t) = X(t, X_0) \in R_0$ for all $t \geq 0$ and diverges to infinity as $t \rightarrow \infty$. It is very likely that the reduced equations (1)-(4), (6) have chaotic solutions for almost all initial conditions in the state space. System (3') and (6') have only linear damping terms, and the instability of their equilibrium points is due to the external wave. The numerical experiment was done only for these two cases.

We obtained the conditions (Table 2.7 and (S.2.3)) for asymptotic phase locking of (2')-(7') as $t \rightarrow \infty$, which depend on the sizes of the attractors for the trajectories. But,

the conditions are too strong for determining the occurrence of asymptotic phase locking of (3') and (6') as $t \rightarrow \infty$ for the values of parameters at which chaotic solutions may appear. The numerical experiments show that system (6') has a strong tendency of asymptotic phase locking as $t \rightarrow \infty$. In (3'), for certain values of parameters, the phases are nearly locked most of the time, but not asymptotically locked as $t \rightarrow \infty$.

Periodic and pseudo-chaotic solutions of system (3) and especially (6) were studied numerically in detail. For certain values of parameters, the first return mappings of the trajectories have properties which are similar to those of the well-known one-dimensional mappings having parabolic graphs. The transitions of attractors are schematically explained by using the simple models in Figures 4.7 and 4.8.

Finally, we considered the statistical properties of the first return mappings of the trajectories of (3) and (6) using the known theorems for simple one-dimensional discrete models. Numerical results suggest that system (3) and (6) have a mixing property for certain values of parameters, which is an important property of the turbulent states.

6.2 Remarks on Further Research

We have shown that some wave-wave interacting systems with a few modes have chaotic behaviors. As mentioned earlier, no additional assumption for randomness was necessary in these systems. In this new approach to plasma

turbulence, there are still many unresolved basic questions.

One of the questions is how to relate the statistical properties of the simple systems with a few modes to the turbulent state in plasmas. In actual plasmas, there are a large number of coupled modes. If a plasma in a turbulent state consists of systems which are weakly coupled with each other and each of which is a few-mode interaction having a chaotic motion, we can regard each system as a quasi-particle, since the phase of the system varies randomly. Then, the whole system may be described by a kinetic equation of quasi-particles [11]. If many waves are strongly coupled, we cannot use directly the results for a few-mode system to analyze the whole system. It has been shown that a multi-mode system has behavior similar to that of a few-mode system [10]. But, very little is known about general multi-mode systems.

There are also unresolved questions about the simple systems studied in this work. First of all, we still do not know exactly under what conditions the reduced equations describe the asymptotic behaviors of the original systems. Furthermore, the relationship between the reduced and original systems is not known if the phases are not locked asymptotically as $t \rightarrow \infty$. None of the statistical properties mentioned in Chapter 4 are proved mathematically. The power spectrum of the variables is one of the important quantities from the physical standpoint. But, at the present time, it

is too difficult to obtain the power spectrum of the chaotic solutions of such systems analytically. Thus, further studies must be done before the turbulent behavior of plasmas can be analyzed via the new approach considered in this work.

REFERENCES

1. Nishikawa, K., "Parametric Excitation of Coupled Waves. I. General Formulation," J. Phys. Soc. Japan, Vol. 24, No. 4, pp. 916-922, April 1968; "Parametric Excitation of Coupled Waves. II. Parametric Plasmon-Photon Interaction," J. Phys. Soc. Japan, Vol. 24, No. 5, pp. 1152-1152, May 1968.
2. Sagdeev, R. Z. and A. A. Galeev, Nonlinear Plasma Theory, W. A. Benjamin, New York, 1969.
3. Tsytovich, V. N., Nonlinear Effects in Plasma, Prenum Press, New York, 1970.
4. Davidson, R. C., Methods in Nonlinear Plasma Theory, Academic Press, New York, 1970.
5. Schwarz, H. J. and H. Hora, Laser Interaction and Related Plasma Phenomena, Vol. 3A, Prenum Press, New York, 1973.
6. Hasegawa, A., Plasma Instabilities and Nonlinear Effects, Springer-Verlag, New York, 1975.
7. Simon, A. and W. B. Thompson, Advances in Plasma Physics, Vol. 6, John Wiley and Sons, New York, 1976.
8. Wilhelmsson, H., Plasma Physics, Nonlinear Theory and Experiments, Prenum Press, New York, 1977.
9. Leontovich, M. A., Reviews of Plasma Physics, Vol. 7, Consultants Bureau, New York, 1979.
10. Flynn, R. W. and W. M. Manheimer, "Stabilization of Instabilities by Mode Coupling," Phys. Fluids, Vol. 14, No. 9, pp. 2063-2065, September 1971.
11. Vyshkind, S. Ya. and M. I. Rabinovich, "The Phase Stochastization Mechanism and the Structure of Wave Turbulence in Dissipative Media," Sov. Phys. JETP,

- Vol. 44, No. 2, pp. 292-299, August 1976.
12. Pikovskii, A. S., M. I. Rabinovich, and V. Yu. Trakhtengerts, "Onsets of Stochasticity in Decay Confinement of Parametric Instability," Sov. Phys. JETP, Vol. 47, No. 4, pp. 715-719, April 1978.
 13. Dubrovin, V. I., V. R. Kogan, and M. I. Rabinovich, "Decay Mechanism for the Onset of Turbulence," Sov. J. Plasma Phys., Vol. 4, No. 5, pp. 658-659, September-October 1978.
 14. Wersinger, J. M., J. M. Finn, and E. Ott, "Bifurcation and Strange Behavior in Instability Saturation by Nonlinear Mode Coupling," Phys. Rev. Lett., Vol. 44, No. 7, pp. 453-456, February 1980.
 15. Wang, P. K. C., "Nonperiodic Oscillations of Langmuir Waves," J. Math. Phys., Vol. 21, No. 2, pp. 398-407, February 1980.
 16. Landau, L. D. and E. M. Lifshitz, Mechanics of Continuous Media, Pergamon Press, Oxford, 1975.
 17. Aizawa, Y., "Synergetic Approach to the Phenomena of Mode-Locking in Nonlinear Systems," Prog. Theor. Phys., Vol. 56, No. 3, pp. 703-716, September 1976.
 18. Ruelle, D. and F. Takens, "On the Nature of Turbulence," Commun. Math. Phys., Vol. 29, No. 3, pp. 167-192, 1971.
 19. Lorenz, E. N., "Deterministic Nonperiodic Flow," J. Atmos. Sci., Vol. 20, pp. 130-141, January 1963.
 20. Robbins, K. A., "A Moment Equation Description of Magnetic Reversals in the Earth," Proc. Natl. Acad. Sci. U.S.A., Vol. 73, No. 12, pp. 4297-4301, December 1976.
 21. May, R. M. and G. F. Oster, "Bifurcations and Dynamic Complexity in Simple Ecological Models," Amer. Natural.,

- Vol. 110, No. 974, pp. 573-599, July-August 1976.
22. Guckenheimer, J., G. F. Oster, and A. Ipaktchi, "The Dynamics of Density Dependent Population Models," J. Math. Biology, Vol. 4, No. 2, pp. 101-147, 1977.
 23. Tomita, K. and I. Tsuda, "Chaos in Belousov-Zhabotinsky Reaction in a Flow System," Phys. Lett., Vol. 71A, No. 5,6, pp. 489-492, May 1979.
 24. Haken, H., "Analogy between Higher Instabilities in Fluids and Lasers," Phys. Lett., Vol. 53A, No. 1, pp. 77-78, May 1975.
 25. Tsytovich, V. N., Theory of Turbulent Plasma, Consultants Bureau, New York, 1977.
 26. Vidyasagar, M., Nonlinear Systems Analysis, Prentice-Hall, New Jersey, 1978.
 27. Treve, Y. M., "Boxing-in the Lorenz Attractor," Preprint.
 28. Feigenbaum, M. J., "Qualitative Universality for a Class of Nonlinear Transformations," J. Stat. Phys., Vol. 19, No. 1, pp. 25-52, January 1978.
 29. Rössler, O. E., "Continuous Chaos - Four Prototype Equations," Bifurcation Theory and Applications in Scientific Disciplines (ed. by O. Gurel and O. E. Rössler), pp. 377-392, New York Academic Sciences, New York, 1979.
 30. Lasota, A. and J. A. Yorke, "On the Existence of Invariant Measures for Piecewise Monotonic Transformations," Trans. Amer. Math. Soc., Vol. 186, pp. 481-488, December 1973.
 31. Li, T. Y. and J. A. Yorke, "Period Three Implies Chaos," Amer. Math. Monthly, Vol. 82, No. 10, pp. 985-992, December 1975.

32. Li, T. Y. and J. A. Yorke, "Ergodic Transformations from an Interval into Itself," Trans. Amer. Math. Soc., Vol. 235, pp. 183-192, January 1978.
33. Pomeau, Y., "Stochastic Behavior of Simple Dynamic Systems," Stochastic Processes in Nonequilibrium Systems (ed. by L. Garrido, P. Seglar and P. J. Shepherd), pp. 236-277, Springer-Verlag, Berlin, 1978.

APPENDIX

PIKOVSKII-RABINOVICH-TRARHTENGERTS' MODEL

Let us assume that all the γ_i 's, v_i 's and v_i' 's are positive. By using the substitution:

$$A_1 \rightarrow iA_1, \quad A_2 \rightarrow A_2, \quad A_3 \rightarrow A_3, \quad vA_0 \rightarrow -h, \quad (A.1)$$

we obtain the following set of equations

$$\left. \begin{aligned} \dot{A}_1 &= -\gamma_1 A_1 - A_2 A_3 + hA_2^*, \\ \dot{A}_2 &= -\gamma_2 A_2 + A_1 A_3^* + hA_1^*, \\ \dot{A}_3 &= -\gamma_3 A_3 + A_1 A_2^* \end{aligned} \right\} \quad (A.2)$$

which is identical to the Pikovskii-Rabinovich-Trarhtengerts' model [12]. Let

$$\xi = \text{Im}(hA_1^* A_2^*), \quad \eta = \text{Im}(A_1 A_2^* A_3^*). \quad (A.3)$$

Then,

$$(d/dt)(\xi + \eta) = -(\gamma_1 + \gamma_2)\xi - (\gamma_1 + \gamma_2 + \gamma_3)\eta. \quad (A.4)$$

According to Ref.[12], the trajectories $\Xi = (\xi(t), \eta(t))$ enter the sector Z between the straight lines L_1 and L_2 :

$$\left. \begin{aligned} L_1 &= \{(\xi, \eta) : \xi + \eta = 0\}, \\ L_2 &= \{(\xi, \eta) : (\gamma_1 + \gamma_2)\xi + (\gamma_1 + \gamma_2 + \gamma_3)\eta = 0\}. \end{aligned} \right\} \quad (A.5)$$

It is true that the trajectories $\Xi = (\xi(t), \eta(t))$ on L_1 enter

Z, since

$$(d/dt)(\xi + \eta) \big|_{(\xi, \eta) \in L_1} = -\gamma_3 \eta, \quad (A.6)$$

which is positive (resp., negative) when η is negative (resp., positive). However, the trajectories $\Xi = (\xi(t), \eta(t))$ on L_2 do not always enter Z. For,

$$\begin{aligned} (d/dt)\{(\gamma_1 + \gamma_2)\xi + (\gamma_1 + \gamma_2 + \gamma_3)\eta\} &= (\gamma_1 + \gamma_2 + \gamma_3)(\gamma_1 + \gamma_2)(\xi + \eta) \\ &\quad - \gamma_3(2\gamma_1 + 2\gamma_2 + \gamma_3)\{(\gamma_1 + \gamma_2)\xi + (\gamma_1 + \gamma_2 + \gamma_3)\eta\} \\ &\quad + h\gamma_3\{\text{Im}(A_1^2 A_3^*) - \text{Im}(A_2^2 A_3)\} = Q, \end{aligned} \quad (A.7)$$

and Q is easily shown to be positive (resp., negative) on L_2 for $\xi > 0$ (resp., $\xi < 0$). Without loss of generality, we set $h > 0$ since the substitution $h \rightarrow -h$, $A_1 \rightarrow -A_1$ and $A_3 \rightarrow -A_3$ leads to the same equation (A.2). On L_2 , we can choose any values of $|A_1|$ and $|A_2|$ independently of r_3 and θ_j 's, since

$$r_1 r_2 \{-h(\gamma_1 + \gamma_2)\sin(\theta_1 + \theta_2) + r_3(\gamma_1 + \gamma_2 + \gamma_3)\sin(\theta_1 - \theta_2 - \theta_3)\} = 0 \quad (A.8)$$

on L_2 . We can also choose the θ_j 's such that $\sin(2\theta_1 - \theta_2) \neq 0$ and $\sin(2\theta_2 + \theta_3) \neq 0$, since (A.8) has two degrees of freedom for the θ_j 's. Now, we assume that $\xi > 0$, then $\eta < 0$ and $\xi + \eta > 0$ on L_2 . On L_2 , we can choose only θ_j 's such that

$$\left. \begin{aligned} \sin(2\theta_1 - \theta_3) < 0 \text{ and } \sin(2\theta_2 + \theta_3) < 0, \text{ or} \\ \sin(2\theta_1 - \theta_3) > 0 \text{ and } \sin(2\theta_2 + \theta_3) > 0. \end{aligned} \right\} \quad (A.9)$$

Hence,

$$Q = (\gamma_1 + \gamma_2)(\gamma_1 + \gamma_2 + \gamma_3)r_1r_2|h\sin(\theta_1 + \theta_2) + r_3\sin(\theta_1 - \theta_2 - \theta_3)| \\ + h\gamma_3\{r_1^2r_3|\sin(2\theta_1 - \theta_3)| + r_2^2r_3|\sin(2\theta_2 + \theta_3)|\}. \quad (A.10)$$

Thus, for sufficiently large $|r_2|/|r_1|$, Q is positive on L_2 . Similarly, Q is negative on L_2 for $\xi < 0$ for sufficiently large $|r_1|/|r_2|$. Hence, trajectory $(\xi(t), \eta(t))$ may leave sector Z .

DATE
FILMED
- 8